

Digitized by the Internet Archive
in 2012 with funding from
LYRASIS Members and Sloan Foundation

<http://archive.org/details/adsorptionstudie00desh>

ADSORPTION STUDIES ON GRAIN DUSTS

by

UJWAL ANANT DESHPANDE

B.S., Indian Institute of Technology (Bombay), 1977

A MASTER'S THESIS

submitted in partial fulfillment of the

requirements for the degree

MASTER OF SCIENCE

Department of Chemical Engineering

KANSAS STATE UNIVERSITY
Manhattan, Kansas

1979

Approved by:

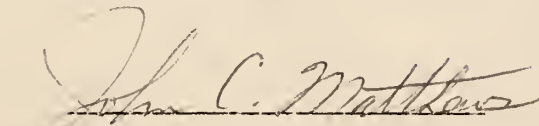

Major Professor

TABLE OF CONTENTS

| | Page |
|---|--------|
| CHAPTER 1. INTRODUCTION | 1 |
| 1.1 Background | 1 |
| 1.2 Types of Adsorption Isotherms | 2 |
| 1.3 The BET Theory | 5 |
| 1.4 Criticism of the BET Theory | 6 |
| 1.5 The Dubinin-Polanyi Theory: Application | 7 |
| CHAPTER 2. SPECIFIC SURFACE AREA MEASUREMENTS USING THE SORPTOMETER | 10 |
| 2.1 The Principle of the 'Sorptometer' | 10 |
| 2.2 The Sample Size and Pretreatment | 13 |
| 2.3 Results | 16 |
| 2.4 Discussion | 16 |
| CHAPTER 3. SPECIFIC SURFACE AREA MEASUREMENTS USING THE STATIC BET APPARATUS | 22 |
| 3.1 The Principle of the Apparatus | 22 |
| 3.2 Description of the Apparatus | 25 |
| 3.3 Specific Sections | 28 |
| 3.3.1 The Sample Tube | 28 |
| 3.3.2 The Vacuum System | 30 |
| 3.3.3 The Mercury Reservoirs | 32 |
| 3.3.4 The Burettes | 32 |
| 3.3.5 The McLeod Gauge | 32 |
| 3.3.6 The Storage Bulbs | 34 |
| 3.3.7 The Purification Trains For the Gases | 35 |
| 3.3.8 The Free Space | 35 |
| 3.3.9 The Dead Space | 36 |
| 3.3.10 Miscellaneous | 36 |
| 3.4 Surface Area Measurements Using Nitrogen | 37 |
| 3.5 Surface Area Measurements Using Carbon Dioxide At 195°K. | 38 |
| 3.6 Surface Area Measurements Using Carbon Dioxide At Room Temperature | 39 |

Sp. Coll.
 LD
 2008
 T4
 1274
 04/5
 52

| | Page |
|---|------|
| 3.7 Adsorption of Krypton | 39 |
| 3.8 Results | 42 |
| 3.9 Discussion | 42 |
| CHAPTER 4. ADSORPTION OF CARBON MONOXIDE AND METHANE | 49 |
| 4.1 Introduction | 49 |
| 4.2 Adsorption of Carbon Monoxide and Methane | 49 |
| 4.3 Results | 50 |
| 4.4 Discussion | 50 |
| CHAPTER 5. OTHER ADSORPTION ISOTHERMS | 62 |
| 5.1 Introduction | 62 |
| 5.2 Various Adsorption Isotherms | 62 |
| 5.3 Application of the Adsorption Isotherm Equations To the Adsorption Data | 66 |
| 5.4 Discussion | 76 |
| ACKNOWLEDGMENTS | 79 |
| REFERENCES | 80 |
| APPENDIX A: Sample Calculation For Determination of Specific Surface Area Using the Sorptometer | 82 |
| APPENDIX B: Particle Size Distribution of the Grain Dust Samples | 87 |
| APPENDIX C: A Sample Calculation For Estimation of External Surface Area Using the Particle Size Distribution | 88 |
| APPENDIX D: A Sample Calculation For Measurement of the Free Space In the Static BET Apparatus | 90 |
| APPENDIX E: A Sample Calculation For Measurement of Dead Space In the Sample Tube of the Static BET Apparatus | 93 |
| APPENDIX F: Calibration of Burettes | 97 |

| | Page |
|---|------|
| APPENDIX G: Calibration of the McLeod Gauge | 99 |
| APPENDIX H: A Sample Calculation For An Adsorption Run On the Static BET Apparatus | 105 |
| APPENDIX I: A Sample Calculation For Measurement of Surface Area Using Carbon Dioxide At Room Temperature | 114 |
| APPENDIX J: Pore Size Distribution Measurements Using the Static BET Apparatus | 119 |
| J-1 Introduction | 119 |
| J-2 Sample Preparation and Experimental Procedure | 122 |
| J-3 Necessary Data | 123 |
| J-4 Results | 123 |
| J-5 Discussion | 133 |

LIST OF FIGURES

| <u>Figure</u> | | <u>Page</u> |
|---------------|---|-------------|
| 1.1 | Types of Adsorption Isotherms | 4 |
| 2.1 | Schematic Diagram of the Sorptometer | 11 |
| 2.2 | Front View of the Sorptometer | 14 |
| 2.3 | Recorder Output for a Sorptometer Run | 15 |
| 3.1 | Simplified Schematic of the Static BET Apparatus | 23 |
| 3.2 | Static BET Apparatus | 26 |
| 3.3 | Sample Tube | 29 |
| 3.4 | Arrangement of Vacuum Pumps | 31 |
| 3.5 | The McLeod Gauge | 33 |
| 3.6 | Schematic of the Modified Static BET Apparatus | 41 |
| 3.7 | BET Plot for Surface Area Measurement of #784-04 (Wheat) Using Krypton at Liquid Nitrogen Temperature | 43 |
| 4.1 | Adsorption of Carbon Monoxide and Methane On #784-08 (Milo) | 51 |
| 4.2 | Adsorption of Carbon Monoxide and Methane On #784-04 (Wheat) | 52 |
| 4.3 | Adsorption of Carbon Monoxide On #784-04 (Wheat) and On #784-08 (Milo) | 53 |
| 4.4 | Adsorption of Methane On #784-04 (Wheat) and On #784-08 (Milo) | 54 |
| 4.5 | Plot of Amount Adsorbed Vs. $\frac{p}{p_{cr} \tau^2}$ For #784-04 (Wheat) | 59 |
| 4.6 | Plot of Amount Adsorbed Vs. $\frac{p}{p_{cr} \tau^2}$ For #784-08 (Milo) | 60 |
| 5.1 | The Harkins-Jura Relative Method for Adsorption of Nitrogen On #784-04 (Wheat) At Liquid Nitrogen Temperature | 67 |

| <u>Figure</u> | | <u>Page</u> |
|---------------|--|-------------|
| 5.2 | The Huttig Plot For Adsorption of Nitrogen On #784-08 (Milo) At Liquid Nitrogen Temperature | 68 |
| 5.3 | The Huttig Plot For Adsorption of Nitrogen On #784-04 (Wheat) At Liquid Nitrogen Temperature | 69 |
| 5.4 | The Lopez-Gonzalez and Deitz Plot For Adsorption of Nitrogen On #784-04 (Wheat) At Liquid Nitrogen Temperature | 70 |
| 5.5 | The Langmuir Plot For Adsorption of Nitrogen On #784-04 (Wheat) At Liquid Nitrogen Temperature | 71 |
| 5.6 | The BET Plot For Adsorption of Carbon Dioxide On #784-08 (Milo) At 195° K | 72 |
| A-1 | The BET Plot | 85 |
| D-1 | Free Space Measurement | 92 |
| G-1 | The McLeod Gauge | 100 |
| H-1 | Adsorption Isotherm For Carbon Dioxide On a Wheat Sample At 195° K | 110 |
| H-2 | The BET Plot | 111 |
| I-1 | Adsorption Isotherm For Carbon Dioxide On a Wheat Sample At 301° K | 115 |
| I-2 | The Dubinin-Polanyi Plot | 118 |
| J-1 | Adsorption Isotherm For Nitrogen On Kaiser Alumina At Liquid Nitrogen Temperature | 126 |
| J-2 | Cumulative Pore Volume Against Pore Diameter For Kaiser Alumina | 128 |
| J-3 | $\frac{d V_p}{d(\log \bar{d}_p)}$ against \bar{d}_p For Kaiser Alumina | 129 |
| J-4 | Adsorption Isotherm For Nitrogen On #784-04 (Wheat) At Liquid Nitrogen Temperature | 130 |
| J-5 | Cumulative Pore Volume Against Pore Diameter For #784-04 (Wheat) | 131 |
| J-6 | $\frac{d V_p}{d(\log \bar{d}_p)}$ against \bar{d}_p For #784-04 (Wheat) | 132 |

LIST OF TABLES

| Table | | Page |
|-------|---|------|
| 1.1 | Information On the Grain Dust Samples | 3 |
| 2.1 | Legend For Fig. 2.1 | 12 |
| 2.2 | Specific Surface Areas of Grain Dust Samples | 17 |
| 2.3 | Surface Areas of Refractory Materials | 19 |
| 2.4 | Comparison of the Specific Surface Area and the External Surface Area of the Dust Samples | 20 |
| 3.1 | Legend For Fig. 3.1 | 24 |
| 3.2 | Legend For Fig. 3.2 | 27 |
| 3.3 | Comparison of the Surface Areas Calculated from Different Measurements | 44 |
| 3.4 | Adsorption of Krypton On A Wheat Sample (#784-04) At Liquid Nitrogen Temperature | 45 |
| 3.5 | Molecular Diameter of Gases | 47 |
| 4.1 | Comparison of the Amounts Adsorbed and the Monolayer Capacities of the Dust Samples For Carbon Monoxide and Methane | 56 |
| 4.2 | Comparison of Lower Explosive Limits and the Amounts Adsorbed For Carbon Monoxide and Methane | 57 |
| 5.1 | Nitrogen Adsorption Data Using Various Adsorption Isotherms | 73 |
| 5.2 | Carbon Dioxide Adsorption Data At 195°K. Using Various Adsorption Isotherms | 74 |
| 5.3 | Krypton Adsorption Data On #784-04 (Wheat) Using Various Adsorption Isotherms | 75 |
| C-1 | Estimation of External Surface Area of A Grain Dust Sample Using the Particle Size Distribution | 89 |
| D-1 | Free Space Measurement | 91 |
| E-1 | Measurement of Dead Space At Liquid Nitrogen Temperature | 94 |
| E-2 | Comparison of the Dead Volumes Measured At Various Temperatures | 96 |

| Table | | Page |
|-------|---|------|
| F-1 | Calibration of Large Burette (B) | 97 |
| F-2 | Calibration of Small Burette (S) | 98 |
| G-1 | Calibration of the Capillary | 101 |
| G-2 | Calibration of McLeod Gauge Bulb | 102 |
| G-3 | Calibration of the Gauge Scale | 104 |
| H-1 | Adsorption Measurement of Carbon Dioxide On A Wheat Dust Sample At Dry Ice-Acetone Temperature | 107 |
| H-2 | Calculations For the BET Plot | 112 |
| I-1 | Adsorption Measurement of Carbon Dioxide On A Wheat Dust Sample At 301.2°K. | 116 |
| I-2 | Calculations For the Dubinin-Polanyi Plot | 117 |
| J-1 | Saturation Pressure and Liquid/Gas Ratio For Nitrogen . . . | 124 |
| J-2 | Values For Statistical Layers of Nitrogen, the Kelvin Diameter and the True Pore Diameter At Various Relative Pressures | 125 |
| J-3 | Measurement of Pore Size Distribution | 127 |

Chapter 1 Introduction

1.1 Background

A dust consists of solid particles of various sizes formed by disintegration processes. Grain dust is always present in grain handling units and is suspected of causing fire, explosion and health hazards. Dust control systems are designed to reduce air pollution and, hopefully, to minimize the fire and explosion hazards.

A number of causes of dust explosions in grain elevators have been identified. The conditions necessary for a dust explosion are similar to those of a combustible gas in an air; proper mixture of dust and air and an external source of heat to raise the temperature of the mixture above the ignition temperature. However, dust explosions are currently an area of active research and are not well understood.

Grain dust, being a porous material, has a surface area in excess of the external area and knowledge of the total area could be important in the combustion processes. The standard method of determining specific surface area of a porous substance is by nitrogen adsorption. The specific surface area can be calculated after determining the amounts adsorbed at various partial pressures by making use of the Brunauer, Emmett and Teller equation (2).

Apart from determining surface area of grain dusts, one can also determine the amount of the combustible gases adsorbed. In biodegradation

of cereal grains, carbon monoxide, carbon dioxide, methane etc. are produced. Whereas carbon dioxide is an inert gas, carbon monoxide and methane are highly explosive and so it is of interest to determine how much of these gases are adsorbed by the dusts.

The purpose of this work is to determine the specific surface areas of various grain dusts and the extent of adsorption of the above mentioned gases on the grain dusts. For this work, the grain dust samples were provided by U.S. Grain Marketing & Research Laboratory, Manhattan, Kansas. These samples were collected at elevators situated at different places in Kansas and were taken from various locations in the elevators. The particle size distribution analysis were made available for all these samples by the donors, and so also their absolute densities. The grain dusts were of corn, wheat, milo, and soybean. Three samples of each of these kinds were provided. The details on the source of these samples are given in Table 1.1.

1.2 Types of Adsorption Isotherms

The adsorption isotherms found experimentally have been classified into five types and almost all isotherms can be identified as belonging to one of these types (11,2). Figure 1.1 shows the types of isotherms.

Type I isotherms are referred to as the Langmuir type because in these cases only monomolecular adsorption takes place. Chemisorption isotherms are type I isotherms. They are also observed when physical adsorption cannot proceed beyond a monolayer because the pores are narrow and so a monomolecular layer is enough to fill them.

Type II isotherms, commonly called sigmoid or S-shaped isotherms, approach a relative pressure of unity asymptotically. They normally represent multimolecular adsorption on non-porous materials.

Table 1.1

Information On the Grain Dust Samples*

| Sample No. | Dust type | Location | Elevator | Date | Absolute Density, ρ ³ (kg./m ³ x 10 ⁻³) |
|------------|-----------|----------|---------------------|---------------|--|
| 784-04 | Wheat | Bin | Cargill-Kansas City | Apr. 5, 1978 | 1.54 |
| 784-06 | Corn | Bin | Cargill-Kansas City | Apr. 20, 1978 | 1.49 |
| 784-08 | Milo | Belt | Cargill-Kansas City | Apr. 20, 1978 | 1.56 |
| 785-04 | Soybean | Bin | Cargill-Wichita | May 9, 1978 | 1.74 |
| 786-01 | Wheat | Cyclone | Far-Mar-Co-Topeka | June 14, 1978 | 1.61 |
| 786-02 | Milo | Cyclone | Far-Mar-Co-Topeka | June 14, 1978 | 1.50 |
| 786-12 | Soybean | Cyclone | Bunge Corp.-Emporia | June 21, 1978 | 1.46 |
| 786-23 | Wheat | Baghouse | Morrison-Salina | June 22, 1978 | 1.50 |
| 786-28 | Milo | Baghouse | Morrison-Salina | June 22, 1978 | 1.43 |
| 786-30 | Soybean | | | | 2.16 |
| 786-43 | Corn | | Topeka Mill-Topeka | June 23, 1978 | 1.62 |
| 774-07 | Corn | Cyclone | | | 1.48 |

*Courtesy of the U.S. Grain Marketing Research Lab., Manhattan, Kansas.

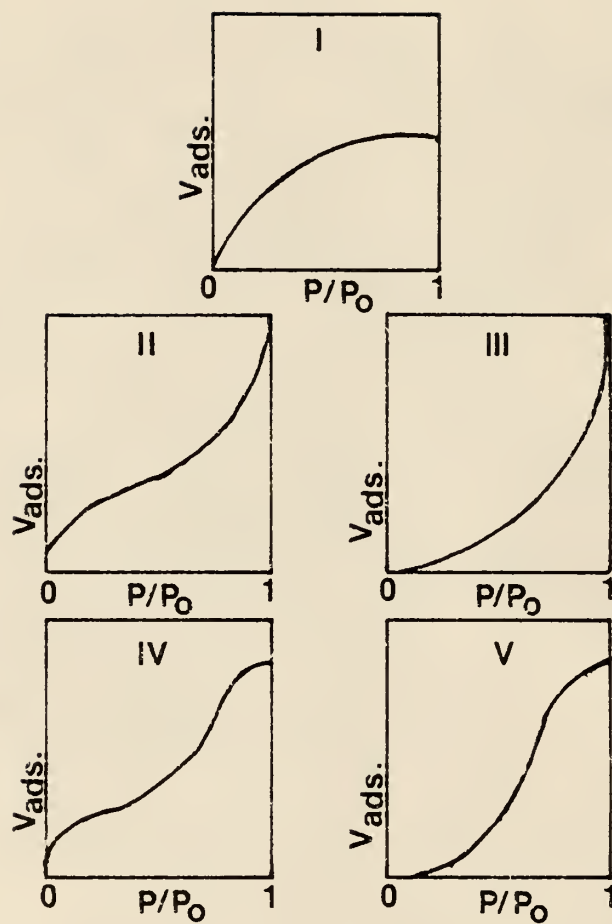


Fig. 1.1 Types of Adsorption Isotherms

Type III and V isotherms are rarely observed. In these cases, unlike in type I, II and IV, the heat of adsorption evolved in the formation of first layer is less than the heat evolved in the adsorption of subsequent layers. Excepting this difference, they resemble type II and IV, respectively. Type IV and V isotherms are observed in case of adsorption on highly porous adsorbents, the flattening of the isotherms at the highest pressures being attributed to the capillary phenomena.

In the low-pressure region, type I, II, and IV are similar to one another and so are type III and V to each other. In the region of very low pressure, almost all types of isotherms approach a linear relationship between amount adsorbed and pressure.

1.3 The BET Theory

As mentioned earlier, surface area of a porous substance can be measured by carrying out physical adsorption on it. There have been several theories put forward to evaluate the monolayer coverage from the adsorption data. The most popular among these is the one proposed by Brunauer, Emmett and Teller (commonly referred to as the BET theory). The generally accepted adsorbate for specific surface area determinations is nitrogen.

The BET theory retains Langmuir's concept of fixed adsorption sites (2), but allows the adsorption to take place to more than a monomolecular layer. The number of layers formed is assumed to be infinity and the state of 'dynamic equilibrium' that Langmuir postulated for his monolayer is assumed to hold for each of these infinite number of layers. Further, it is assumed that the heat of adsorption in all layers beyond the first is equal to the latent heat of condensation and that the frequency of oscillation of the molecules perpendicular to the surface is the same for molecules in all layers after the first.

The BET equation, relating volume adsorbed to pressure, may be written as

$$\frac{p}{v(p_0 - p)} = \frac{1}{v_m c} + \frac{c-1}{v_m c} \cdot \frac{p}{p_0} \quad (1.1)$$

where, p = Equilibrium partial pressure of the adsorbate, N/m^2

p_0 = Vapor pressure of the adsorbate at the existing temperature, N/m^2

v = Volume (STP) of the adsorbate adsorbed, m^3

v_m = Volume (STP) of the adsorbate corresponding to a monolayer, m^3

and, $c = e^{(E_1 - E_L)/RT}$ (1.2)

where, E_L = Latent heat of condensation of the adsorbate, kJ

E_1 = Heat of adsorption evolved in the formation of 1st layer, kJ

According to equation (1.1), a plot of $\frac{p}{v(p_0 - p)}$ against p/p_0 should

give a straight line of slope $\frac{(c-1)}{v_m c}$ and intercept $\frac{1}{v_m c}$. The application

of this equation is limited to the range of p/p_0 from 0.05 to about 0.30

(1).

1.4 Criticism of the BET Theory

Despite the success of the BET equation for the determination of monolayer capacity, of being applicable to all the types of adsorption isotherms, of reproducing the same parameters from isotherms at different temperatures, and of predicting heats of adsorption from a single isotherm, the BET theory is far from being perfect and has drawn much criticism (1,2).

The failure of the BET equation below a relative pressure of 0.05 is attributed by the authors to non-uniformity of the surface which causes the heat of adsorption for the first layer to vary from one part of the surface to another. The failure above a relative pressure of about 0.35 is

considered due to the existence of narrow pores which limit the thickness of the film.

Some workers, on the contrary, regard the limited validity of the BET equation as being due to shortcoming of the model itself. The assumption that the adsorbate has liquid-like properties after the first layer is difficult to justify since, as shown experimentally, both planar and porous solids exposed to saturated vapor sometimes take up only a limited amount and not the indefinitely large amount as postulated by the BET theory.

Also, the co-ordination number of molecules is near 12 in a bulk liquid and this "structure" mainly gives rise to the latent heat of liquefaction. Now, the BET theory assumes that the co-ordination number is 12 for an adsorbed molecule in any layer after the first and so each molecule which condenses in any layer after the first yields its full latent heat of liquefaction. However, in the absence of horizontal neighbors, the co-ordination number is much less than 12, and so the heat evolved should be only a fraction of the latent heat (2).

1.5 The Dubinin-Polanyi Theory: Application

Whereas the BET equation has been widely employed in determination of surface areas of porous materials, its applicability in the relative pressure range of 0.05 to 0.30 can be very restrictive. This range is convenient when the adsorption is being carried out at the normal boiling point of the adsorbate. However, sometimes this is too low a temperature. For example, when pores offer significant diffusional resistance, the amounts of the gas adsorbed in a reasonable time are much less than the equilibrium values. To overcome this resistance to diffusion one has to carry out the adsorption at higher temperatures. Since vapor pressure of a gas increases

enormously with temperature, it may not be possible to maintain the BET range of relative pressure in a glass adsorption apparatus. In such case, one has to either have an apparatus that can withstand high pressure, or have an equation that gives the monolayer capacity of the solid adsorbent and can be used at the existing low relative pressure. The equation proposed by Dubinin, M.M. and Polanyi, M. satisfies the latter condition.

The Dubinin-Polanyi equation (14) may be written as

$$\log W = \log W_0 - 0.434 (k/\beta^2) \epsilon^2 \quad (1.3)$$

where, W = Volume of the adsorbate adsorbed, m^3/kg . adsorbent

W_0 = Limiting volume of the adsorption space, m^3/kg . adsorbent

k = A constant

β = Relative differential molar work of adsorption of the vapor for the chosen standard substance, a constant for an adsorbate.

and, ϵ = Differential molar work of adsorption, kJ.

$$= RT \ln (p_s/p) \quad (1.4)$$

where, R = Universal gas constant

$$= 8314.3 \text{ N}\cdot\text{m}/\text{kmole } ^\circ\text{K}$$

T = Temperature of the system, $^\circ\text{K}$

p_s = Saturation pressure of the adsorbate at the system temperature,
 N/m^2

p = Equilibrium partial pressure of the adsorbate, N/m^2 .

If the adsorption can be assumed to be restricted to a monolayer only, the monolayer capacity of the solid is the limiting volume of the adsorption space, W_0 (16) and thus it is possible to determine the monolayer capacity by plotting $\log a$ against $(\log(p_s/p))^2$ and determining the intercept on the ordinate.

This method of determining the surface area of a porous substance has been used in the case of adsorption of carbon dioxide on coal at room temperature and the results obtained agreed very well with those obtained using a high pressure apparatus and the BET equation (9).

Chapter 2

Specific Surface Area Measurements Using the Sorptometer

2.1 The Principle of the 'Sorptometer'

The 'Sorptometer' (5) is a flow-type adsorption measurement apparatus manufactured by 'Perkin-Elmer'. A schematic of the apparatus is shown in Fig. 2.1 and the various parts are identified in Table 2.1. A gas mixture of helium as inert and nitrogen as adsorbate, of any composition can be made by adjusting the flow rates of each of these gases. The gas mixture passes over the sample in the sample tube and the effluent is monitored by a thermal conductivity detector. With the gas mixture flowing, the sample tube is cooled to liquid nitrogen temperature by immersing it in a bath containing liquid nitrogen. At this lower temperature, the sample adsorbs a certain amount of nitrogen thus depleting the flowing mixture of nitrogen. This depletion of nitrogen is recorded on the recorder chart as a peak, the area of which is proportional to the amount of nitrogen adsorbed. When the adsorption is completed, the recorder pen comes back to zero or its original position. The liquid nitrogen bath is then removed and the rise in temperature of the sample causes it to release the adsorbed nitrogen. This causes the enrichment of the effluent gas with nitrogen which is, again, sensed by the thermal conductivity detector and another peak is produced, however, in the reverse direction of the adsorption peak. The areas of these two peaks should be the same as all the gas that was adsorbed must be desorbed. However the desorption peak is used in the calculations since it is sharper with less tailing. After this, a known amount of



Fig. 2.1 Schematic Diagram of the Sorptometer

Table 2.1

Legend for Fig. 2.1

| | |
|------------|---|
| Gas 1 | - Adsorbate (Nitrogen) Inlet Port |
| Gas 2 | - Carrier (Helium) Inlet Port |
| Cal. Gas | - Calibration Gas Inlet Port |
| W | - Soap Bubble Flowmeter |
| D1, D2, D3 | - Dryers |
| E1, E2, E3 | - Filter Discs |
| F1, F2 | - Toggle Valves |
| G1, G2 | - Pressure Regulators |
| H | - Needle Valve |
| I1, I2 | - Pressure Gauges |
| J1, J2 | - Restrictors |
| K | - Flowmeter |
| L1, L2 | - Gas Shut off Valves |
| M | - Mixing Tank |
| S1, S2 | - Calibration Valves (shown in "Charge" position) |
| C1, C2 | - Calibration Valve Loops |
| N | - Cold Trap |
| O1, O2 | - Dewar Flasks |
| T1, T2, T3 | - Sample Bypass Valve |
| U | - Sample Tube |
| Q | - Constant Temperature Bath |
| P1, P2 | - Heat Exchangers |
| R | - Detector |

nitrogen is injected into the stream and the resulting peak is recorded. This peak serves as the calibration peak.

By comparing the areas of the desorption and the calibration peaks, the amount of nitrogen adsorbed can be calculated. By changing the composition of the gas mixture and repeating the measurement, the adsorption isotherm can be obtained, from which the specific surface area of the sample can be determined by the BET method.

In using a flow procedure such as the Sorptometer, the assumptions are made that adsorption on the sample is negligible at room temperature and that adsorption on the sample tube is negligible.

Figure 2.2 gives the front view of the Sorptometer. Further details may be found in (5).

2.2 The Sample Size and Pretreatment

The amounts of sample used in the surface area measurements of grain dusts were typically between 0.5×10^{-3} and 1.0×10^{-3} kg. and the signal from the detector was normally attenuated by a factor of 2. This sample size was within the physical dimensions available for the sample tube and it normally produced large peaks (Fig. 2.3).

The sample to be used in the Sorptometer has to be pretreated for removal of any gases present on the sample material. Typically there is moisture present in porous materials, which is normally removed by exposing the sample to elevated temperatures in an inert atmosphere. The temperature and the exposure time depend upon the nature of sample material. The normal temperatures used are between 373 and 773⁰K. and the normal exposure times are between 1 and 5 hours. Generally the selected temperature and the necessary time are inversely proportional. Higher tempera-

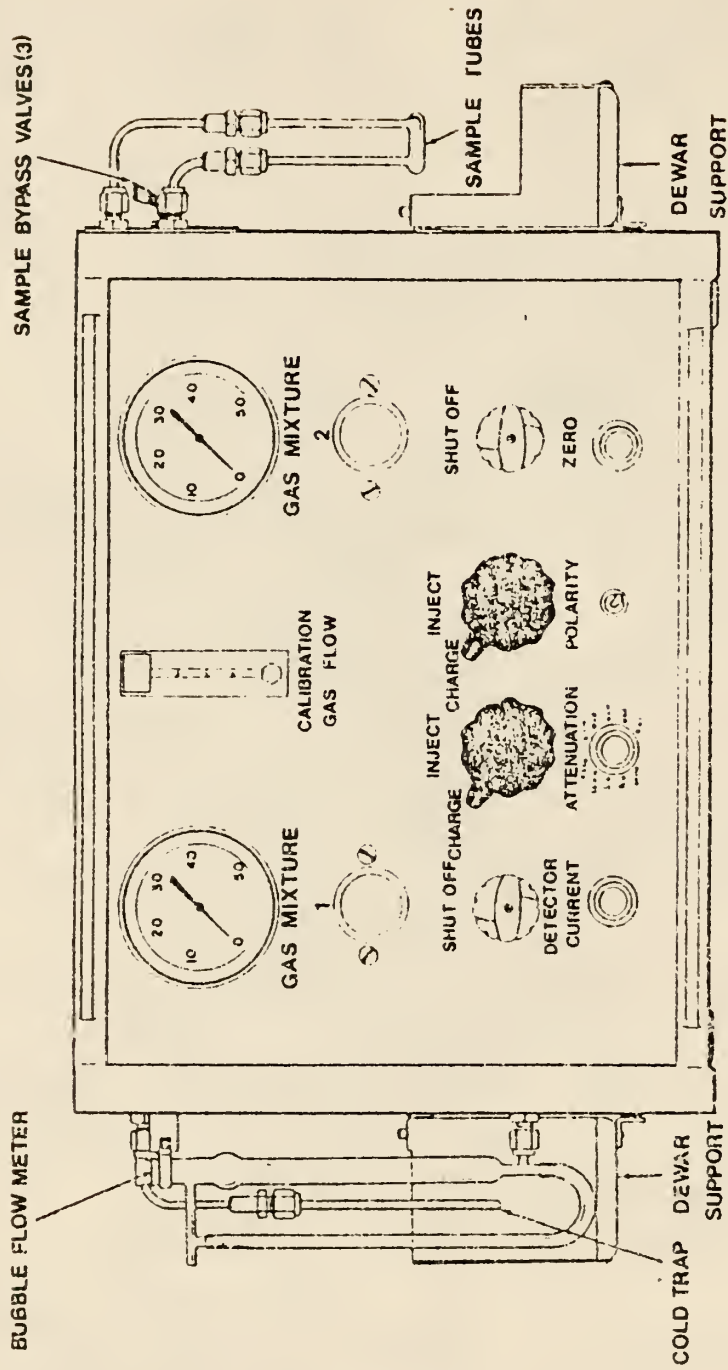


Fig. 2.2 Front View of the Sorptometer

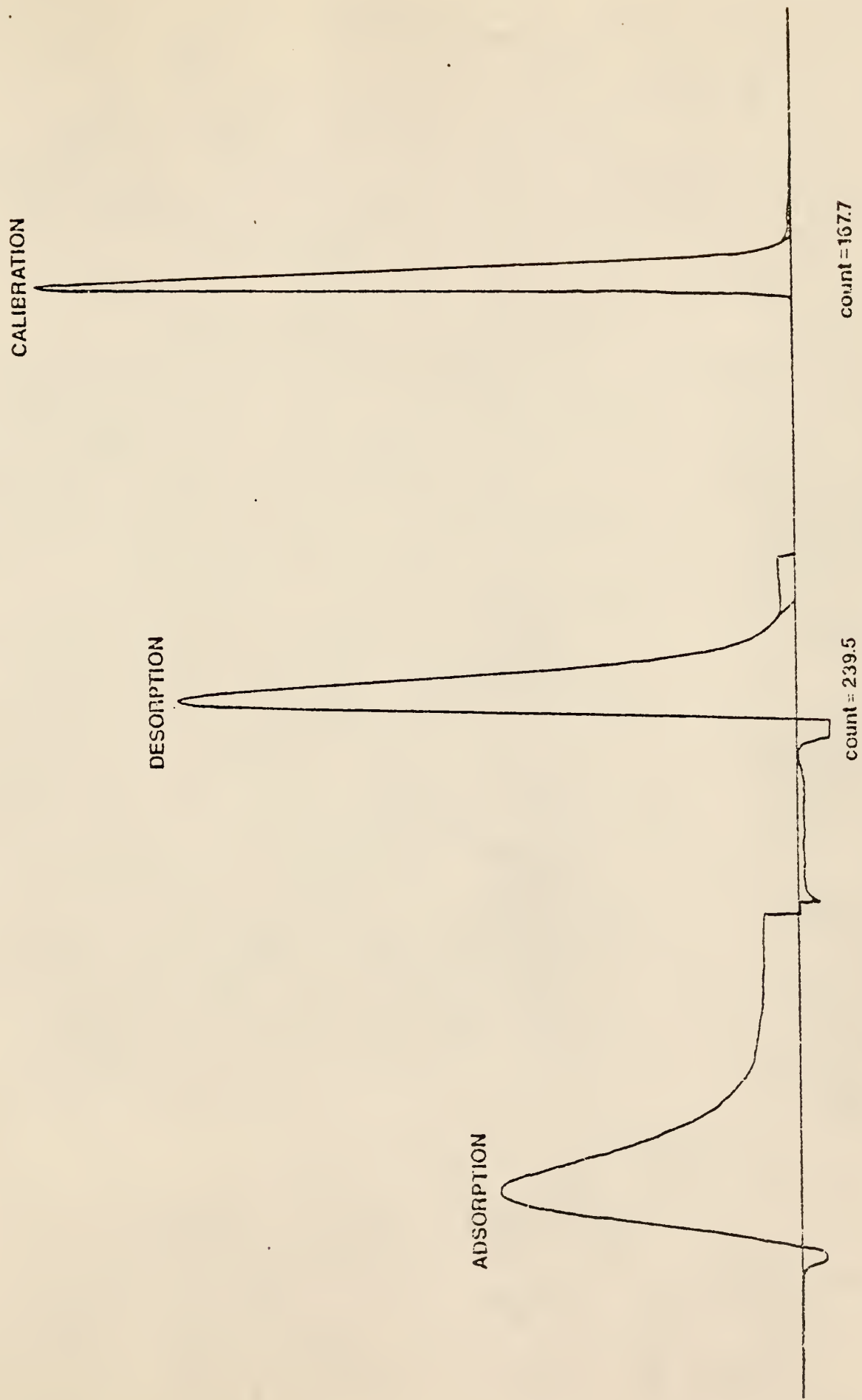


Fig. 2.3 Recorder Output for a Sorptometer Run

tures are preferred unless they cause physical or chemical changes in the sample. For samples which cannot withstand high temperatures, the degassing may be carried out overnight.

The grain dusts undergo pyrolysis at temperatures above $\sim 395^{\circ}\text{K}$. (4). So they could not be degassed at high temperatures. To degas them, therefore, three different treatments were utilized and their results compared.

1) Place the sample in an oven at 383°K . for 2 hours and immediately after removing the sample tube from the oven, pass helium through it for 15 minutes.

2) Place the sample in an oven at 383°K . for 18 hours and immediately after removing the sample tube from the oven, pass helium through it for 15 minutes.

3) Place the sample in a desiccator containing phosphorous pentoxide (P_2O_5) for a minimum of 7 days at room temperature.

On degassing, all the grain dusts were found to have undergone a 10-15% weight loss. After pretreatment, the sample tube was always capped with rubber policemen to avoid any contamination of the sample prior to the adsorption measurements.

2.3 Results

The specific surface areas of various grain dusts as measured using the Sorptometer, after various pretreatments, are shown in Table 2.2. A complete set of sample calculations is given in Appendix A. The multiple entries in a column in Table 2.2 are the repetition measurements for the sample using the same pretreatment.

2.4 Discussion

From Table 2.2, one can see that the specific surface area of various grain dust samples varied between 420 and $2070 \text{ m}^2/\text{kg}$. (0.42 and $2.07 \text{ m}^2/\text{g}$).

Table 2.2
Specific Surface Areas of Grain Dust Samples

| Sample | Using Sorptometer | | | | | Using Static System | | |
|------------------|------------------------------|-------------------------------|--|--|---|-------------------------------|----------------------------------|----------------------------------|
| | 383° K. for 2 hrs. (1) | 383° K. for 18 hrs. (2) | 383° K. for 1 week for 1 week (3) | P ₂ O ₅ Desiccator (4) | Average of (2) (3) and (4) (5) | Nitrogen (77.4° K.) (6) | CO ₂ (195° K.) (7) | CO ₂ (298° K.) (8) |
| 786-01 (Wheat) | | 1.70 | | | 1.70 | | | |
| 786-23 (Wheat) | | 1.03 | | | 1.03 | | | |
| 784-04 (Wheat) | 1.54 | 1.77 | 1.80 1.46 | 1.81 1.93 | 1.77 | 2.24 | 8.94 | 17.84 |
| 786-02 (Milo) | 1.76 | 1.89 1.93 | 2.07 | | 1.96 | | | |
| 786-28 (Milo) | | 0.84 | | | 0.84 | | | |
| 784-08 (Milo) | | 1.22 | | 1.05 1.14 | 1.18 | 1.15 | 4.93 | 40.30 |
| 786-12 (Soybean) | 0.42 | 0.51 0.60 | 0.69 | | 0.60 | | | |
| 786-30 (Soybean) | | 1.12 | | | 1.12 | | | |
| 785-04 (Soybean) | | 1.04 | | 0.92 1.04 | 1.00 | 1.14 | 6.52 | 12.17 |
| 786-43 (Corn) | | 1.52 | | | 1.52 | | | |
| 774-07 (Corn) | | 1.75 | | | 1.75 | | | |
| 784-06 (Corn) | 0.75 | 1.30 | 1.10 | 0.71 0.99 1.01 | 1.02 | | | |

Note: All values are in (m²/kg x 10⁻³)

The Sorptometer has been observed to be able to measure, reasonably accurately the surface areas of refractory materials in the range from 1000 to 3,100,000 m²/kg. (1 to 3100 m²/g.) as shown in Table 2.3. The reproducibility that was obtained on the grain dust samples is of the same order as the reproducibility that was obtained for an alumina sample of specific surface area of around 1000 m²/kg. (1 m²/g.).

On the whole, one cannot conclude that the pretreatment of putting the sample in desiccator containing P₂O₅, is better than the pretreatment of putting it in an oven at 383°K. for 18 hours, or vice versa. The results obtained in both cases are essentially within the reproducibility that has been observed in the Sorptometer measurements.

However, it may be noted that the surface area values obtained after the treatment of putting a sample in oven at 383°K. for 2 hours are typically lower than those obtained after other pretreatments. It was concluded that the pretreatment of putting a sample in oven at 383°K. for 2 hours is inadequate to drive off all the gases or vapors bound on the grain dusts.

As will be seen in Chapter 3, the measurements made on the static BET apparatus agree well with those made on the Sorptometer. Noting that the Sorptometer is a flow type apparatus, the agreement between the data obtained from these two techniques is worth mentioning.

Table 2.4 gives the values of total specific surface area and the external surface area (assuming spherical particles), as calculated from the particle size distribution, for various grain dust samples. Appendix B gives the particle size distribution for these samples and Appendix C gives a sample calculation of the external surface area. The values of the specific surface areas obtained in case of the grain dusts are an order of magnitude greater than the external surface area values. This shows that

Table 2.3

Surface Areas of Refractory Materials (3)

| Catalyst Support | Surface Area, ($\text{m}^2/\text{kg} \times 10^{-3}$) | | % Deviation |
|---------------------------|---|----------------|-------------|
| | Reported Value | Measured Value | |
| Amoco Active Carbon | 3070 | 3137 | +2 |
| Davison Grade 979 Alumina | 400 | 427 | +7 |
| Davison Grade 980-25 | 325 | 312 | -4 |
| Norton SA-5102 Alumina | 0.7-1.3 | 0.86 | — |
| Kaiser Alumina 201 | — | 322 | — |

Table 2.4

Comparison of the Specific Surface Area and the External
Surface Area of the Dust Samples

| Sample | Average Specific Surface Area Using the Sorptometer, S_s ($m^2/kg. \times 10^{-3}$) | External Surface Area Calculated From the Particle Size Distribution S_{ext} ($m^2/kg. \times 10^{-3}$) |
|------------------|---|--|
| 786-01 (Wheat) | 1.70 | 0.173 |
| 786-23 (Wheat) | 1.03 | 0.359 |
| 784-04 (Wheat) | 1.77 | 0.389 |
| 786-02 (Milo) | 1.96 | 0.275 |
| 786-28 (Milo) | 0.84 | 0.036 |
| 784-08 (Milo) | 1.18 | 0.172 |
| 786-12 (Soybean) | 0.60 | 0.033 |
| 786-30 (Soybean) | 1.12 | 0.057 |
| 785-04 (Soybean) | 1.00 | 0.186 |
| 786-43 (Corn) | 1.52 | 0.199 |
| 774-07 (Corn) | 1.75 | 0.226 |
| 784-06 (Corn) | 1.02 | 0.244 |

nitrogen does enter at least some pores, although as will be seen in Chapter 3, it apparently does not enter all the pores of the grain dusts.

It may be noted that with the pretreatment of putting the samples in desiccator containing P_2O_5 , only the moisture present in the samples could be removed. On the other hand, by putting them in an oven at $383^{\circ}K.$, any gas or vapor bound to the sample, including moisture could be removed. But, in heating them to $383^{\circ}K.$, there is always a possibility of sample undergoing some chemical changes. However fairly consistent results obtained after these varied pretreatments show that there were no other gases, present in significant amounts, on the sample other than moisture, and that there was no significant structural change undergone by the sample in heating it to $383^{\circ}K.$

Chapter 3

Specific Surface Area Measurements Using the Static BET Apparatus

3.1 The Principle of the Apparatus

A simplified schematic of the apparatus is shown in Fig. 3.1 and the terminology used is explained in Table 3.1. The apparatus is a standard volumetric BET apparatus. The volumes of the burette bulbs were determined prior to assembling the various parts of the system (Appendix F). The system in Durland Hall has two sets of burettes and sampling tubes on a single vacuum system. Besides the vacuum system, they also share the purification trains and the McLeod gauge.

After connecting the various parts of the system, the "free space" of the system has to be determined. The free space is the space over the burettes, over the stopcock C, below the stopcock B and above the zero position in the manometer. It is essentially made up of the capillary tubings used to connect the above parts. The free space measurement is made by admitting helium into the space and using the burette bulbs to change the volume of the gas by known amounts. By measuring the corresponding pressure changes and using the ideal gas law the free space volume can be determined. A sample calculation is shown in Appendix D.

Prior to an adsorption measurement, the "dead space" in the sample tube has to be determined. The void space below the sample tube stopcock, C, including that in the sample tube and in the pores of the sample is referred to as the dead space of the system. To make this measurement,

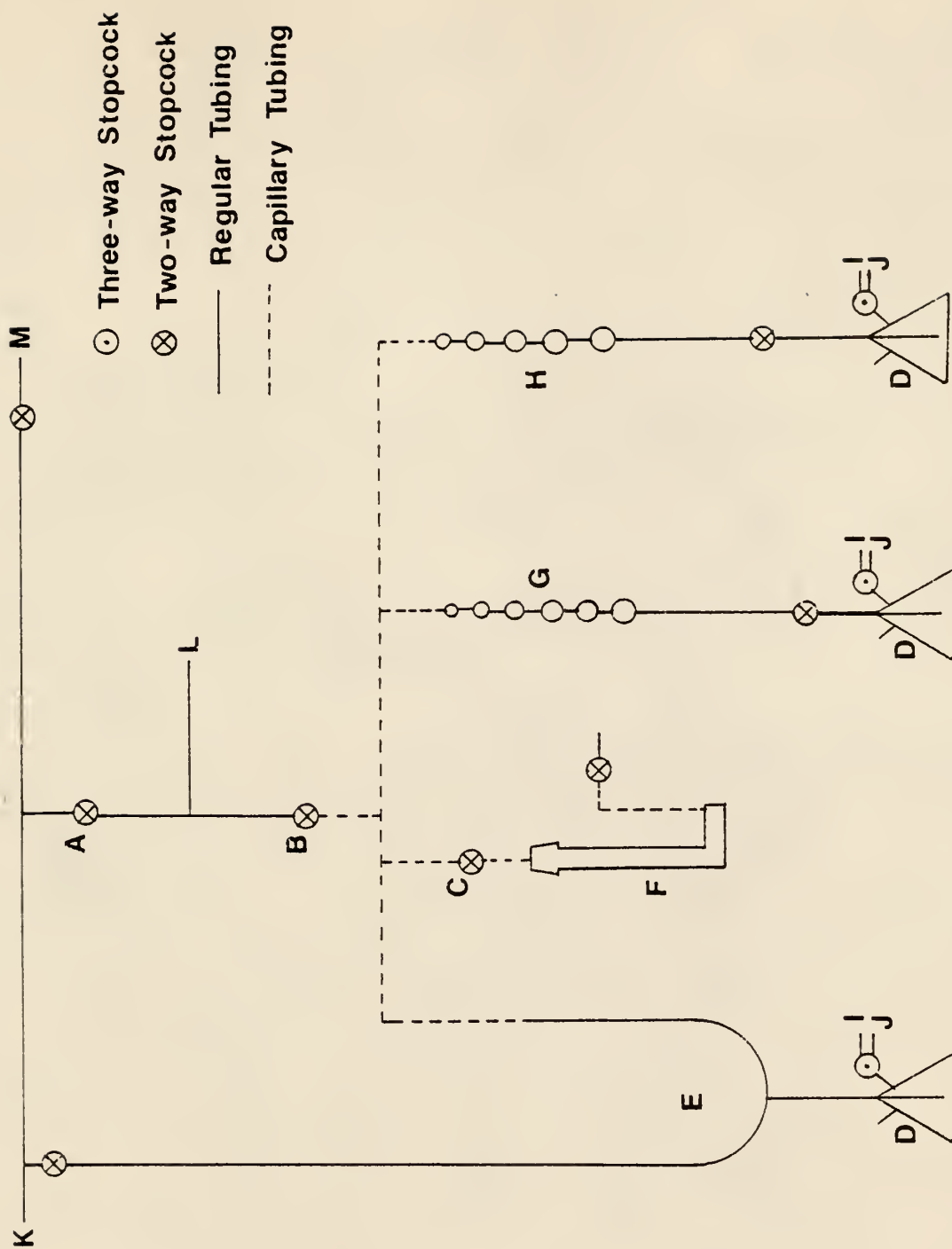


Fig. 3.1 Simplified Schematic of the Static BEF Apparatus

Table 3.1

Legend For Fig. 3.1

| | |
|-------|---|
| A,B,C | Key-Position stopcocks |
| D | Mercury reservoirs |
| E | Manometer to measure gas pressure over the sample and the gas burette |
| F | Sample tube |
| G | Small gas burette |
| H | Large gas burette |
| I | To source of air pressure |
| J | To vacuum chamber |
| K | To diffusion pump |
| L | To gas storage |
| M | To atmosphere |

the entire system is first evacuated, then the sample tube stopcock, C, is closed, stopcock B is opened and helium is admitted into the system. Stopcock B is then closed and the gas is thus trapped in the system. The amount taken in is measured assuming the ideal gas law by measuring the pressure using the manometer, since the volume of the burette bulbs is known. A number of readings are taken by changing the level of mercury in the burettes and adjusting the level of mercury in the manometer. Stopcock C is then opened. The gas enters the sample tube and the pressure in the system drops. The level of mercury in the monometer is re-adjusted and sufficient time is given for the system to reach the equilibrium. The volume of the dead space can then be calculated, again using the ideal gas law. A number of such measurements are made and the average value of the volume of the dead space is used in the adsorption measurements. A sample calculation for the dead space measurement is shown in Appendix E.

The entire system is then re-evacuated and adsorption gas is admitted into the system. The same procedure as the dead space measurement is followed and the amount of the gas adsorbed is calculated. This amount corresponds to the equilibrium pressure in the system and so gives one point on the adsorption isotherm. To obtain more points, the level of mercury in the burettes is changed, the level of mercury in the manometer is readjusted and the new equilibrium pressure in the system is noted. The calculation procedure is explained in detail in Appendix H.

3.2 Description of the Apparatus

A schematic diagram of the apparatus is shown in Fig. 3.2 and the terminology used is explained in Table 3.2. The apparatus consists of three main sections integrated together: the sample tube, burettes, manometer and mercury reservoirs; the storage bulbs and the open-end manometer;

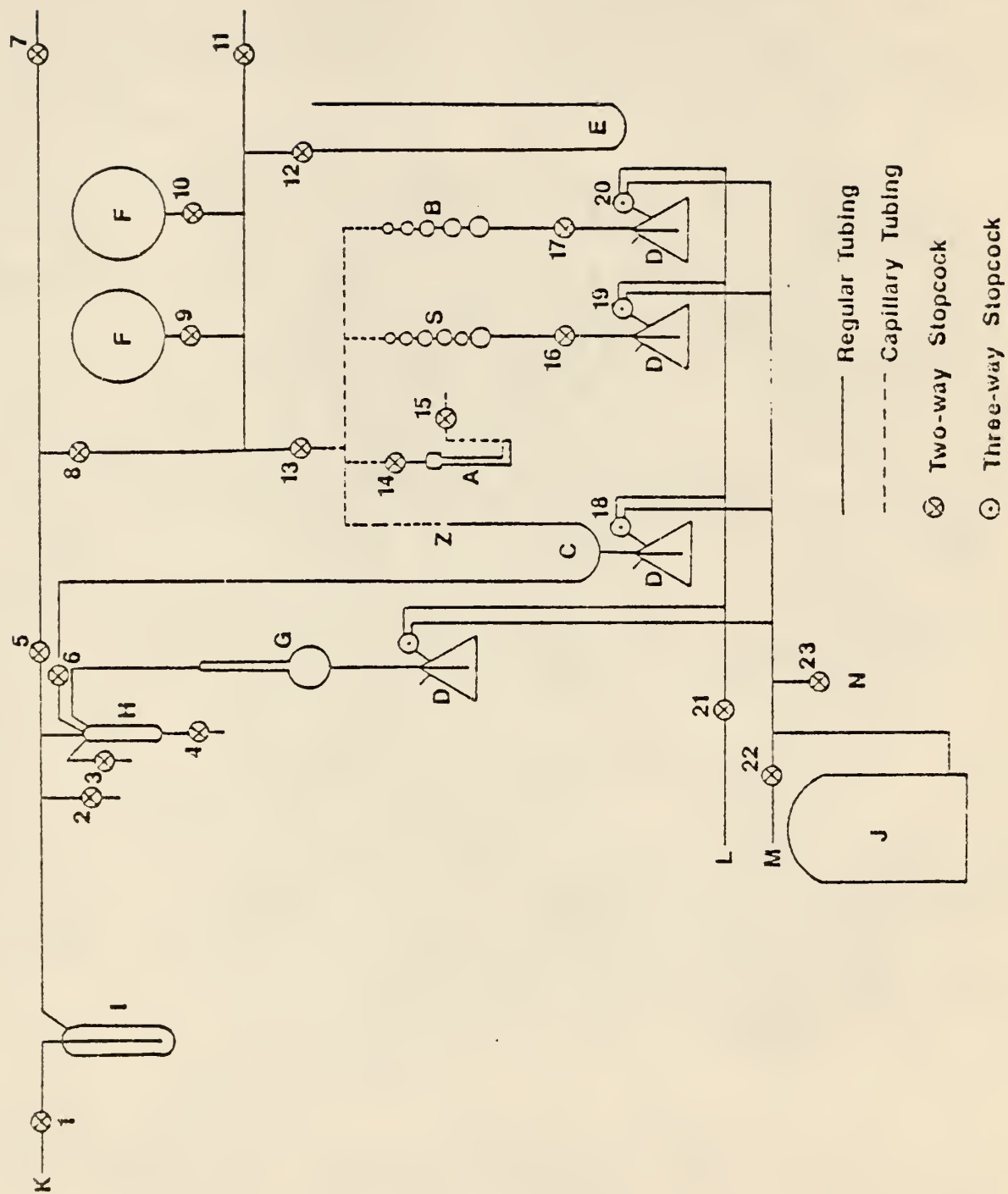


Fig. 3.2 Static BET Apparatus

Table 3.2

Legend For Fig. 3.2

| | |
|---|---|
| A | Sample tube |
| B | Large gas burette |
| C | Manometer to measure gas pressure over the sample and the gas burette |
| D | Mercury reservoirs |
| E | Manometer to measure gas pressure in the gas storage bulbs |
| F | Gas storage bulbs |
| G | McLeod gauge |
| H | Mercury trap |
| I | Cold trap |
| J | Vacuum chamber |
| K | To diffusion pump |
| L | To source of air pressure |
| M | To mechanical pump |
| N | To atmosphere |
| S | Small gas burette |
| Z | Reference position on the manometer C |

the vacuum system consisting of an oil diffusion pump in series with a mechanical pump, a cold trap and a McLeod gauge to measure the level of vacuum. The various parts of the system were made and assembled by Mr. Mitsugi Ohno.

In the first section of the apparatus, where the adsorption measurements are made, capillary glass tubing was used wherever possible to reduce the free space and thus improve the accuracy in the measurements. Also, wherever necessary, high vacuum pyrex stopcocks manufactured by Fisher Scientific Co. were used. All stopcocks were greased using Apiezon "N" grease manufactured by Fisher Scientific Co.

Much of the system has been described previously (3). However the second set of burettes and sample tube were added specifically for the grain dust measurements. Further the system does change as it gets broken (e.g. the McLeod gauge) or modified. For these reasons the system is described in detail below.

3.3 Specific Sections

3.3.1 The Sample Tube

Although the accuracy of the measurements improves as the sample size is increased, the weight of the sample tube correspondingly goes up and this limits the size of the sample and so also the size of the sample tube.

Fig. 3.3 is the diagram of the sample tube that was used for the adsorption measurements on the grain dust samples. The flow-through nature of the design permits passing a gas over the sample if needed. The glass rod inserted in the sample tube minimizes the void volume in the sample tube.

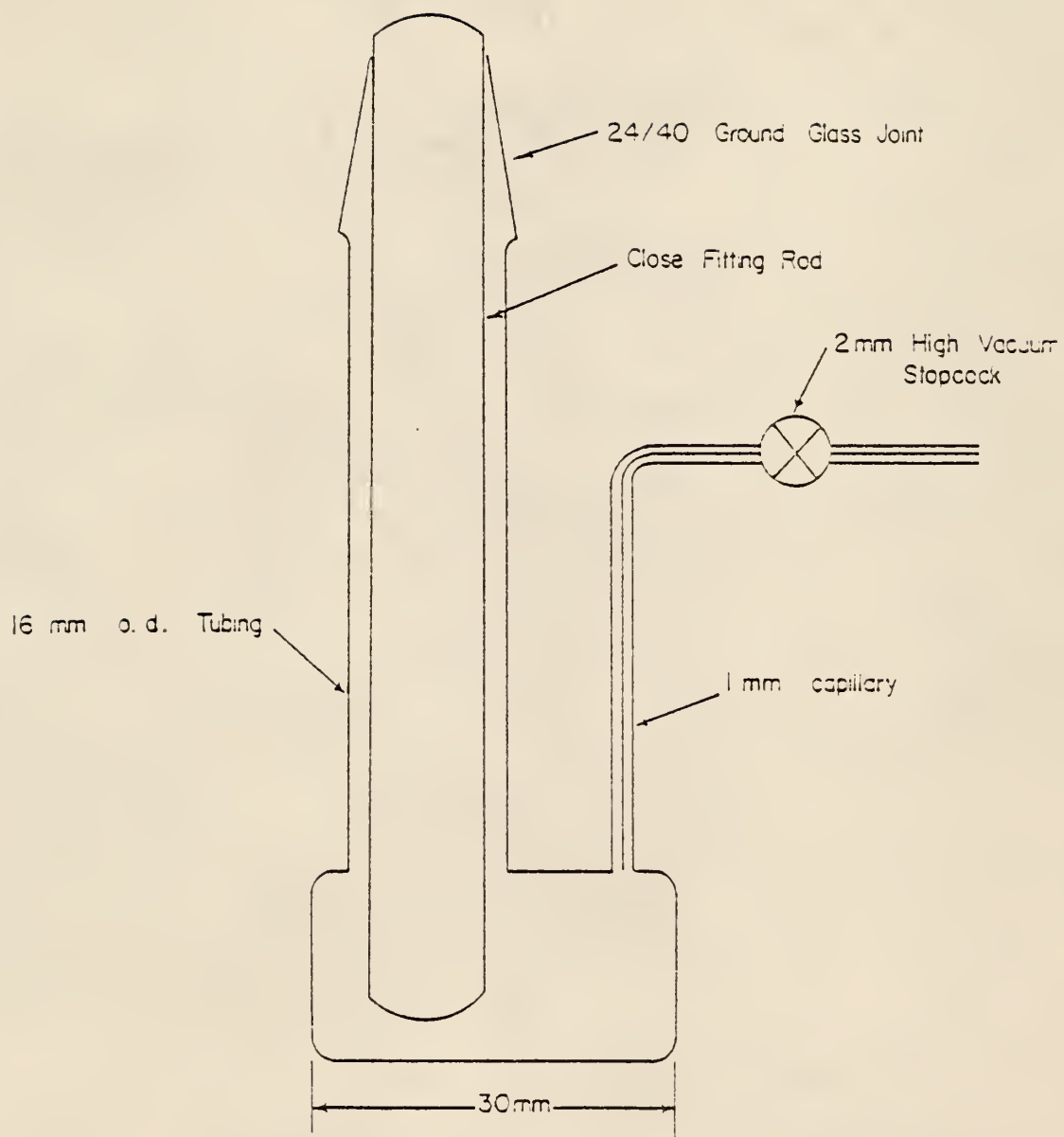


Fig. 3.3 Sample Tube

3.3.2 The Vacuum System

The vacuum system consists of a "Speedivac" Chevron Baffle oil diffusion pump by Edwards High Vacuum Ltd., in series with a "Speedivac" High Vacuum mechanical pump. The diffusion pump is water cooled. The pumping system is as shown in Fig. 3.4.

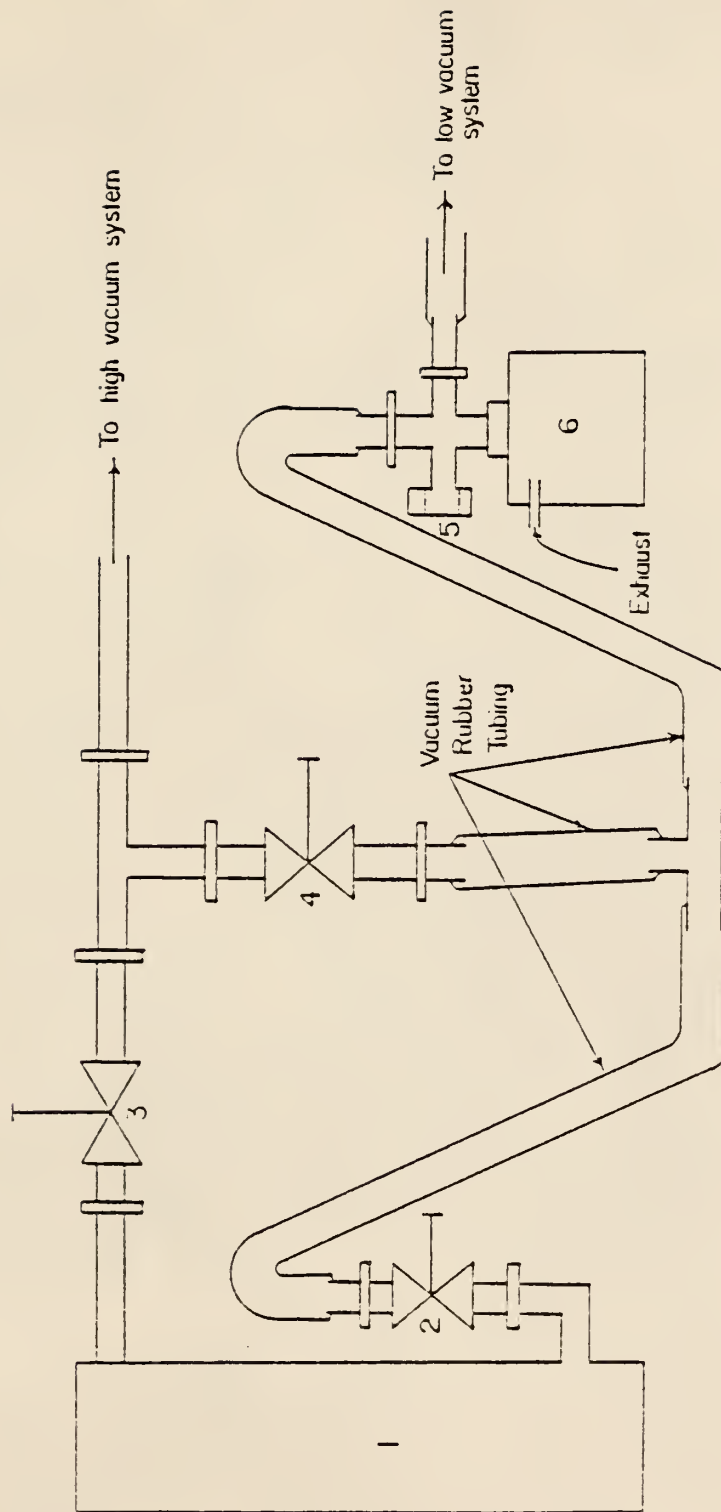
The start up procedure for the system is as follows.

- (a) Close the air admittance valve and all other openings to the atmosphere.
- (b) Open the roughing valve and backing valve.
- (c) Turn on the cooling water supply, then switch on the rotary pump.
- (d) When the backing pressure reaches about 66 N/m^2 (0.5 mm Hg) or better, switch on the diffusion pump heater.
- (e) After a warming period of 10 to 15 minutes, close the roughing valve and open the high vacuum isolation valve.

The shut down procedure for the system is as follows.

- (a) Switch off the diffusion pump heater.
- (b) Close the high vacuum isolation valve and open the roughing valve.
- (c) After the diffusion pump cools, close the backing valve.
- (d) Turn off the water supply. Admit air to the system by opening the air admittance valve and switching off the rotary pump simultaneously.

Normally the diffusion pump is kept evacuated in order to prevent the oil from absorbing air. To prevent oil vapors from entering the rest of the system, including the sample tube, there is a liquid nitrogen cold trap between the pumps and the rest of the system. Also, since the same pumps are used for evacuating the low vacuum side (used for pulling the mercury down into the mercury reservoirs, Section 3.3.3) a large vacuum



1. Diffusion Pump
2. Backing Valve
3. High Vacuum Isolation Valve
4. Roughing Valve
5. Air Admittance Valve
6. Backing Pump

Fig. 3.4 Arrangement of Vacuum Pumps

chamber of ~ 17 liters is connected to the low vacuum side. This helps maintain the vacuum on the low vacuum side for a longer period of time and avoids frequent evacuation.

3.3.3 The Mercury Reservoirs

500 ml. conical flasks partially filled with mercury have been used as the mercury reservoirs. They supply the mercury for changing the level of mercury in the burettes, manometer and the McLeod gauge when adsorption or vacuum level measurements are made. The pressure in the reservoirs is changed with three-way stopcocks, one arm of which is at atmospheric pressure and the other is at vacuum.

3.3.4 The Burettes

The burettes are used to change the volume of the entrapped adsorption gas by a known amount. They are, as shown in Fig. 3.1, a number of glass bulbs attached together by short capillaries. There are two burettes, the smaller one has six bulbs and the larger five. The bulbs have been calibrated using mercury (Appendix F). The two burettes together constitute a volume of about 364 ml.

3.3.5 The McLeod Gauge

A McLeod gauge is used to measure the pressure in the system. It operates on the principle that a known amount of gas at the pressure of the system obeys Boyle's law when compressed to a pressure much higher than the system pressure and to a volume much smaller than the initial value.

The gauge is shown in Fig. 3.5. It consists of a capillary of uniform cross-section, closed at the top end and connected to a large bulb at the bottom. It is in this capillary where the gas originally at the pressure of the system is compressed. A 200 ml. round bottomed flask was

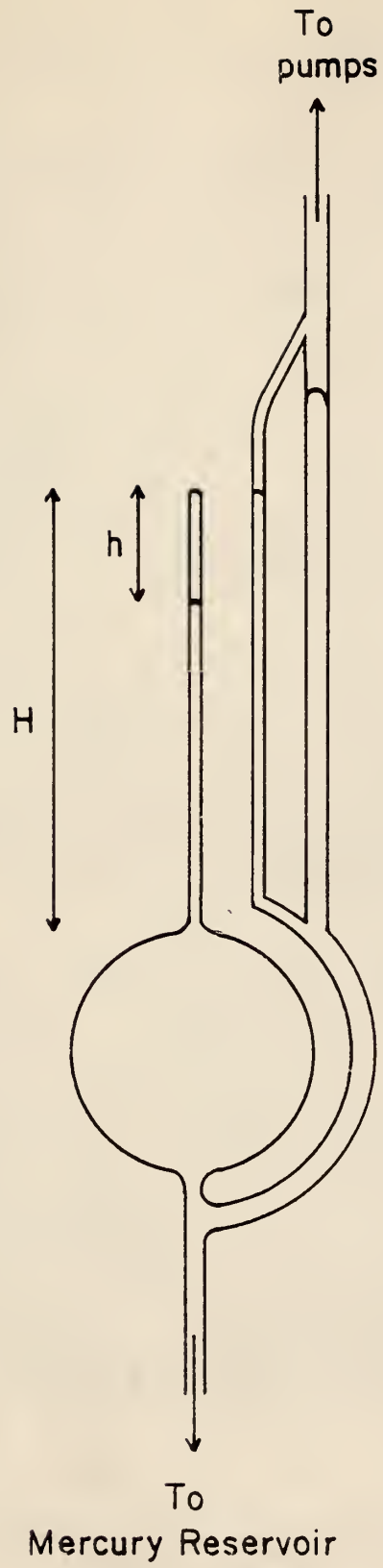


Fig. 3.5 The McLeod Gauge

used as the bulb, the other end of which is connected to the mercury reservoir. Between the bulb and the reservoir is a side line which is parallel to the capillary and open to the vacuum system. There is another capillary, parallel to the side line, of the same size as the one on top of the bulb, the mercury level in which is taken as standard so as to eliminate the capillary effects in the main capillary tube. The volume of the capillary and the bulb have been determined using mercury. The top end of this capillary has been marked as the reference.

As one pushes the mercury from the reservoir into the gauge, the amount of the gas in the bulb and the capillary is trapped and compressed by the mercury. The mercury is raised until its level in the side arm capillary reaches the reference mark. The level of mercury in the main capillary then corresponds to a particular value of pressure in the system. The capillary has been calibrated and the calculations are shown in Appendix G.

The lowest pressure reading on a McLeod gauge can be improved by either increasing the volume of the bulb, or decreasing the diameter of the capillary used. However, increasing the bulb volume increases the weight of mercury that the glass tubing above the reservoir has to support and so its strength limits the size of the bulb that can be used. Decreasing the diameter of the capillary tubing used below a certain value causes the mercury to stick to the glass walls and to break into small threads. The McLeod gauge used can measure pressure from 53.3 N/m^2 (0.4 mm Hg) up to $1.33 \times 10^{-3} \text{ N/m}^2$ (1×10^{-5} mm Hg). It was made and attached to the system by Mr. Mitsugi Ohno.

3.3.6 The Storage Bulbs

In order to store the purified gases that are used either for adsorption or as inert gas for the dead space or the free space measurements,

round bottomed flasks of capacity of about 3 liters were used. Prior to their first fillings, they were heated and evacuated to $1.33 \times 10^{-3} \text{ N/m}^2$ ($1 \times 10^{-5} \text{ mm Hg}$). Also, in order to prevent leakage of air into the bulbs, the gases were always stored at a pressure slightly higher than atmospheric. The bulbs were strengthened by reinforcing them with masking tape.

3.3.7 The Purification Trains for the Gases

The gases used for adsorption and for the dead space and free space measurements were first purified by passing them through purification trains, and then stored in the storage bulbs.

Helium which was used for the measurements of the dead space and the free space, was obtained from Airco Inc., of 99.995% purity and it was passed over a bed of copper wires at 623° K for removal of oxygen and moisture was removed by passing the gas over 3A molecular sieves. The gas was then passed over activated coconut charcoal of 6 to 14 mesh size at liquid nitrogen temperature for removal of other condensable gases or vapors. The helium thus purified was then stored.

Nitrogen that was used was first passed over 3A molecular sieves, followed by a flask surrounded by a mixture of dry ice and acetone.

Matheson Research Purity grade carbon dioxide of minimum of 99.995% purity was used in the adsorption work. It was passed over 3A molecular sieves for removal of any moisture present, before storing it in a storage bulb.

3.3.8 The Free Space

As mentioned above, the space made of capillary tubing that connects the burettes, the sample tube and the manometer is referred to as the free space. It is desirable to reduce it to the least possible volume. This space is always at room temperature during any measurement. A sample

calculation for the free space measurement is shown in Appendix D. The sample tube is protected from the mercury vapors by gold foil. Gold forms an amalgam with mercury and thus prevents the vapors from entering the sample tube.

3.3.9 The Dead Space

The void space in the sample tube, including the pores of the sample, is referred to as the dead space in the sample tube. A sample calculation for its measurement using helium is shown in Appendix E. It is desirable to have as little dead space as possible and it is for this reason that the glass rod is inserted in the sample tube. In the case of extremely fine samples, a little glass wool may be needed to prevent blow over during evacuation.

It is assumed in the calculations that the entire dead space has the same temperature as the sample. This may not be the case at temperatures far from ambient and indeed, in the calculations, it is found that the dead space has a smaller value at a lower temperature (Appendix E). However, the error is minimized since the same effect occurs while carrying out the adsorption measurements.

3.3.10 Miscellaneous

To maintain the sample tube at a constant temperature during low temperature adsorption measurements, it was surrounded with a Dewar flask of capacity ~ 900 ml. containing the appropriate coolant. The exact temperature of a bath containing a mixture of dry ice and acetone was measured using a Copper-Constantan Thermocouple and the exact temperature of a liquid nitrogen bath was measured using the nitrogen vapor thermometer described previously (3). The temperature of the sample was controlled near room temperature by using the TU-14 Tempunit model of the thermoregulator manufactured by Techne Inc.

There is a mercury trap installed to prevent the mercury from the manometer or the McLeod gauge from being thrown into the large high vacuum line in case of sudden pressure fluctuations in the system. Also, there is a liquid nitrogen cold trap to prevent oil vapors from the diffusion pump from entering the rest of the system.

3.4 Surface Area Measurements Using Nitrogen

Adsorption of nitrogen at liquid nitrogen temperature and use of the BET equation to calculate the monolayer capacity of the solid is the standard method of measuring the specific surface area of porous substances. It has proven to be useful in case of many materials, particularly refractory catalysts and catalysts supports. However, in case of coals and other carbonaceous materials, the method has had problems, apparently due to large resistance to pore diffusion at very low temperatures (7). It was suspected from the Sorptometer runs that this could be the case for grain dust. However, the surface area measurements on the static apparatus using nitrogen were carried out for the purpose of comparing the results with those obtained from the Sorptometer.

Prior to putting the sample in the sample tube, it was kept in a desiccator containing P_2O_5 for an extended period of time. This removes most of the moisture present in the sample and thus reduces the time required for evacuating the sample. After evacuating the sample, the dead space in the sample tube was measured at liquid nitrogen temperature, using helium. The system was then re-evacuated to 1.33×10^{-3} N/m² (1×10^{-5} mm Hg) and the adsorption measurements made. Equilibrium was observed within a few minutes. The level of the liquid nitrogen in the Dewar flask was maintained constant throughout the course of the measurements.

The vapor pressure of the liquid nitrogen was measured using the nitrogen vapor thermometer described previously (3).

3.5 Surface Area Measurements Using Carbon Dioxide at 195°K

Reasonable agreement was found between the Sorptometer runs and the static apparatus runs. However, as mentioned earlier, it was suspected that nitrogen could not enter all the pores in a reasonable time, giving, therefore, low values of specific surface area. To explore this possibility, it was decided to carry out adsorption at a higher temperature to at least diminish the pore diffusion resistance. But, if nitrogen is used at a higher temperature, a high-pressure apparatus is needed in order to operate at the pressures which would still give the relative pressure in the range of the BET equation validity. It was, thus, decided to use carbon dioxide at 195°K, which has also been used in the study of coals (8).

Again, prior to putting the sample in the sample tube, it was kept in a P_2O_5 desiccator for an extended period (> 4 weeks). It was then put in the sample tube and evacuated to around $1.33 \times 10^{-3} \text{ N/m}^2$ (1×10^{-5} mm Hg), and again the dead space in the sample tube measured prior to the adsorption measurements. The temperature of the sample tube was maintained at 195°K using a mixture of dry ice and acetone in a Dewar flask surrounding the sample tube. Dry ice was made using the 'Redi-ice' unit manufactured by 'Metallurgical Supply Company' and was added frequently to the Dewar flask to maintain the temperature as close to 195°K as possible. The contents of the Dewar flask were stirred frequently and the temperature was measured using a Copper-Constantan thermocouple. The BET equation was used to calculate the monolayer capacity and the area

covered by solid carbon dioxide at 193.3°K was used to calculate the specific surface area.

3.6 Surface Area Measurements Using Carbon Dioxide at Room Temperature

The higher values of surface area obtained in case of adsorption of carbon dioxide at 195°K indicate that diffusional resistance indeed could have caused the surface area values from the nitrogen adsorption to be low. However, if this was the case, the carbon dioxide adsorption at 195°K might not have been complete either. Walker et al. (9) claim that the carbon dioxide adsorption at 298°K gave the correct value of surface area in the case of coal. Since the vapor pressure of carbon dioxide is around 6.49×10^6 N/m² (64 atm) at 298°K, the BET equation could not be used for the measurements made on the glass apparatus. However, the coal work at 298°K using the Dubinin-Polanyi equation was successful in terms of agreement with the surface area calculated using the BET equation on the measurements made in a metallic apparatus. It was thus decided to try the high temperature adsorption on grain dusts and make use of the Dubinin-Polanyi equation to calculate their monolayer capacities.

Again, prior to the adsorption measurements, the dead space in the sample tube was measured at room temperature. The temperature around the sample tube was maintained constant using the thermoregulator, referred to in Section 3.3.10. The sample calculations showing the use of the Dubinin-Polanyi equation are given in Appendix I.

3.7 Adsorption of Krypton

Fairly consistent results were obtained with the adsorption of nitrogen on the static BET apparatus. However, it was thought that relatively large amounts of the adsorbate gas taken in was staying in the burettes, the free space and the dead space of the system compared to the amount

adsorbed, thus lessening the accuracy of the measurements. This problem is encountered when surface areas are low, say, less than $1000 \text{ m}^2/\text{kg}$.

It is impossible to reduce the free space and the dead space in a system beyond some minimum value. It is, however, possible to reduce the amount of gas not adsorbed at the desired relative pressure. This can be achieved if the partial pressure of the gas is reduced and so also the vapor pressure, so that the relative pressure is the same as before.

Krypton has a vapor pressure of $\sim 270 \text{ N/m}^2$ at liquid nitrogen temperature. It was, therefore, decided to determine the surface area of a grain dust sample using krypton at liquid nitrogen temperature and compare the results with those obtained using nitrogen.

3.7.1 Modification of the Apparatus

The existing static BET apparatus could be used for measurements of krypton adsorption after modification. A schematic of the modified apparatus is shown in Fig. 3.6.

As mentioned earlier, Krypton has a vapor pressure of $\sim 270 \text{ N/m}^2$ at liquid nitrogen temperature. The existing McLeod gauge cannot be used to measure pressures higher than $\sim 53 \text{ N/m}^2$ and the manometer cannot read a pressure below $\sim 133 \text{ N/m}^2$. So neither of these could be used for the krypton adsorption measurements. It was, therefore, necessary to use a different McLeod gauge. The model 10-224-B, manufactured by 'The Virtis Company' was used for this work. It has a pressure range of from 0.667 to 667 N/m^2 . To connect this to the free space of the system, a three-way stopcock was used at the position 'B' in Fig. 3.6 and the two were connected using high-vacuum rubber tubing of 6.4 mm I.D., #14-182A manufactured by 'Fisher Scientific Company'.

Exactly the same procedure as described in Section 3.1 was followed, except that the pressure was now measured using the McLeod gauge instead

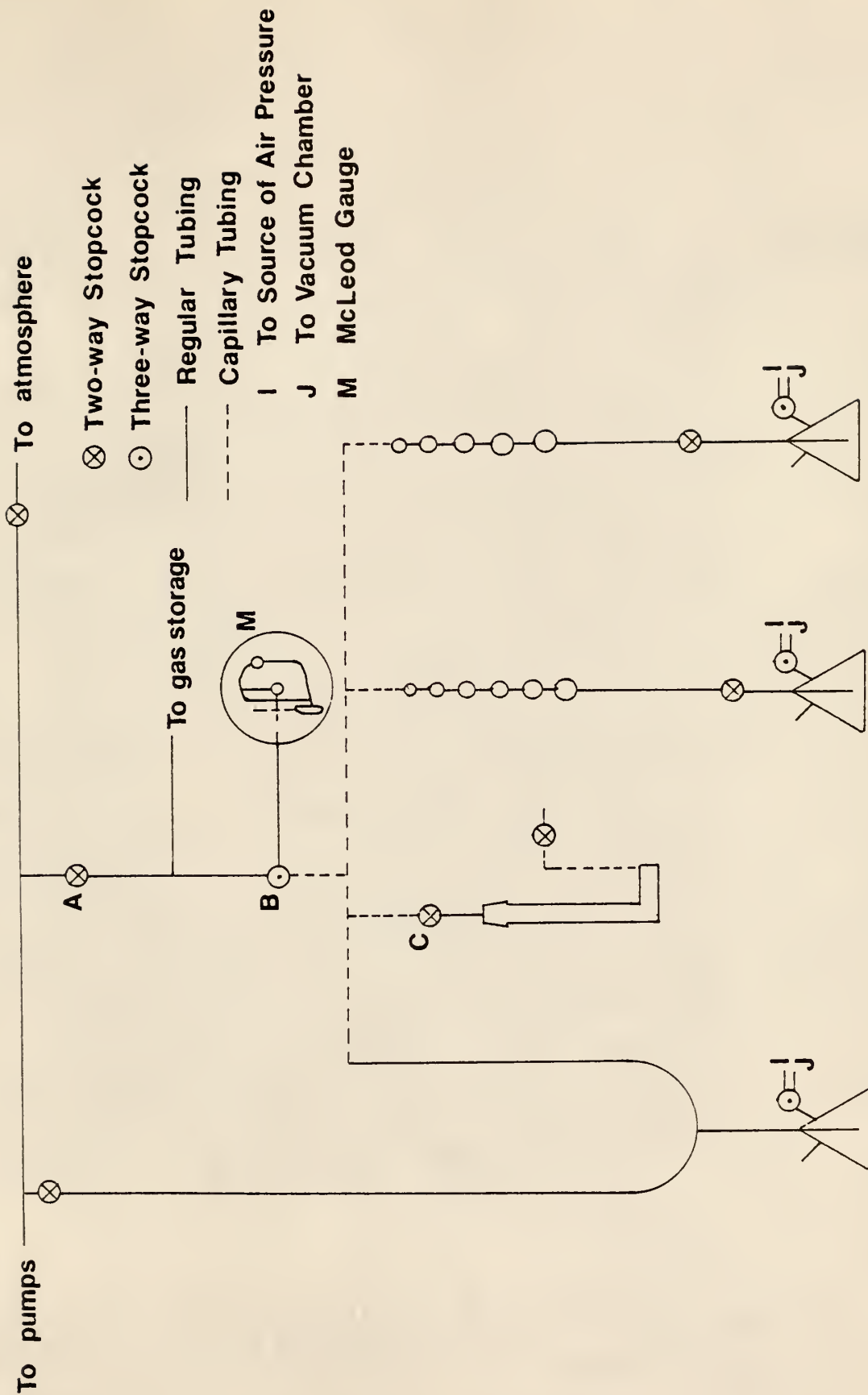


Fig. 3.6 Schematic of the Modified Static BET Apparatus

of the manometer. It may, however, be noted that now the free space consisted of the previous free space and the space in the McLeod gauge.

3.8 Results

The specific surface area values obtained from the adsorption of nitrogen at 77.4°K , the adsorption of carbon dioxide at 195°K , and that at the room temperature have been tabulated for various grain dust samples in Table 3.3. Also shown are the mean values of the surface areas obtained from the Sorptometer measurements. Table 3.4 shows the calculations for determination of the surface area of the wheat sample (#784-04) by krypton adsorption and Fig. 3.7 gives the BET plot for this measurement.

3.9 Discussion

From Table 3.3, it can be seen that the specific surface areas of a sample obtained from the Sorptometer measurements and from the nitrogen adsorption measurements made on the static BET apparatus agree reasonably well. The deviation between the two values is within the accuracy of the Sorptometer in most cases.

Comparing the measurements from the nitrogen adsorption and the carbon dioxide adsorption at 195°K , one can see that the carbon dioxide values are higher in all the cases. This suggests that pore diffusional resistance may be important in the case of nitrogen. The comparison of the carbon dioxide adsorption measurements at the two temperatures show that the specific surface areas are higher at room temperatures. This suggests that the temperature of 195°K was not high enough to completely eliminate the diffusional resistance. In the case of coal, carbon dioxide was found to enter all the pores at 298°K .

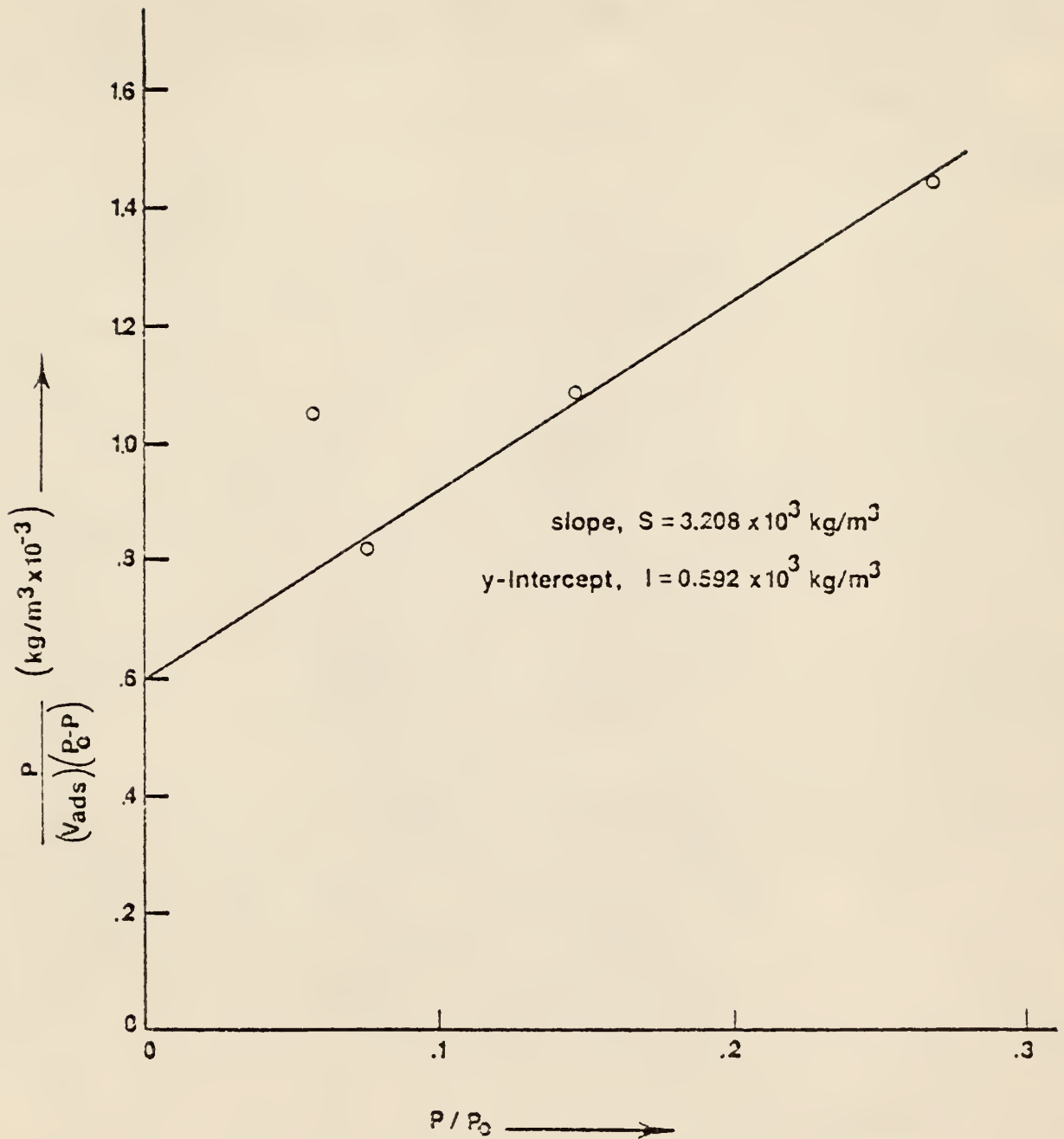


Fig. 3.7 BET Plot for Surface Area Measurement of #784-04 (Wheat)
Using Krypton at Liquid Nitrogen Temperature

Table 3.3
 Comparison of the Surface Areas Calculated From
 Different Measurements

| Sample | Nitrogen Adsorption At 77.4°K | CO ₂ Adsorption At 195°K | CO ₂ Adsorption At 298°K | Average of the Sorptometer Measurements |
|------------------|-------------------------------|-------------------------------------|-------------------------------------|---|
| 784-04 (Wheat) | 2.24 | 8.94 | 17.84 | 1.77 |
| 784-08 (Milo) | 1.15 | 4.93 | 40.30 | 1.18 |
| 785-04 (Soybean) | 1.14 | 6.52 | 12.17 | 1.00 |

Note: All values are in (m²/kg x 10⁻³)

Table 3.4

Adsorption of Krypton on a Wheat Sample (#784-04) at
Liquid Nitrogen Temperature

| Run No. | Bath Temperature T_b ($^{\circ}\text{K}$) | Vapor Pressure of Krypton, P_o (N/m^2) | Pressure in the System, P (N/m^2) | Amount of the Gas Adsorbed, n_{ads} (kmole/kg Sample $\times 10^5$) | $\frac{P}{P_o}$ | $\frac{P}{(P_o - P)} (V_{\text{ads}})$ ($\text{kg}/\text{m}^3 \times 10^{-3}$) |
|---------|---|--|---|---|-----------------|--|
| 1 | 77.24 | 273.54 | 73.33 | 1.133 | 0.268 | 1.442 |
| 2 | 77.33 | 278.60 | 16.00 | 0.260 | 0.057 | 1.044 |
| 3 | 77.40 | 282.58 | 21.33 | 0.448 | 0.076 | 0.817 |
| 4 | 77.25 | 274.10 | 40.00 | 0.702 | 0.146 | 1.086 |

From the BET plot (Fig. 3.7),

$$\text{Slope, } S = 3.208 \times 10^3 \text{ kg}/\text{m}^3$$

$$\text{y-Intercept, } I = 0.592 \times 10^3 \text{ kg}/\text{m}^3$$

$$\text{Monolayer capacity, } v_m = \frac{I}{S+I} = 0.263 \times 10^{-3} \text{ m}^3/\text{kg}$$

$$\text{Coverage by adsorbed krypton, } s_o = 5.2432 \times 10^6 \text{ m}^2/\text{m}^3 \quad (2)$$

$$\text{Specific surface area, } S_s = v_m s_o = 1.38 \times 10^3 \text{ m}^2/\text{kg}$$

A surface area of $1380 \text{ m}^2/\text{kg}$ was obtained from the adsorption of krypton on the wheat sample (#784-04) at liquid nitrogen temperature (Table 3.4). The average value of the several measurements made on the Sorptometer on this sample was $1770 \text{ m}^2/\text{kg}$ while the nitrogen adsorption on the static apparatus gave a value of $2240 \text{ m}^2/\text{kg}$. However, it may be expected that krypton gives smaller surface area value than does nitrogen by considering the diameters of the molecules as calculated from van der Waal's equation (Table 3.5). Krypton molecules being larger than nitrogen, should enter fewer pores. The difference between the values of the molecular diameters of these gases is, however, not large and this explains why the difference in the surface area values calculated from the adsorption measurements is small. It may also be noted from the results that the majority of the surface area in the porous structure of wheat dust is offered by pores of size less than the diameter of nitrogen molecule (0.315 nm).

The above comparison is possible because these adsorption measurements were made at the same temperature. However, a similar comparison for the measurements with carbon monoxide, methane (Chapter 4) and carbon dioxide cannot be made although they all were made at the dry-ice temperature (195°K). The difficulty is that the surface area cannot be calculated using the carbon monoxide and the methane measurements as their critical temperatures are less than the dry-ice temperature.

During the calculation of the amount of the gas adsorbed, it could be clearly seen that the fraction of the gas not adsorbed was very small in these measurements. For example, in the worst case, out of 7.597×10^{-8} kmole of krypton taken into the system, 1.214×10^{-8} was in the free space and the burettes, 0.167×10^{-8} kmole was in the dead space and

Table 3.5
Molecular Diameter of Gases (15)

| Gas | Molecular diameter (nm) | | |
|-----------------|-------------------------|------------------------------|------------------------|
| | From Viscosity | From van der Waal's equation | From heat conductivity |
| Carbon monoxide | 0.319 | 0.312 | — |
| Carbon dioxide | 0.334 | 0.323 | 0.340 |
| Krypton | — | 0.369 | 0.314 |
| Nitrogen | 0.315 | 0.315 | 0.353 |

6.216×10^{-8} kmole was adsorbed on the sample which corresponds to 82% of the total gas intake.

It can be seen in the BET plot (Fig. 3.7) that whereas three points lie on the straight line, the fourth point is far off. Since any attention given to this point would have raised the surface area of the sample closer to the values obtained from either the Sorptometer measurements or the nitrogen adsorption measurements on the static BET apparatus, thus reaffirming the conclusion drawn from this work, it was decided to draw a straight line through the other three points only.

The fairly good agreement between the krypton work and the nitrogen work on the wheat sample led us to think that carrying out krypton adsorption on another sample or taking more data on the wheat would not yield new information, but only confirm what has been said here. It was, therefore, decided to stop the krypton work after one dust sample only.

Chapter 4

Adsorption of Carbon Monoxide and Methane

4.1 Introduction

As mentioned in Chapter 1, this work is in connection with exploring the cause of grain dust explosions in grain storage elevators. As part of the project, it is important to determine the extent of adsorption of combustible gases on the grain dusts.

While grains are stored in the elevators, they undergo biodegradation with the passage of time. The gases evolved due to the biodegradation include carbon monoxide and methane, which are explosive. If these gases, upon evolution, are adsorbed on the internal surfaces of the grain dusts, they could contribute to the danger of an explosion.

4.2 Adsorption of Carbon Monoxide and Methane

Measurements of adsorption of carbon monoxide and methane were made with the static BET apparatus. The same procedures as described in Chapter 3 were followed for these measurements. The measurements were made both at ambient and at dry ice temperatures. The dead volume in the sample tube was determined prior to the adsorption measurements.

The gases used in this work were high purity gases further purified by passing them through a cold trap. The carbon monoxide used was Ultra High Purity (99.8% min.) manufactured by 'Matheson', which was passed through a bulb containing 3A molecular sieves and then cooled to 195° K. with a

mixture of dry ice and acetone to remove moisture and other condensable vapors that might be present.

The methane was Ultra High Purity (99.97% min.) manufactured by 'Matheson', which was again passed through a bulb containing 3A molecular sieves and then cooled to 195^o K.. The gases thus purified were stored in the storage flasks, to be used later.

4.3 Results

The adsorption measurements of carbon monoxide and methane made on a milo sample (#784-08) are shown in Fig. 4.1, and those made on a wheat sample (#784-04) are shown in Fig. 4.2. For comparing adsorption of a gas on these two grain dust samples, Figures 4.3 and 4.4 show the adsorption isotherms for carbon monoxide and methane, respectively, at the different temperatures.

4.4 Discussion

As should be the case, more adsorption was observed for a given gas on an adsorbent at a lower temperature. For a particular sample, it was found that more methane was adsorbed at a particular pressure and temperature than carbon monoxide. This was expected since methane has a higher critical temperature than carbon monoxide. For a particular gas, the wheat dust was found to adsorb somewhat more than milo at the same temperature. This should be expected since the wheat dust has about 1.5 times higher surface area than milo, as calculated from the nitrogen adsorption. However, the amounts of carbon monoxide and methane adsorbed by wheat are more than 1.5 times those by the milo sample. For example, the wheat dust adsorbs 3.15×10^{-6} kmole of carbon monoxide per kg. of sample at $5.33 \times 10^4 \text{ N/m}^2$ (400 mm.Hg) and at room temperature, compared

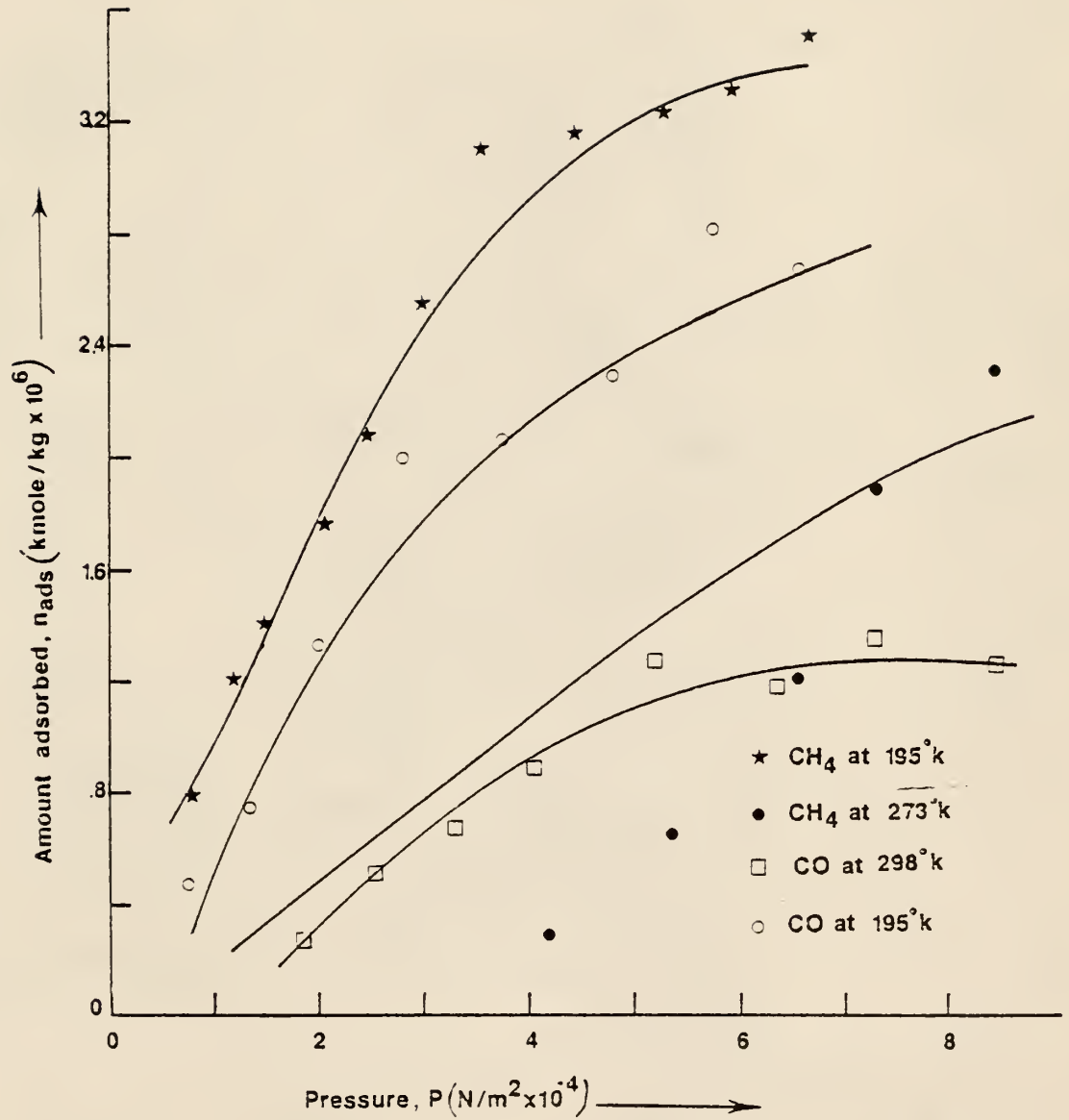


Fig. 4.1 Adsorption of Carbon Monoxide and Methane On #784-08 (Milo)

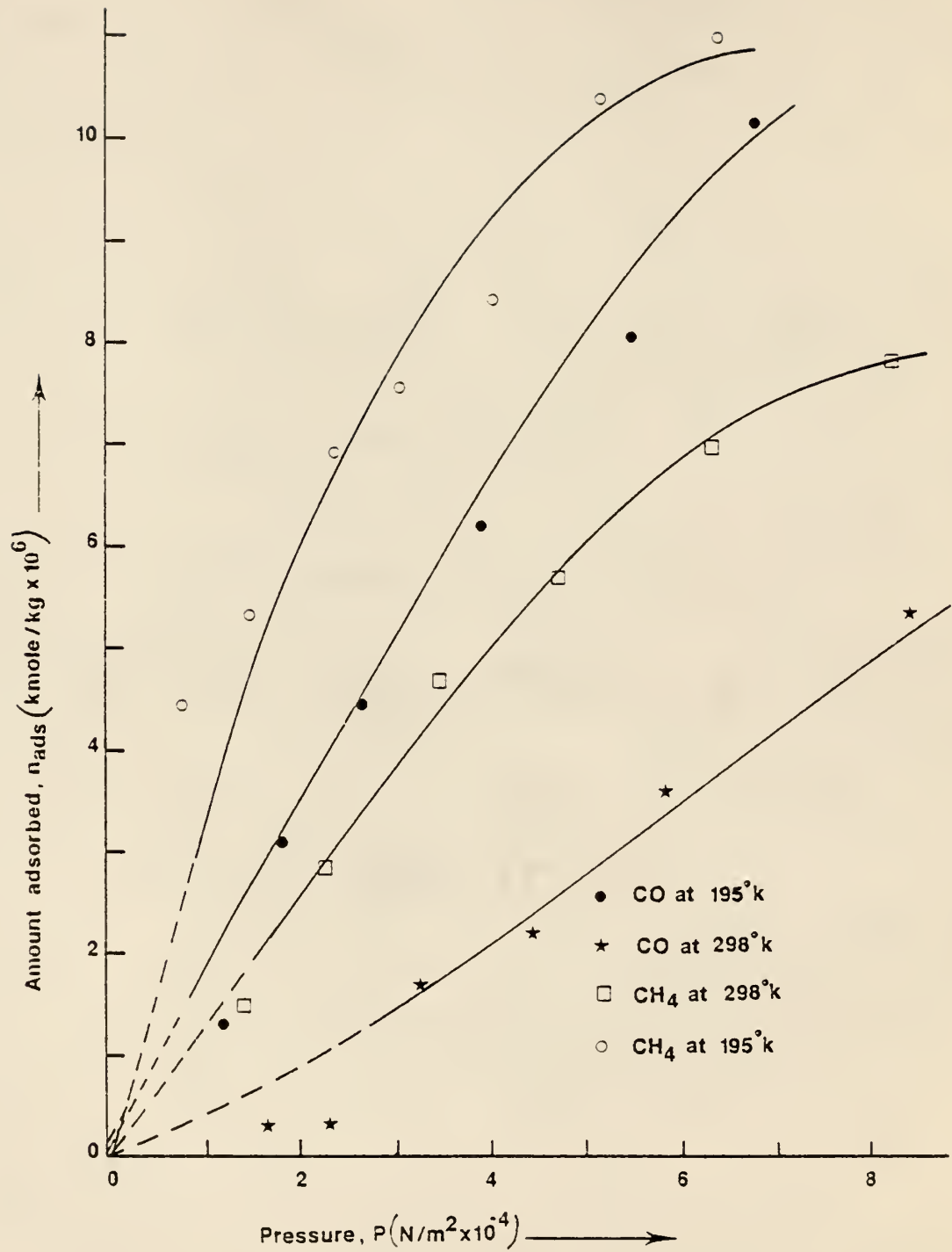


Fig. 4.2 Adsorption of Carbon Monoxide and Methane On #784-04 (Wheat)

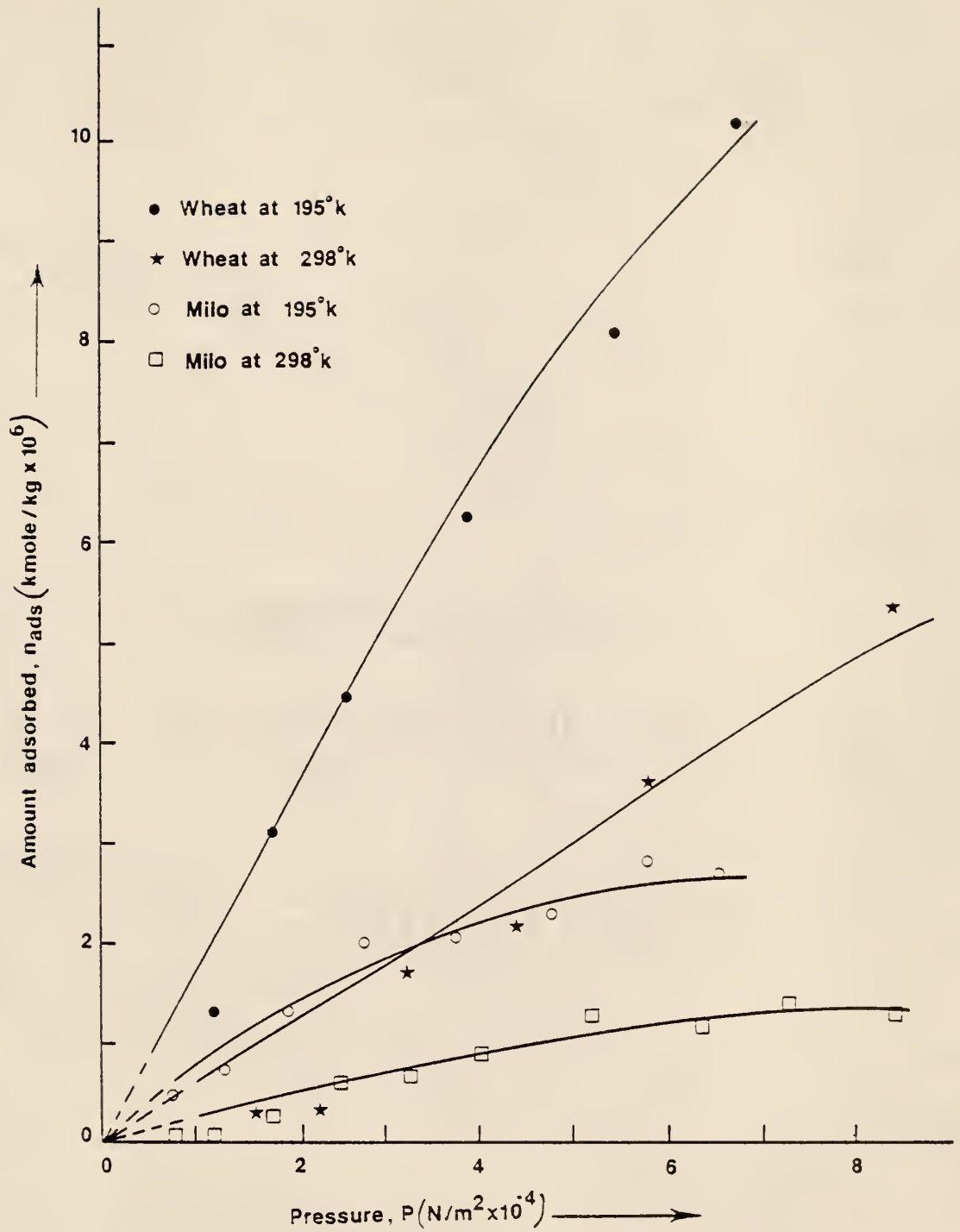


Fig. 4.3 Adsorption of Carbon Monoxide On #734-C4 (Wheat) and On #784-08 (Milo)

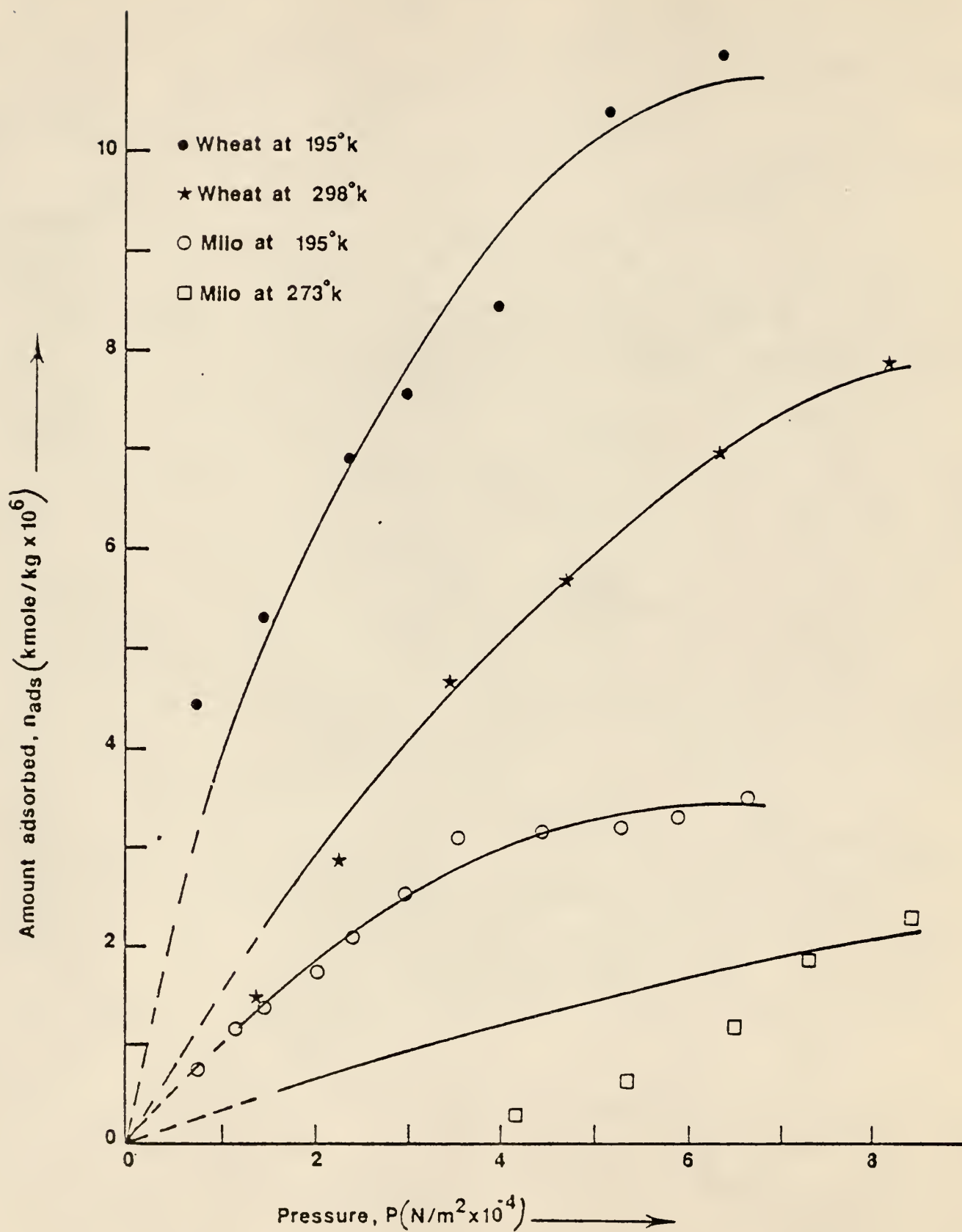


Fig. 4.4 Adsorption of Methane On #784-04 (Wheat) and On #784-08 (Milo)

to 1.1×10^{-6} kmole/kg. by milo. Also, 10.33×10^{-6} kmole/kg. of methane are adsorbed by wheat at 5.33×10^4 N/m² (400 mm.Hg) and at 195° K., compared to 3.375×10^{-6} kmole/kg. by milo.

To compare these values with the monolayer capacities, Table 4.1 gives the monolayer capacities of the samples for these gases. These monolayer capacities are based on the assumptions that the nitrogen adsorption measurements on the static BET apparatus give the correct values of specific surface area of the samples and that the values of area covered by a molecule of a gas in the adsorbed state, σ_m do not change with temperature. Under the second assumption, the values (19) of σ_m for methane and carbon monoxide at 90.2° K are, 0.172 and 0.168 nm²/molecule, respectively.

As can be seen, the amounts of carbon monoxide or methane adsorbed are less than the monolayer capacities of the samples. This was expected since the adsorption measurements are at temperatures above the critical temperature of these gases.

To compare the amounts of these gases adsorbed with their lower explosive limits ('LEL'), Table 4.2 gives the LEL and the amounts adsorbed by the wheat and milo samples for carbon monoxide and methane. The LEL have been compared with the values of volume per cent of these gases in the void space which have been calculated based on the assumptions that both the dust samples have an absolute density of 1600 kg./m³ and an apparent density of 800 kg./m³. Whereas the densities for these samples are not precisely these values, they are in the neighborhood and the precise LEL would be close to the tabulated values.

By comparing different values, it can be seen that at low partial pressures of either carbon monoxide or methane (as would be the case in stored grain), the amounts adsorbed do not give rise to explosive mixtures. However, at high pressures, adsorption on wheat gives rise to

Table 4.1
 Comparison of the Amounts Adsorbed and the Monolayer
 Capacities of the Dust Samples For Carbon Monoxide
 and Methane

| Sample | Specific Surface Area, S_s ($m^2/kg. \times 10^{-3}$) | Adsorbate Gas | Temperature ($^{\circ}K.$) | Monolayer Capacity, (n_{ads}) ($kmole/kg. \times 10^5$) | Pressure, P ($N/m^2 \times 10^{-4}$) | Amount Adsorbed, n_{ads} ($kmole/kg. \times 10^5$) |
|--------------------|--|--------------------|---------------------------------|---|--|---|
| #784-04 (Wheat) | 2.24 | Methane | 195 | 2.162 | 6.373 | 1.099 |
| | | | 298 | 2.162 | 8.190 | 0.787 |
| #784-08 (Milo) | 1.15 | Carbon Monoxide | 195 | 2.214 | 6.733 | 1.016 |
| | | | 298 | 2.214 | 8.397 | 0.537 |
| | | Methane | 195 | 1.110 | 6.493 | 0.379 |
| | | | 273 | 1.110 | 8.427 | 0.230 |
| Carbon Monoxide | 195 | 1.136 | 6.553 | 0.268 | | |
| | 298 | 1.136 | 8.433 | 0.126 | | |

Table 4.2
 Comparison of Lower Explosive Limits and the Amounts Adsorbed
 For Carbon Monoxide and Methane

| Sample | Gas | Temperature (°K) | Lower Explosive Limit (18), % in air | Pressure, P ($N/m^2 \times 10^{-4}$) | Amount adsorbed, n_{ads} | |
|--------------------|--------------------|---------------------|---|--|-----------------------------|---------------------------|
| | | | | | ($kmole/kg. \times 10^6$) | Volume % in void space |
| #784-04 (Wheat) | Methane | 298 | 5.6 | 1.427 4.660 | 1.459 | 5.71 |
| | | | | | 5.700 | 22.27 |
| #784-08 (Millo) | Carbon Monoxide | 298 | 12.5 | 1.663 5.810 | 0.320 | 1.25 |
| | | | | | 3.619 | 14.16 |
| | Methane | 273 | 5.6 | 4.180 5.343 7.297 | 0.297 | 1.16 |
| | | | | | 0.659 | 2.58 |
| Carbon Monoxide | 298 | 12.5 | 1.833 5.197 | 0.278 | 1.09 | |
| | | | | 1.274 | 4.99 | |

explosive mixtures of carbon monoxide or methane, but milo does not. Yet, as mentioned above, these high partial pressures are unlikely to exist in the grain dusts.

In order to compare the amounts of carbon monoxide and methane adsorbed on a particular sample at temperatures above their respective critical temperatures, relative pressures are calculated by using the idea of the reduced temperatures successfully utilized by Dubinin (14). The plots of the amount of gas adsorbed against $\frac{p}{p_{cr} (T/T_{cr})^2}$ are shown in Figures 4.5 and 4.6 for the wheat sample and the milo sample, respectively. While there is considerable scatter, particularly among the milo data, experimental points do suggest a single curve. This means that the same amounts of carbon monoxide and methane are adsorbed on a grain dust sample at a particular "apparent" relative pressure. If a sample offers the same surface area for both the gases to adsorb, this result would be expected.

It should be noted that the adsorption measurements with nitrogen or carbon dioxide made at a temperature below their critical temperatures do not merge into these curves. In fact, for the same value of $\frac{p}{p_{cr} \tau^2}$, the values of amounts of gas adsorbed per unit mass of the sample are about an order of magnitude higher for carbon dioxide and about 1.5 times higher for nitrogen than for carbon monoxide or methane. It seems, thus, that a "universal" adsorption isotherm is obtained for gases only above their critical temperatures.

It should be also noted that at room temperature, since the amounts of carbon monoxide and methane adsorbed were very small, the accuracy of the measurements was very low. For example, in the case of adsorption of methane on a milo sample (#784-08), although a large amount of sample was taken (13.965×10^{-3} kg.), even at the highest pressure reading of

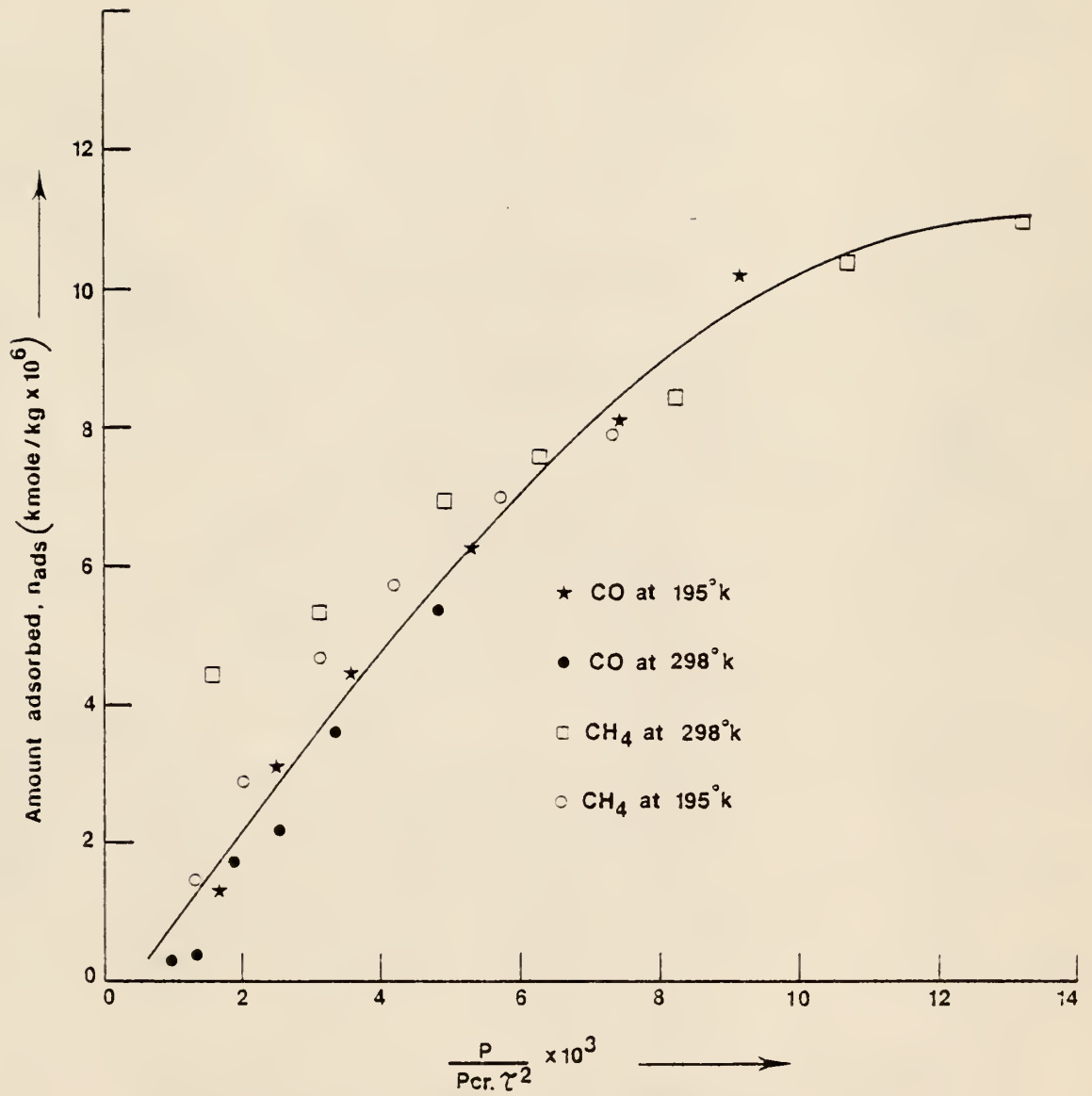


Fig. 4.5 Plot of Amount Adsorbed Vs. $\frac{p}{p_{cr} \tau^2}$ For #784-04 (Wheat)

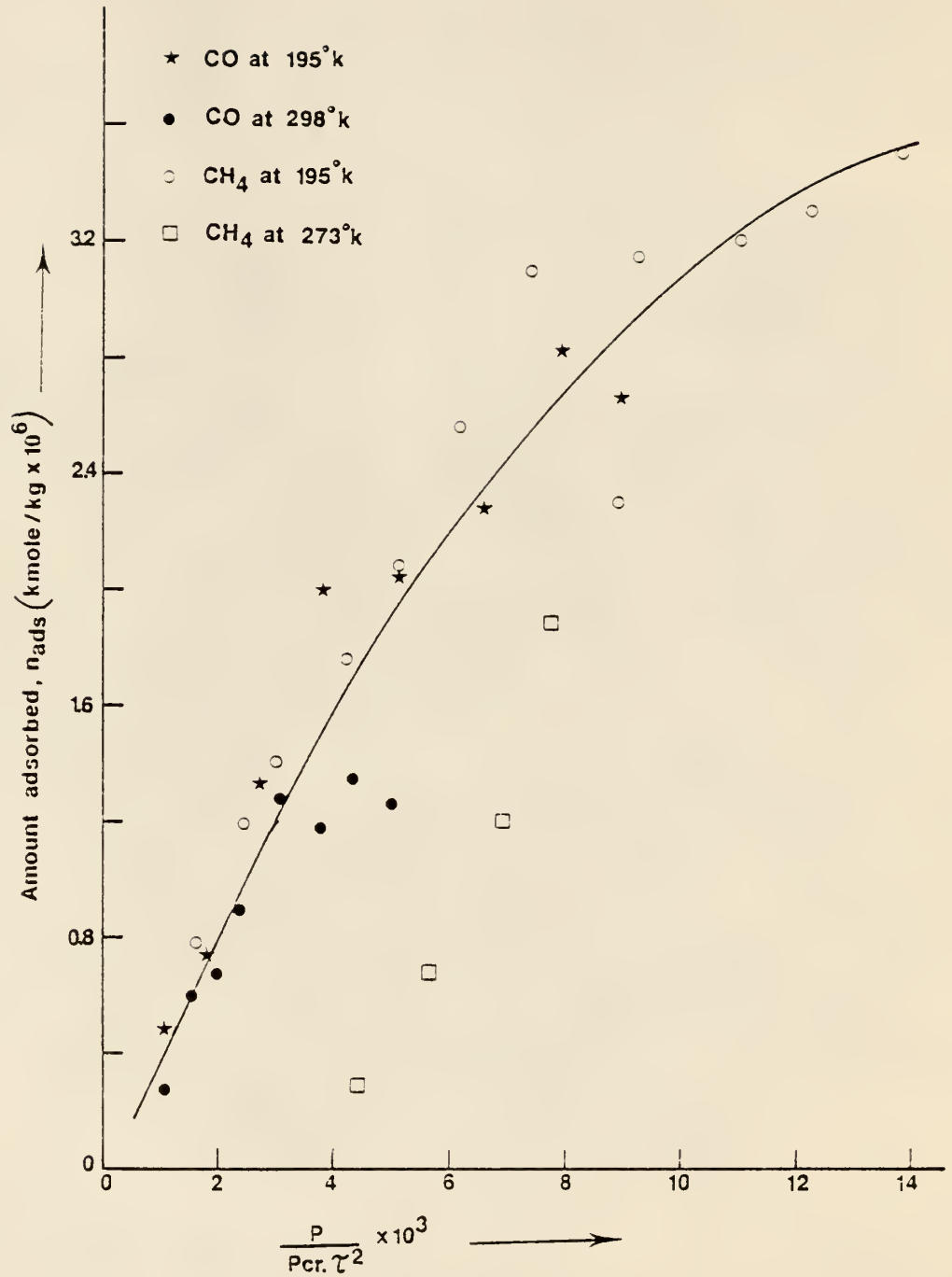


Fig. 4.6 Plot of Amount Adsorbed Vs. $\frac{p}{p_{cr} \tau^2}$ For #784-08 (Milo)

$8.43 \times 10^4 \text{ N/m}^2$ (632 mm.Hg), out of 1.368×10^{-6} kmole of methane taken in, 0.212×10^{-6} kmole of the gas was in the free space and the burette-bulbs, 1.124×10^{-6} in the dead space and only 0.032×10^{-6} kmole was adsorbed by the sample, which corresponds to only about 2.3% of the total amount of the gas taken in. The drop in accuracy in the measurements can also be observed from the scatter obtained in case of these measurements.

Chapter 5

Other Adsorption Isotherms

5.1 Introduction

In the previous chapters, it has been shown how to determine the specific surface areas of grain dust samples using the BET equation and the Dubinin-Polanyi equation. Whereas the experimental data obtained fitted these equations in their respective ranges of applications, it is of interest to see how they fit some of the other adsorption isotherm equations existing in the literature. It is with this intention that the data were tried with these equations and the monolayer capacities were calculated in each case and compared with those obtained from the BET and the Dubinin-Polanyi equations.

5.2 Various Adsorption Isotherms

There are many adsorption isotherms in the literature and several have been summarized by Young and Crowell, (2). Some of them are applicable to a particular kind of solid only and almost all of them are restricted to a limited relative pressure range. Among them, the BET equation has been accepted most widely and it, supposedly, gives the correct value of the surface area of a solid.

Langmuir's equation is based on the assumption that a solid surface adsorbs only a monolayer of adsorbate and is essentially a model of chemisorption rather than of physical adsorption. It assumes a dynamic equilibrium between the adsorbed phase and the gas phase. The BET theory has

expanded this idea from the Langmuir theory and assumes dynamic equilibrium between consecutive layers. The Langmuir equation may be written

$$v = \frac{v_m b p}{1 + b p} \quad (5.1)$$

where, v = Amount of the gas adsorbed at pressure p , m^3

v_m = Amount of the gas that is necessary to form a monolayer over the solid, m^3

p = Equilibrium pressure in the system, N/m^2

b = A constant, m^2/N

Rearranging, yields

$$\frac{p}{v} = \frac{p}{v_m} + \frac{1}{b v_m} \quad (5.2)$$

If p/v is plotted against p , a straight line of slope $1/v_m$ and intercept on the ordinate equal to $1/bv_m$ should be obtained.

Since the Langmuir equation assumes only a monolayer, this equation would be valid for isotherms of type I only. However, one may also apply it in the low relative pressure region of types II and IV isotherms, when the monolayer is yet to be completed.

In 1948 a modification to the BET theory was suggested by Huttig (2). The difference between the two theories is in their mechanisms. Huttig assumes that evaporation from the i th layer is unaffected by the presence of the $(i+1)$ th layer, whereas the BET contention is that $(i+1)$ th layer molecules are completely effective in preventing evaporation of underlying molecules.

The Huttig equation may be written,

$$\frac{v}{v_m} = \frac{cp/p_o}{1 + cp/p_o} (1 + p/p_o) \quad (5.3)$$

where, the nomenclature is same as that in the BET equation,

which may also be written as

$$\frac{p}{p_0 v} \left(1 + \frac{p}{p_0} \right) = \frac{1}{c v_m} + \frac{p}{v_m p_0} \quad (5.4)$$

A plot of $\frac{p}{p_0 v} \left(1 + \frac{p}{p_0} \right)$ against $\frac{p}{p_0}$ should, therefore, yield a straight line

with slope $1/v_m$ and intercept on the ordinate equal to $\frac{1}{c v_m}$.

It may be noted that the amount adsorbed at $p = p_0$ is not infinite in this case, as in the BET equation, but equal to $2c/(1+c)$ layers. Also, this equation may be regarded as a Langmuir equation multiplied by a factor $(1+p/p_0)$ which takes into account the adsorption in the second and higher layers. For the majority of gas-solid systems the monolayer capacity values, v_m , calculated from the Huttig equation exceed the BET values by 2-20 per cent, depending on the value of the constant c (2).

Lopez-Gonzalez and Deitz (2), noting the fact that the BET equation predicts too high and the Huttig equation too low an amount adsorbed above $p/p_0 = 0.30$, have compromised by adding the equations with the result

$$\frac{p}{2v p_0} \left(\frac{p}{p_0 - p} + \frac{p_0 + p}{p_0} \right) = \frac{1}{c v_m} + \left(\frac{c-2}{c v_m} \right) \frac{p}{p_0} \quad (5.5)$$

where, the nomenclature is the same as that in the BET and the Huttig equation.

Thus a plot of $\frac{p}{2v p_0} \left(\frac{p}{p_0 - p} + \frac{p_0 + p}{p_0} \right)$ against p/p_0 is a straight line with slope $\frac{1}{c v_m}$ and an intercept on the ordinate equal to $\frac{1}{c v_m}$.

This equation has been found to fit the nitrogen isotherms on various samples of bentonite up to the relative pressure of 0.8 (2). The v_m values

calculated from the slopes and the intercepts lay midway between the BET and the Huttig values.

Apart from these isotherms, all of which have been basically derived from the Langmuir equation, there are several more in the literature. Most of them are empirical in nature.

The Freundlich isotherm is purely empirical. It may be written

$$v = B p^{1/n} \quad (5.6)$$

where, B and n are constants.

The monolayer capacity of the adsorbent cannot be determined from the Freundlich isotherm.

There is another called the Harkins-Jura Relative method. The Harkins-Jura equation (hereinafter referred to as the HJ equation) is also basically empirical in nature and may be written

$$\ln p/p_0 = B - A/v^2 \quad (5.7)$$

where, A and B are constants.

A plot of $\ln p/p_0$ against $1/v^2$ should yield a straight line, with slope (-A). The specific surface of an adsorbent is related to the constant A by the relation

$$S_s = kA^{\frac{1}{2}} \quad (5.8)$$

where, S_s = Specific surface area of the adsorbent, m^2/kg .

k = A constant.

The constant k must be determined by calibration, using an independent surface area measurement. It is assumed that k is a function only of the temperature and of the nature of the adsorbate and is independent of the nature of the solid surface. Besides the need for predetermination of the constant k, the limitation in this method is that in the relative

pressure region of the validity of the BET equation ($p/p_0 = 0.05-0.30$), a linear HJ plot is obtained only when the constant c in the BET equation is between 50 and 250. For values of c below 10, as is the case for most of the grain dust samples, the linear portion exists only beyond $p/p_0 = 0.4$.

5.3 Application of the Adsorption Isotherm Equations To the Adsorption Data

The data of the adsorption of nitrogen at liquid nitrogen temperature and that of carbon dioxide at 195° K. on wheat, milo and soybean dust samples as also the adsorption of krypton at liquid nitrogen temperature on wheat were tested using the various adsorption isotherm equations. Some of the plots obtained from the experimental data are shown in Figures 5.1 - 5.6. The values of the BET parameter c and the values of monolayer capacity v_m as calculated from these isotherms are given in Tables 5.1, 5.2 and 5.3 for the nitrogen data, the carbon dioxide data, and the krypton data, respectively.

As mentioned earlier, the HJ equation requires precalibration and also it applies only beyond $p/p_0 = 0.4$ for the values of the BET constant c obtained for grain dust. Although only the BET range of the relative pressure was covered in most of the adsorption measurements, for the two sets of data used later for the pore size distribution measurements (Appendix J), the entire range of the relative pressure was covered and so the precalibration can be carried out with them. From these data of adsorption of nitrogen on an alumina and a wheat sample, the HJ plots of $\ln p/p_0$ Vs. $1/v^2$ were made beyond $p/p_0 = 0.4$. Reasonably good straight lines were obtained for both of these sets of data (For example, see Fig. 5.1). The values

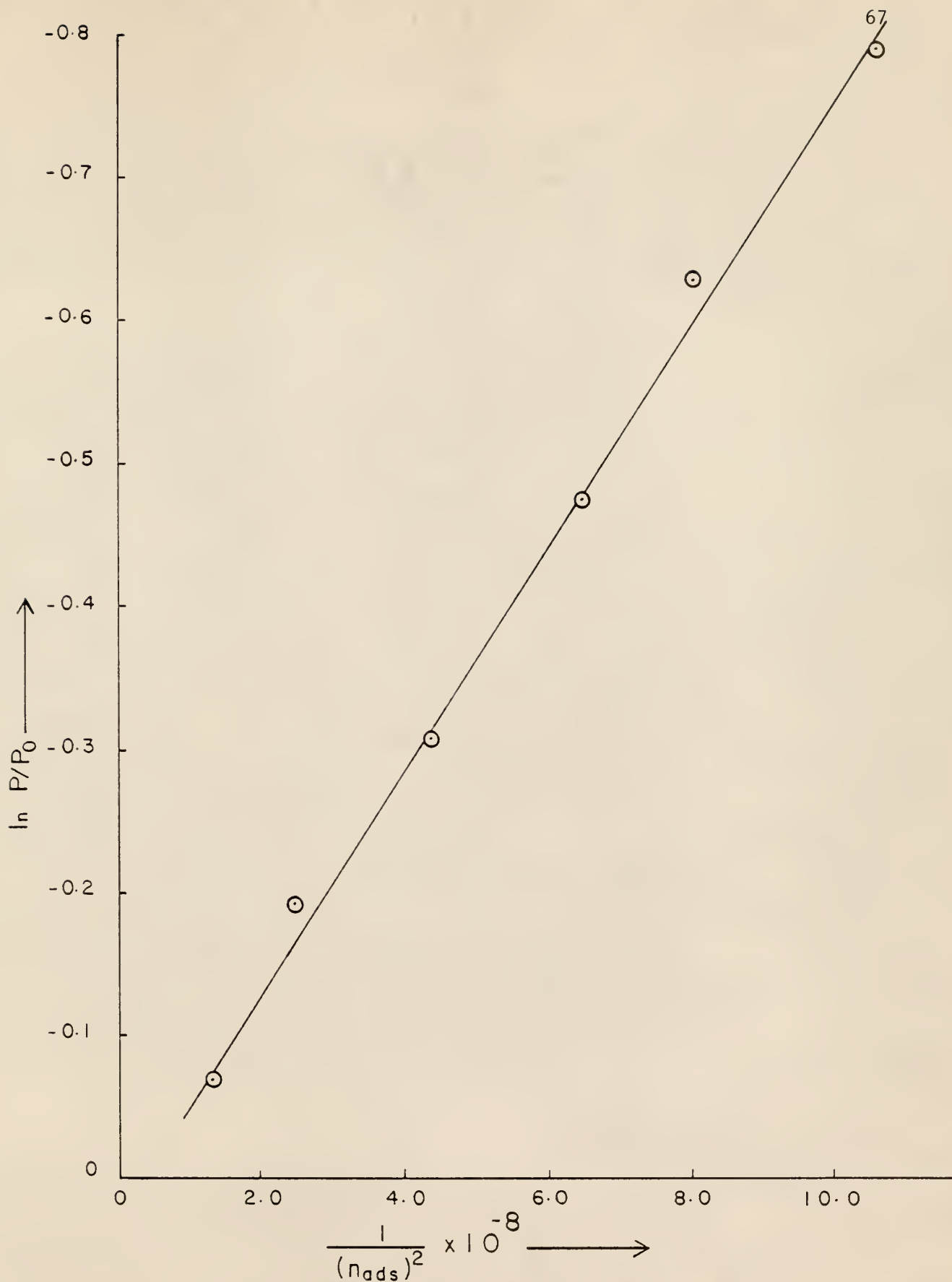


Fig. 5.1 The Harkins-Jura Relative Method for Adsorption of Nitrogen
On #784-04 (Wheat) At Liquid Nitrogen Temperature

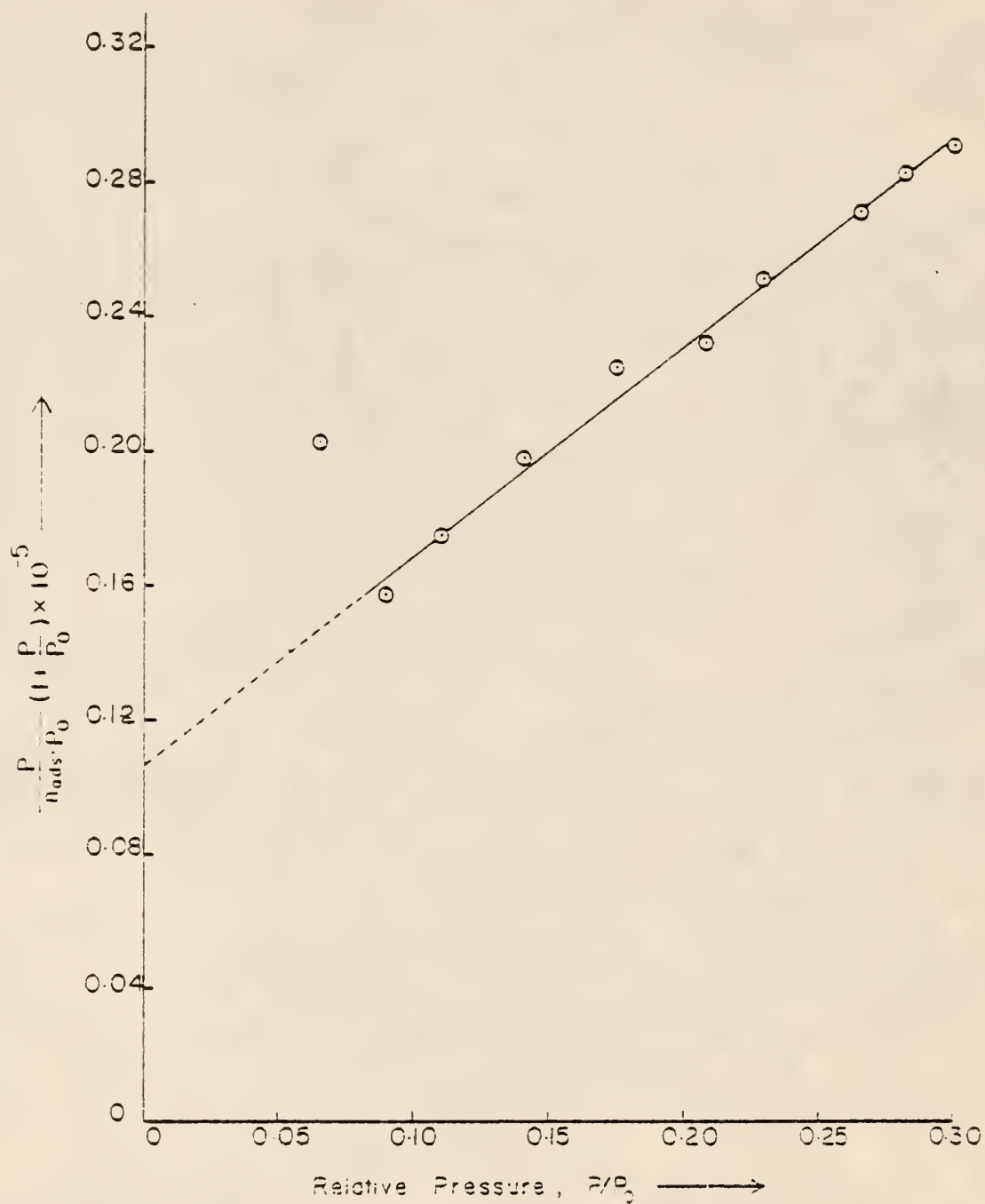


Fig. 5.2 The Huttig Plot For Adsorption of Nitrogen On #784-08 (Milo) At Liquid Nitrogen Temperature

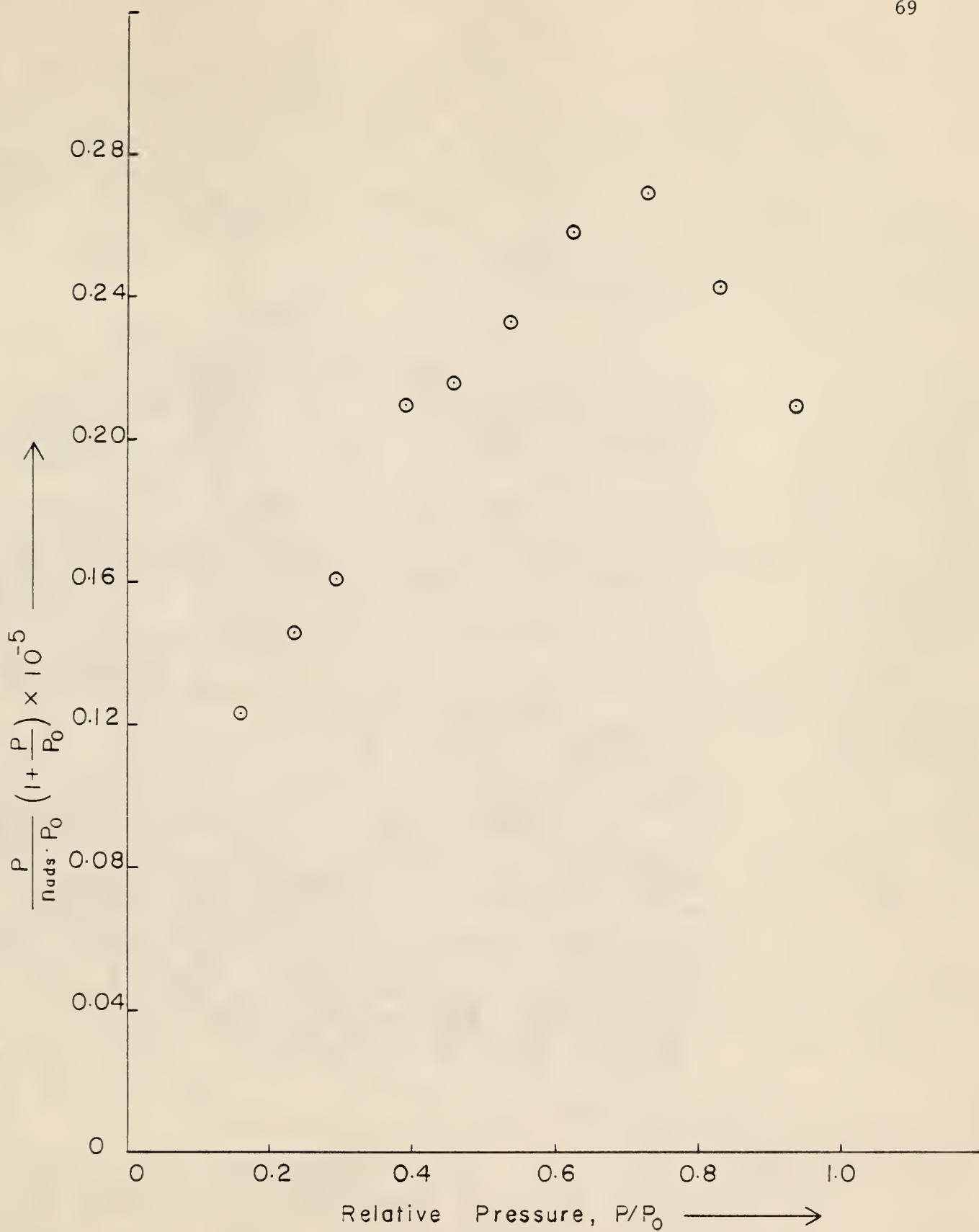


Fig. 5.3 The Huttig Plot For Adsorption of Nitrogen On #784-04 (Wheat) At Liquid Nitrogen Temperature

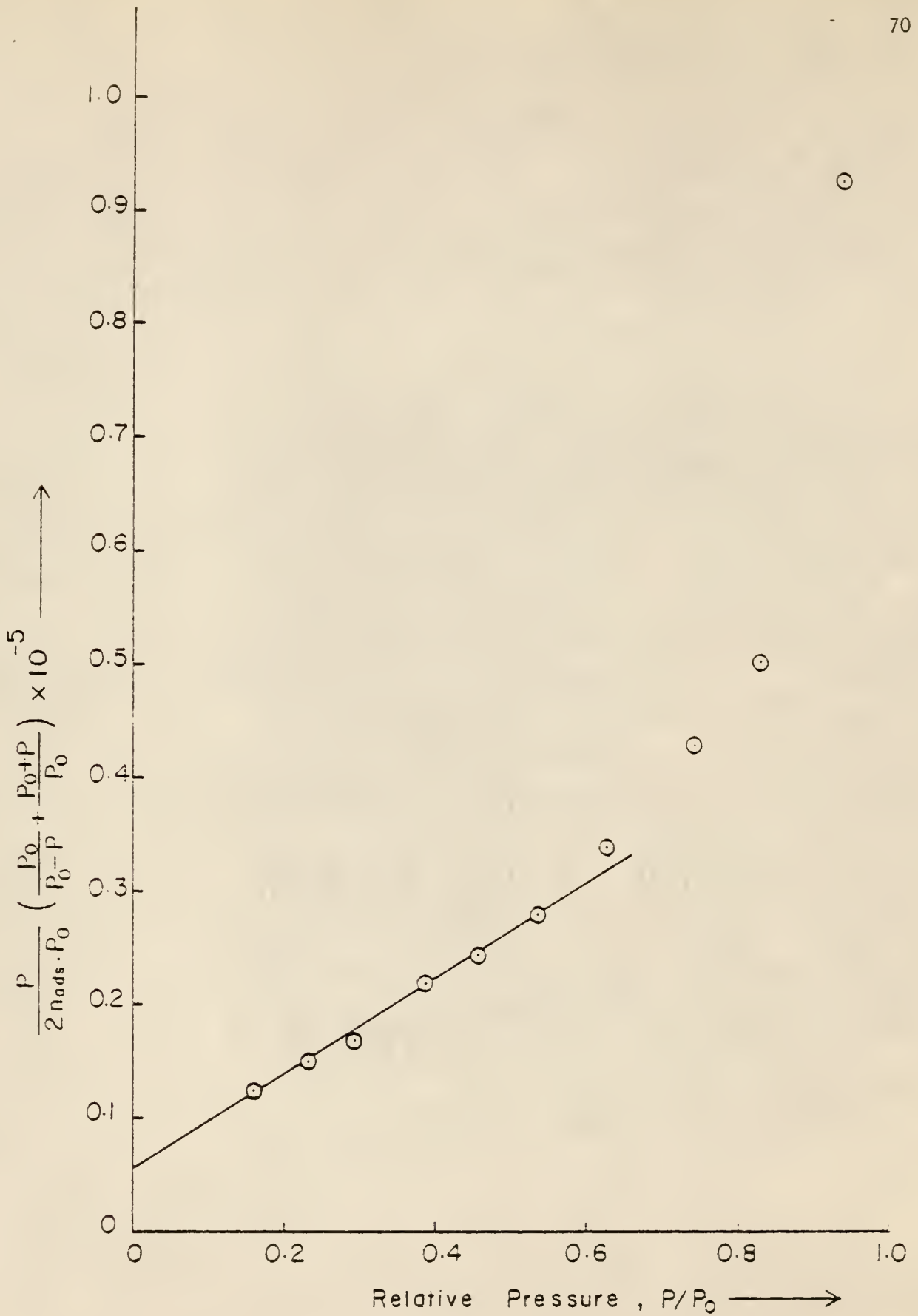


Fig. 5.4 The Lopez-Gonzalez and Deitz Plot For Adsorption of Nitrogen On #784-04 (Wheat) At Liquid Nitrogen Temperature

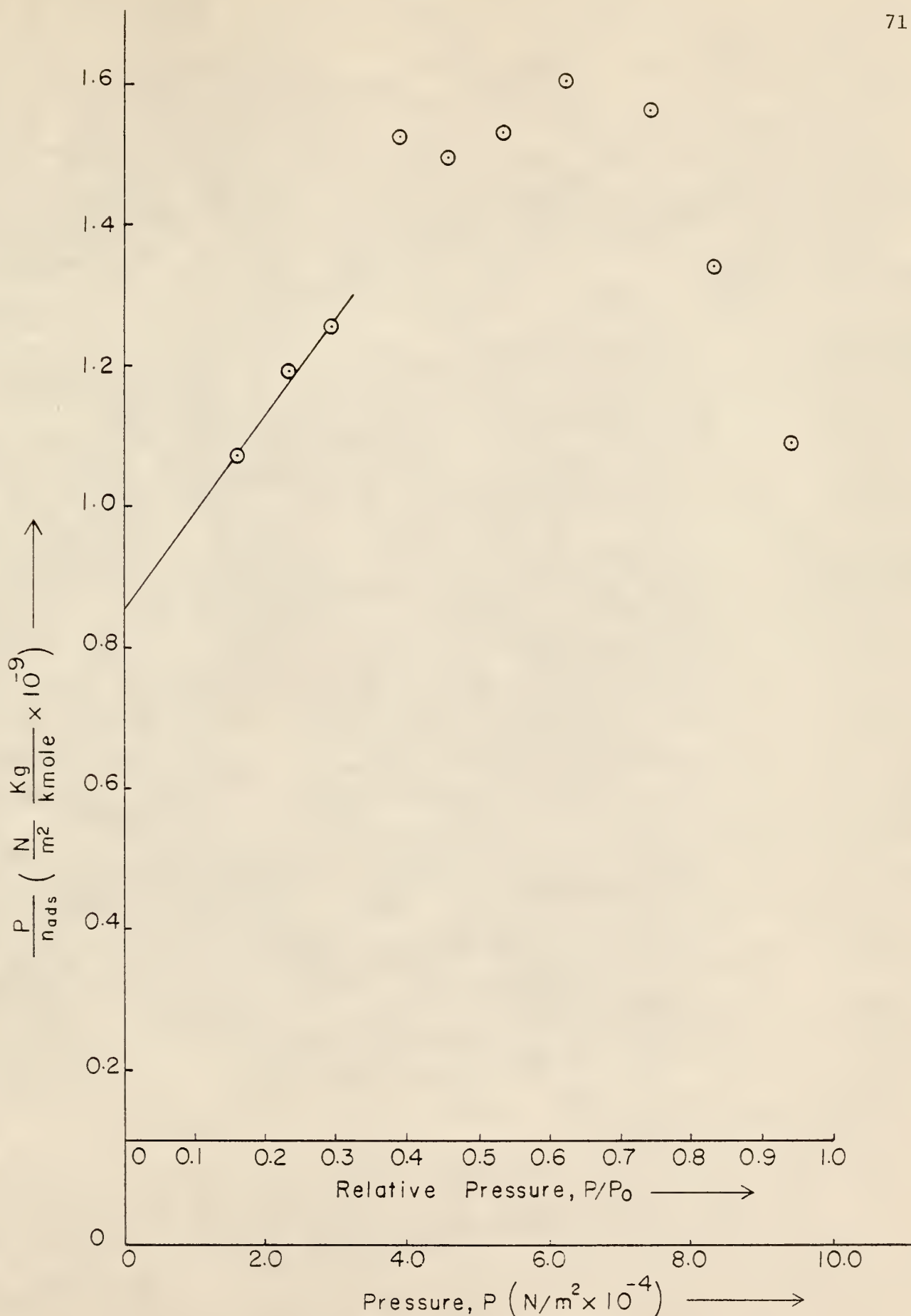


Fig. 5.5 The Langmuir Plot For Adsorption of Nitrogen On #784-04 (Wheat) At Liquid Nitrogen Temperature

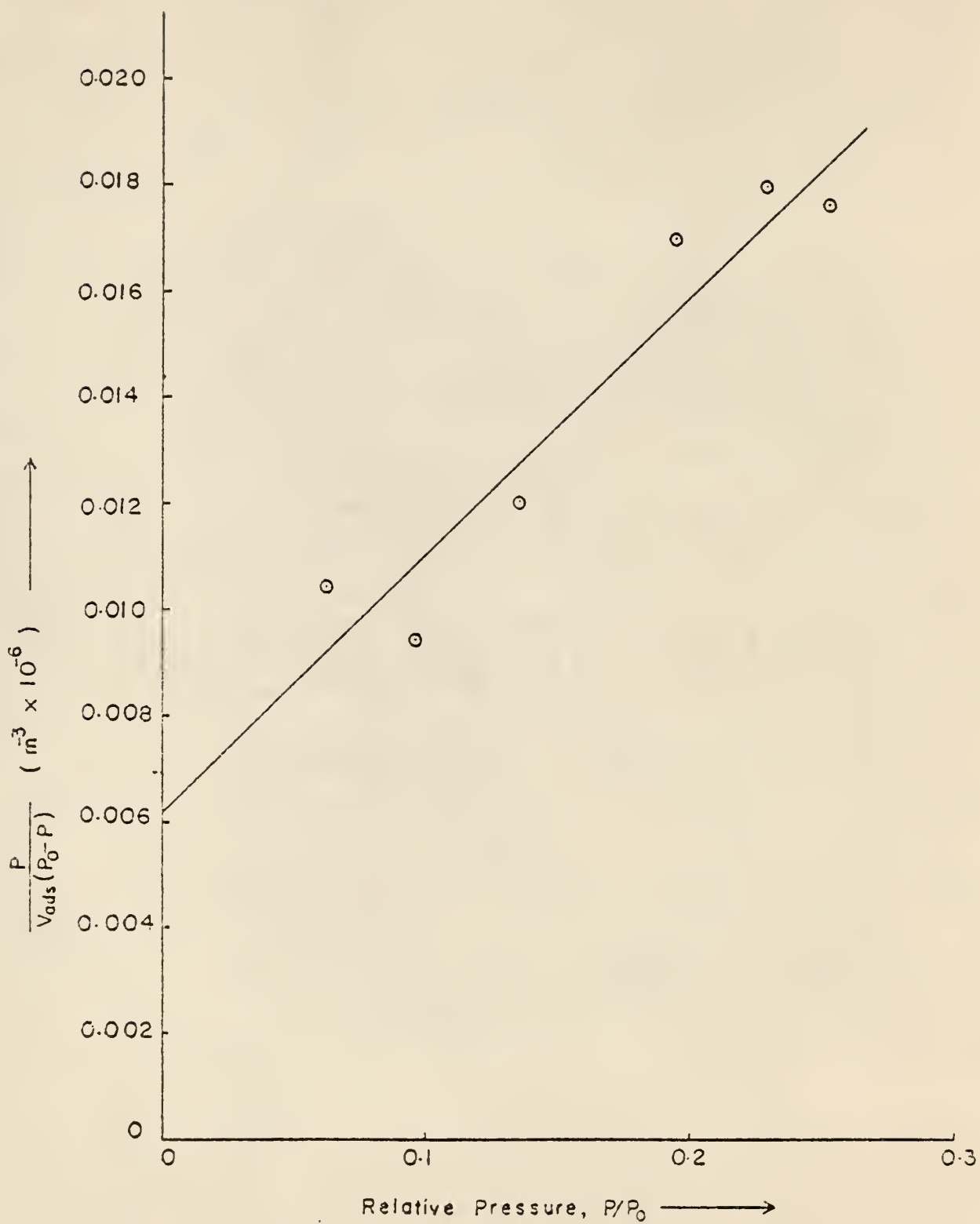


Fig. 5.6 The BET Plot For Adsorption of Carbon Monoxide On #784-08 (Milo) At 195^o K

Table 5.1
Nitrogen Adsorption Data Using Various Adsorption Isotherms

| Isotherm | Wheat (#784-04) | | Milo (#784-08) | | Soybean (#785-04) | |
|--------------------------|-----------------------|---|-----------------------|---|-----------------------|---|
| | The BET Constant, c | Monolayer Capacity, v_m ($m^3/kg. \times 10^3$) | The BET Constant, c | Monolayer Capacity, v_m ($m^3/kg. \times 10^3$) | The BET Constant, c | Monolayer Capacity, v_m ($m^3/kg. \times 10^3$) |
| BET, by Sorptometer | 7.717 | 0.426 | 4.757 | 0.279 | 28.059 | 0.238 |
| BET, by Static Apparatus | 6.544 | 0.511 | 9.383 | 0.263 | 17.458 | 0.261 |
| Huttig | 3.614 | 0.792 | 9.186 | 0.282 | 13.734 | 0.300 |
| Lopez-Gonzalez & Deitz | 10.895 | 0.469 | 10.402 | 0.257 | 16.159 | 0.275 |
| Langmuir | - | 1.635 | - | 0.406 | - | 0.435 |

Table 5.2
Carbon Dioxide Adsorption Data At 195°K. Using Various Adsorption Isotherms

| Isotherm | Wheat (#784-04) | | Milo (#784-08) | | Soybean (#785-04) | |
|--------------------------|-----------------------|---|-----------------------|---|-----------------------|---|
| | The BET Constant, c | Monolayer Capacity, v_m ($m^3/kg. \times 10^3$) | The BET Constant, c | Monolayer Capacity, v_m ($m^3/kg. \times 10^3$) | The BET Constant, c | Monolayer Capacity, v_m ($m^3/kg. \times 10^3$) |
| BET, by Static Apparatus | 124.15 | 2.3584 | 8.95 | 1.301 | 10.25 | 1.721 |
| Huttig | 51.33 | 2.640 | 6.54 | 1.657 | 6.37 | 2.332 |
| Lopez-Gonzalez & Deitz | 74.82 | 2.484 | 7.74 | 1.450 | 7.72 | 2.016 |
| Langmuir | - | 3.676 | - | 2.710 | - | 3.926 |

Table 5.3

Krypton Adsorption Data On #784-04 (Wheat)
Using Various Adsorption Isotherms

| Isotherm | The BET Constant, c | Monolayer Capacity, v_m ($m^3/kg. \times 10^3$) |
|---------------------------|---------------------------|---|
| BET | 6.422 | 0.263 |
| Huttig | 3.840 | 0.191 |
| Lopez-Gonzalez & Deitz | 5.302 | 0.308 |
| Langmuir | - | 0.715 |

of the slopes, A , obtained were used in Eq. (5.8) to determine the values of the calibration constant k . The respective values of k obtained are 1249.4 and 0.1796 m^{-1} .

5.4 Discussion

As can be seen from Tables 5.1, 5.2 and 5.3, the data tested for validity of the above stated adsorption isotherms are nitrogen adsorption at liquid nitrogen temperature, carbon dioxide adsorption at 195° K . and krypton adsorption at liquid nitrogen temperature. The data obtained from adsorption of carbon dioxide at room temperature and that from adsorption of carbon monoxide and methane have not been tested for validity of the above stated adsorption isotherm equations because, the carbon dioxide data are at too low a relative pressure and the carbon monoxide and the methane data are above their critical temperatures. Under these conditions, the Huttig equation and the Lopez-Gonzalez and Deitz equation (hereinafter referred to as the LG&D equation) would not apply. Also, a horizontal Langmuir isotherm would be obtained which would correspond to infinite monolayer capacity, since at an extremely low relative pressure, the amount adsorbed is directly proportional to pressure.

Among the data considered, most give straight line plots for the Huttig and the LG&D equations, indicating good agreement between the data and the equations. The data of nitrogen adsorption on the soybean dust sample (#785-04), that on the milo dust sample (#784-08) and the krypton adsorption on wheat (#784-04), however, contain (apparently) one bad point each. Excluding this point, straight line fits are obtained for the Huttig, LG&D, BET and Langmuir isotherms (For example, see Fig. 5.2). This "bad point" occurs at low relative pressure where accuracy is low because of the small amounts adsorbed.

Straight line fits have been obtained probably because the measurements were restricted to the BET range of relative pressure in most cases. In the data of nitrogen adsorption on wheat, which were used in the pore size distribution measurements, one can see that the Huttig and the LG&D equations are obeyed by the data only upto the relative pressures of about 0.30 and 0.65, respectively, after which the points deviate from the straight line (Figures 5.3 and 5.4). It seems, thus, that the Huttig and the LG&D equations are valid upto these relative pressures only. This is probably because beyond $p/p_0 = 0.30$, the BET equation predicts higher amounts adsorbed than is experimentally observed, and the Huttig equation predicts lower amounts, due to the difference in the assumptions made in their derivation. The LG&D equation being the addition of the two, cancels these discrepancies until a higher p/p_0 . This finding is in agreement with that found with bentonite samples as cited in Section 5.2. As can be seen from Tables 5.1, 5.2 and 5.3, the values of the monolayer capacity v_m were consistent for any particular sample as calculated from the BET, the Huttig and the LG&D equations. The values of the BET constant c were not as consistent, although they were all of same order of magnitude, for a particular sample. This has been observed by other workers also (17).

The data seemed to obey the Langmuir isotherm equation at low relative pressures, although not at higher relative pressure values (For example, see Fig. 5.5). This was expected since the Langmuir model assumes monolayer adsorption only. The values of the monolayer capacity v_m calculated from the Langmuir equation were found to be always higher than those found using other equations. Again this was expected since in applying the Langmuir equation to a set of data, one makes an assumption that the

adsorption isotherms are of type I and so the entire amount adsorbed is assumed to be used in the formation of a monolayer.

ACKNOWLEDGMENTS

The author wishes to express his deep sense of gratitude to Dr. John C. Matthews for his invaluable guidance and constant encouragement throughout this work. Thanks are due to Dr. B.G. Kyle and Dr. F.S. Lai for serving on the advisory committee. The author also extends his gratitude to the U.S. Grain Marketing & Research Laboratory, Manhattan for financial support of the entire project. Thanks are also due to Mr. Mitsugi Ohno for constructing and assembling the glass apparatus and to Mr. Duane Morey, who was very helpful in equipment construction and modification.

REFERENCES

1. Gregg, S.J., "The Surface Chemistry of Solids", Second Edition, Reinhold Publishing Corporation, N.Y. (1961).
2. Young, D.M. and Crowell, A.D., "Physical Adsorption of Gases", First Edition, Butterworth & Co. (Publishers) Limited, London (1962).
3. Handa, P.K., "The Redispersion of the Supported Metal Catalysts", M.S. Thesis, Kansas State University (1978).
4. Chiotti, P. and Morris, V., "Low Temperature Pyrolysis of Grain Dust", 'Cereal Foods World', 23 (6), 314-322 (1978).
5. Instructions - The Perkin Elmer Shell Model 212-D Sorptometer.
6. Model 212-D Sorptometer: Determination of Pore Volume and Pore Size Distribution.
7. Anderson, R.B., Hall, W.K., Lecky, J.A. and Stein, K.C., "Sorpton Studies on American Coals", J1. of Phys. Chem., 60, 1548-1558 (1956).
8. Kipling, J.J., Sherwood, J.N., Shooter, P.V., and Thompson, N.R., "The Pore Structure and Surface Area of High-Temperature Polymer Carbons", 'Carbon', 1, 321-328, (1964).
9. Walker, P.L., Jr. and Patel, R.L., "Surface Areas of Coals From Carbon Dioxide Adsorption At 298°K.", 'Fuel', 49, 91-94 (1970).
10. Perry, R.H. and Chilton, C.H., "Chemical Engineers' Handbook", Fifth Edition, McGraw-Hill Book Company.
11. Emmett, P.H., "Catalysis", Vol. II, Reinhold Publishing Corporation (1954).
12. Smith, J.M., "Chemical Engineering Kinetics", Second Edition, McGraw-Hill Book Company.
13. DeBoer, J.H., "The Structure and Properties of Porous Materials", (D.H. Everett and F.S. Stone, eds.), Butterworth, Colston Papers, Vol. 10, London (1958).
14. Dubinin, M.M., "Theory of Bulk Saturation of Microporous Activated Charcoals During Adsorption of Gases and Vapors", 'Russian J1. of Physical Chemistry', 39, 697-704 (1965).
15. Weast, R.C., "Handbook of Chemistry and Physics", 56th Edition, CRC Press Inc. (1976).
16. Marsh, H. and Siemieniowska, T., "The Surface Areas of Coals As Evaluated From the Adsorption Isotherms of Carbon Dioxide Using the Dubinin-Polanyi Equation", 'Fuel', 44, 355-367 (1965).

17. Ross, S., "On Physical Adsorption IV. A Comparison of Two Theories of Multilayer Adsorption", 'Jl. of Physical and Colloid Chemistry', 53, 383-391 (1949).
18. Thorpe, Edward, "A Dictionary of Applied Chemistry", Vol. II, Longmans, Green and Co. Ltd., London (1927).
19. Faeth, P.A., "Adsorption and Vacuum Technique", Institute of Science and Technology, The University of Michigan, Ann Arbor, Mich., Oct. 1962.

Appendix A

Sample Calculation for determination of specific surface area using the sorptometer.

SAMPLE: 784-04 (Wheat)

Pretreatment: 1 week in oven at 110°C

| SYMBOL | MEASUREMENT OR CALCULATION | DIMENSION | RESULT |
|-----------------------|---|----------------------------|---|
| w_2 w_1 w | Weight of Sample | tube + tube: sample: | sample: 11.28732×10^{-3} kg 11.90203×10^{-3} kg 0.61471×10^{-3} kg |
| P_T | Barometric Pressure at $T^\circ\text{K}$ Temperature | N/m^2 | 96349.7 |
| T_R | Room temperature | $^\circ\text{K}$ | 298.72 |
| f | Correction factor for STP conditions: $\bar{f} = \frac{P_T \cdot 273}{760 \cdot T_R} = 0.3595 \frac{P_T}{T_R}$ | | 0.8697 |
| | Inlet pressure of carrier gas (Helium) | in. | 25 |
| t_c | Soap film transit time | sec. | 43.75 |
| v_{meter} | Volume of bubble flow meter between two calibration marks (3) | m^3 | 20.0699×10^{-6} |
| F_c | Flow rate of the carrier gas (helium): $F_c = \frac{v_{\text{meter}}}{t_c}$ | $\text{m}^3/\text{sec.}$ | 0.45874×10^{-6} |

| SYMBOL | MEASUREMENT OR CALCULATION | DIMENSION | | | | RESULT | |
|-----------|--|--------------------------|-----------|--------------------------|-----------|-------------------------------------|---------|
| P_0 | Saturation pressure of N_2 at the temperature of the liquid N_2 used | N/m^2 | average | <input type="checkbox"/> | measured | <input checked="" type="checkbox"/> | 98865.7 |
| s_0 | Area covered by one m^3 (STP) monolayer nitrogen (5) | $m^2/m^3 \times 10^{-6}$ | | | | | 4.3688 |
| SYMBOL | Measurement or Calculation | DIMENSION | FIRST RUN | SECOND RUN | THIRD RUN | | |
| | Inlet pressure of the adsorption gas (N_2) | in. | 13 | 19.5 | 29.5 | | |
| t_c | Soap film transit time for total gas flow | sec. | 37.25 | 34.95 | 32.25 | | |
| F_c | Total ($He + N_2$) flow rate: $F_c = \frac{V_{meter}}{t_c}$ | $m^3/sec. \times 10^6$ | 0.53879 | 0.57425 | 0.62232 | | |
| F_a | Adsorption gas (N_2) flow rate $F_a = F_c - F_c$ | $m^3/sec \times 10^6$ | 0.08005 | 0.11551 | 0.16358 | | |
| A_{des} | Area of the desorption peak | counts | 182.5 | 202 | 236.5 | | |
| V_{cal} | Volume of the injection tube used | $m^3 \times 10^6$ | 0.1395 | 0.1395 | 0.1395 | | |
| A_{cal} | Area of the calibration peak | counts | 173 | 158 | 152 | | |

| SYMBOL | MEASUREMENT OR CALCULATION | DIMENSION | FIRST RUN | SECOND RUN | THIRD RUN |
|-----------|---|-------------------------|-----------|------------|-----------|
| V_{ads} | Volume of adsorbed gas $V_{ads} = \frac{A_{des}}{A_{cal}} \frac{V_{cal}}{V_{cal}}$ | $m^3 \times 10^6$ | 0.19991 | 0.24227 | 0.29485 |
| V_{ads} | Volume of adsorbed gas corrected to standard temperature pressure: $V_{ads} = V_{ads}^f$ | $m^3 \times 10^6$ | 0.17385 | 0.21070 | 0.25642 |
| P | Partial pressure of nitrogen $P = \frac{F_a}{F_t} P_T$ | N/m^2 | 14314.5 | 19379.8 | 25326.4 |
| P/P_0 | Relative pressure of nitrogen (X) | | 0.145 | 0.196 | 0.256 |
| | $(P_0 - P)$ | N/m^2 | 84551.2 | 79485.9 | 73539.3 |
| | $V_{ads} (P_0 - P)$ | $N \cdot m$ | 0.01470 | 0.01675 | 0.01886 |
| | $\frac{P}{V_{ads} (P_0 - P)}$ (Y) | $m^{-3} \times 10^{-6}$ | 0.974 | 1.157 | 1.343 |

A graph of $\frac{P}{V_{ads} (P_0 - P)}$ vs: P/P_0 is plotted (Fig. A-1)

THREE-POINT CALCULATION

| SYMBOL | MEASUREMENT OR CALCULATION | DIMENSION | RESULT |
|--------|-----------------------------|-------------------------|--------|
| 1 | The slope of the BET plot | $m^{-3} \times 10^{-6}$ | 3.325 |
| 3 | y-intercept of the BET plot | $m^{-3} \times 10^{-6}$ | 0.495 |

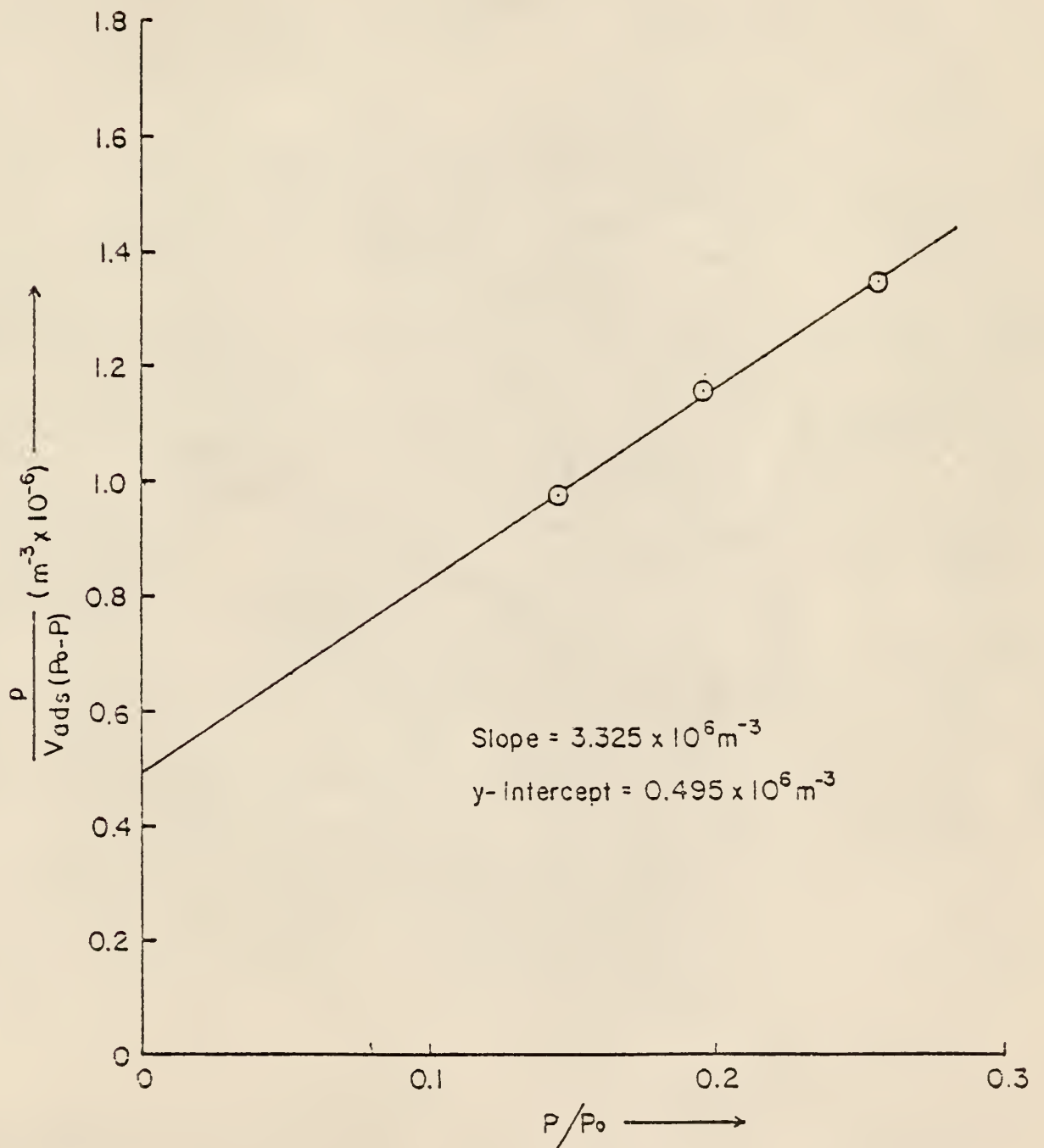


Fig. A-1 The BET Plot

| SYMBOL | MEASUREMENT OR CALCULATION | DIMENSION | RESULT |
|--------|---|-------------------------|--------|
| V_m | Volume of adsorbed nitrogen for a monolayer: $V_m = \frac{1}{\alpha + \beta}$ | $m^3 \times 10^6$ | 0.262 |
| S | $V_m^s o$ | m^2 | 1.144 |
| S_s | Specific surface area of the sample $S_s = \frac{V_m^s o}{w}$ | $m^2/kg \times 10^{-3}$ | 1.86 |

Appendix B

Particle Size Distributions of the Grain Dust Samples*

| Sample # | 784-04 | 784-06 | 784-08 | 785-04 | 786-01 | 786-02 | 786-12 | 786-23 | 786-28 | 786-30 | 786-43 | 774-07 |
|------------------------------|--------|--------|--------|---------|--------|--------|---------|--------|--------|---------|--------|--------|
| Type | Wheat | Corn | Milo | Soybean | Wheat | Milo | Soybean | Wheat | Milo | Soybean | Corn | Corn |
| Diameter, d (μ m) | | | | | | | | | | | | |
| 710 | | | | | | | 76.6 | | 86.9 | 84.9 | | |
| 500 | | | | | | | 55.3 | | 70.8 | 72.3 | | |
| 350 | | | | | | | 40.3 | | 55.7 | 63.9 | | |
| 250 | | | | | | | 29.3 | | 39.7 | 56.0 | | |
| 177 | | | | | | | 20.8 | | 25.8 | 48.4 | | |
| 125 | | | 84.0 | | | | 15.5 | | 16.4 | 41.4 | | |
| 88 | | 91.7 | 81.0 | 97.3 | | | 15.0 | 89.0 | 13.3 | 40.6 | 83.0 | 85.0 |
| 62 | 99.4 | 87.2 | 73.0 | 95.7 | 98.7 | 98.7 | 12.3 | 86.8 | 9.6 | 37.3 | 81.0 | 81.3 |
| 44 | 96.5 | 80.0 | 61.8 | 91.5 | 87.2 | 94.8 | 8.7 | 83.7 | 8.3 | 26.1 | 79.0 | 76.3 |
| 31 | 92.4 | 71.9 | 49.8 | 73.7 | 67.9 | 88.3 | 5.5 | 78.4 | 6.7 | 16.5 | 72.0 | 70.4 |
| 22 | 84.8 | 53.9 | 36.9 | 47.5 | 35.9 | 67.5 | 4.0 | 70.1 | 4.4 | 12.0 | 59.8 | 54.0 |
| 10 | 41.2 | 12.6 | 6.1 | 9.5 | 3.8 | 15.6 | 1.2 | 27.2 | 1.2 | 4.9 | 9.0 | 10.6 |
| 5 | 9.6 | 3.1 | 2.4 | 1.4 | 1.4 | 2.6 | | 8.3 | | 1.2 | 1.3 | 1.9 |
| 3 | 1.2 | 1.8 | 1.4 | | | 1.3 | | 3.1 | | | | 1.3 |
| 2 | | | | | | | | 1.0 | | | | |

Note: All figures are 'Per cent of weight less than d'.

* Courtesy of the U.S. Grain Marketing & Research Lab., Manhattan, Kansas

Appendix C

A Sample Calculation For Estimation of External Surface Area Using the Particle Size Distribution

The particle size distributions of the grain dust samples used in this work are given in Appendix B. For estimation of external surface area offered by the particles the assumption is made that the particles between two sieves all have diameter equal to the average of the two sieve sizes. Another assumption is that all particles are perfect spheres. The density of the sample must also be known.

For an i th mass fraction of the sample of mass f_i absolute volume of the fraction = f_i/ρ m^3/kg ,

where, ρ = Density of the sample (kg/m^3)

\therefore External surface offered by this fraction = $\frac{6f_i}{d_i\rho}$ m^2/kg

where, d_i = Diameter of the particles in the i th fraction (m.)

\therefore Total external surface offered by all the fractions

$$\begin{aligned}
 &= \sum_i \frac{6f_i}{d_i\rho} \\
 &= \frac{6}{\rho} \sum_i \frac{f_i}{d_i} \\
 &= \frac{6}{100\rho} \sum_i \frac{(\% \text{ sample with diameter } d_i)}{d_i} \quad (\text{m}^2/\text{kg})
 \end{aligned}$$

A sample calculation of external surface area is shown in Table C-1.

Table C-1

Estimation of External Surface Area of A Grain
Dust Sample Using the Particle Size Distribution

Sample: 784-04 (Wheat)

Absolute density, $\rho = 1540 \text{ kg/m}^3$

| Size of the fraction, d (m x 10 ⁶) | Mass % of the sample with size d | $\frac{\text{Mass \% sample}}{d}$ (m ⁻¹ x 10 ⁻⁶) |
|--|----------------------------------|--|
| 1 | - | - |
| 2.5 | 1.2 | 0.48 |
| 4 | 8.4 | 2.1 |
| 7.5 | 31.6 | 4.2133 |
| 16 | 43.6 | 2.725 |
| 26.5 | 7.6 | 0.2868 |
| 37.5 | 4.1 | 0.1093 |
| 53 | 2.9 | 0.0547 |
| 88 | 0.6 | 0.0068 |
| | | $\Sigma = 9.9760 \times 10^6 \text{ m}^{-1}$ |

$$\begin{aligned}
 \therefore \text{External surface area} &= \frac{(\Sigma) \times 6}{\rho \times 100} \\
 &= \frac{9.9760 \times 10^6 \times 6}{1540 \times 100} \\
 &= 388.7 \\
 &\approx 390 \text{ m}^2/\text{kg}
 \end{aligned}$$

Appendix D

A Sample Calculation For Measurement of the Free Space
In the Static BET Apparatus

For an ideal gas at constant temperature, the following relationship between pressure and volume of a trapped gas holds.

$$PV = \text{constant} = A$$

but,

$$V = V_0 + V'$$

where,

V_0 = Volume of the free space of the system

V' = Volume of the burette bulbs filled with gas

hence,

$$P(V_0 + V') = A$$

or

$$PV' = A - PV_0$$

Therefore, if a plot of PV' vs P is made, it would be a straight line with a negative slope of value V_0 .

Table D-1 shows the measurements made on system B of the vacuum system and Fig. D-1 shows the plot of PV' vs P .

Table D-1

Free Space Measurement

System: B

Room Temperature = 296^oK. (73^oF.)

| S.No. | Bulb(s) filled with gas (He) | Volume of the bulb(s) filled with gas v' ($m^3 \times 10^6$) | Pressure P ($N/m^2 \times 10^{-4}$) | Pv' ($N \cdot m$) |
|-------|---------------------------------|--|---|--------------------------|
| 1 | 2B + 1S | 29.88 | 9.207 | 2.751 |
| 2 | 2B + 2S | 41.35 | 6.993 | 2.891 |
| 3 | 2B + 3S | 59.41 | 5.060 | 3.006 |
| 4 | 2B + 4S | 81.91 | 3.760 | 3.080 |
| 5 | 3B + 4S | 109.33 | 2.867 | 3.134 |
| 6 | 4B + 4S | 164.82 | 1.937 | 3.192 |
| 7 | 4B + 6S | 226.98 | 1.417 | 3.216 |

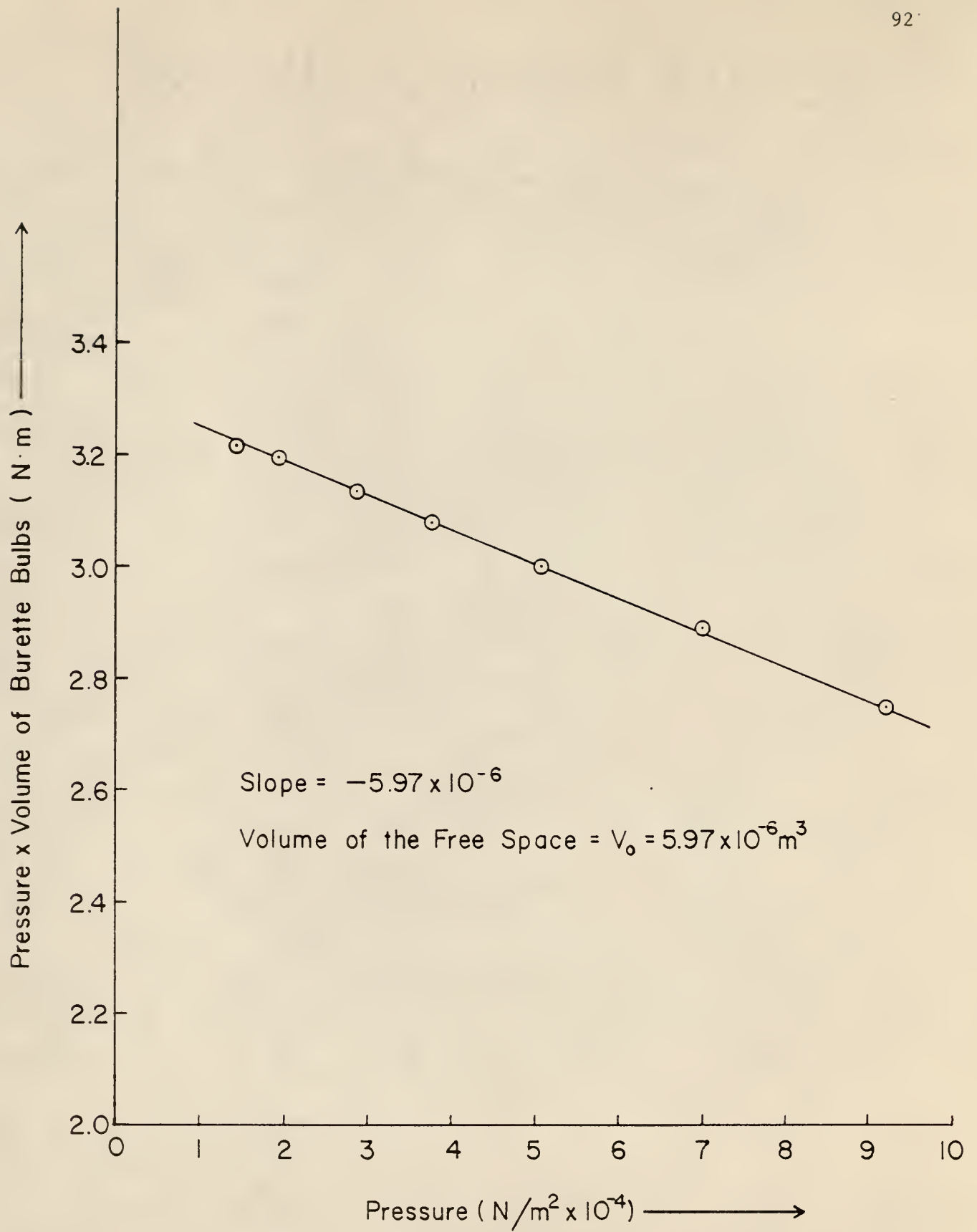


Fig. D-1 Free Space Measurement

Appendix E

A Sample Calculation For Measurement of Dead Space In the Sample Tube of the Static BET Apparatus

According to the Ideal gas law,

$$n_{\text{Tot}} = \frac{PV_1}{RT_1} + \frac{PV_d}{RT_2}$$

where,

n_{Tot} = Total number of kmoles of helium trapped in the system

P = Equilibrium pressure in the system (N/m^2)

V_1 = Volume of the free space + Volume of the burette bulbs filled with helium (m^3)

V_d = Volume of the dead space (m^3)

T_1 = Room temperature ($^{\circ}\text{K}$)

T_2 = Temperature of the constant temperature bath surrounding the sample tube ($^{\circ}\text{K}$)

R = Universal gas constant (= $8314.3 \text{ N}\cdot\text{m/k mole } ^{\circ}\text{K}$.)

Table E-1 shows the measurements made for the calculation of the dead volume.

From Table E-1,

Average of PV_1 for "closed" stopcock position = $1.70258 \text{ N}\cdot\text{m}$

$$\begin{aligned} \therefore n_{\text{Tot}} &= \frac{PV_1}{RT_1} = \frac{1.70258}{8314.3 \times 297.6} \\ &= 6.8799 \times 10^{-7} \text{ kmole} \end{aligned}$$

S.No.5

$$p = 2.740 \times 10^4 \text{ N/m}^2$$

$$\begin{aligned} 6.8799 \times 10^{-7} &= \frac{2.740 \times 10^4 \times 5.97 \times 10^{-6}}{8314.3 \times 297.6} + \frac{2.740 \times 10^4 V_d}{8314.3 \times 77.33} \\ &= 0.6605 \times 10^{-7} + 0.4261 \times 10^{-1} V_d \end{aligned}$$

$$V_d = 14.5959 \times 10^{-6} \text{ m}^3$$

Table E-1
Measurement of Dead Space At Liquid Nitrogen
Temperature

System: B

Room Temperature, $T_1 = 297.6^\circ\text{K}$. (76°F .)

Vapor pressure of the liquid nitrogen, $P_0 = 1.01 \times 10^5 \text{ N/m}^2$

Temperature of the constant temperature bath, $T_2 = 77.33^\circ\text{K}$.

Sample taken: 784-04 (Wheat)

Mass of the sample taken = $5.48582 \times 10^{-3} \text{ kg}$.

Mass of glass wool placed = $14.05 \times 10^{-6} \text{ kg}$.

Pretreatment: The sample is placed in a P_2O_5 desiccator for ~ 4 months and then evacuated upto $1.33 \times 10^{-3} \text{ N/m}^2$ ($1 \times 10^{-5} \text{ mm.Hg}$) within 2 hrs.

| S.No | Position of the sample tube stopcock | Bulb(s) filled with gas (He) | Volume of the gas in the free space and in the burettes V_1 ($\text{m}^3 \times 10^6$) | Pressure P ($\text{N/m}^2 \times 10^{-4}$) | PV_1 ($\text{N}\cdot\text{m}$) |
|------|--------------------------------------|------------------------------|--|--|---------------------------------------|
| 1 | Closed | 3B + 4S | 115.29 | 1.483 | 1.7102 |
| 2 | | 2B + 4S | 87.88 | 1.933 | 1.6989 |
| 3 | | 2B + 2S | 47.32 | 3.587 | 1.6971 |
| 4 | | 1B + 2S | 29.57 | 5.763 | 1.7041 |
| 5 | Open | None | 5.97 | 2.740 | |
| 6 | | 1B + 1S | 18.10 | 2.290 | |
| 7 | | 1B + 2S | 29.57 | 1.983 | |
| 8 | | 2B + 2S | 47.32 | 1.640 | |
| 9 | | 2B + 4S | 87.88 | 1.130 | |

S.No.6

$$P = 2.290 \times 10^4 \text{ N/m}^2$$

$$6.8799 \times 10^{-7} = \frac{2.290 \times 10^4 \times 18.10 \times 10^{-6}}{8314.3 \times 297.6} + \frac{2.290 \times 10^4 V_d}{8314.3 \times 77.33}$$

$$= 1.6750 \times 10^{-7} + 0.3561 \times 10^{-1} V_d$$

$$\therefore V_d = 14.6155 \times 10^{-6} \text{ m}^3$$

S.No.7

$$p = 1.983 \times 10^4 \text{ N/m}^2$$

$$\therefore 6.8799 \times 10^{-7} = \frac{1.983 \times 10^4 \times 29.57 \times 10^{-6}}{8314.3 \times 297.6} + \frac{1.983 \times 10^4 V_d}{8314.3 \times 77.33}$$

$$= 2.3697 \times 10^{-7} + 0.3084 \times 10^{-1} V_d$$

$$\therefore V_d = 14.6228 \times 10^{-6} \text{ m}^3$$

S.No.8

$$p = 1.640 \times 10^4 \text{ N/m}^2$$

$$6.8799 \times 10^{-7} = \frac{1.640 \times 10^4 \times 47.32 \times 10^{-6}}{8314.3 \times 297.6} + \frac{1.640 \times 10^4 V_d}{8314.3 \times 77.33}$$

$$= 3.1357 \times 10^{-7} + 0.2550 \times 10^{-1} V_d$$

$$\therefore V_d = 14.6807 \times 10^{-6} \text{ m}^3$$

S.No.9

$$p = 1.180 \times 10^4 \text{ N/m}^2$$

$$\therefore 6.8799 \times 10^{-7} = \frac{1.180 \times 10^4 \times 87.88 \times 10^{-6}}{8314.3 \times 297.6} + \frac{1.180 \times 10^4 V_d}{8314.3 \times 77.33}$$

$$= 4.1901 \times 10^{-7} + 0.1835 \times 10^{-1} V_d$$

$$\therefore V_d = 14.6579 \times 10^{-6} \text{ m}^3$$

$$\text{Average } V_d = 14.6346 \times 10^{-6} \text{ m}^3$$

$$\therefore \text{Volume of the dead space} = 14.6346 \times 10^{-6} \text{ m}^3$$

A comparison of the values of the dead space measurements at different temperatures is made in Table E-2.

Table E-2

Comparison the Dead Volumes Measured At
Various Temperatures

| Sample No. | Type | Mass of the sample taken ($\text{kg} \times 10^3$) | S.No. | Temperature ($^{\circ}\text{K}.$) | Volume of the dead space ($\text{m}^3 \times 10^6$) | $\frac{(i)}{(i)}$ | $\frac{(ii)}{(i)}$ |
|------------|---------|--|-------|-------------------------------------|---|-------------------|--------------------|
| 784-08 | Milo | 13.965 | (i) | 293.7 | 31.2912 | 0.8625 | 0.6546 |
| | | | (ii) | 195.0 | 26.9871 | | |
| | | | (iii) | 77.3 | 20.4817 | | |
| 785-04 | Soybean | 9.143 | (i) | 299.6 | 27.707 | 0.8623 | 0.7016 |
| | | | (ii) | 196.7 | 23.891 | | |
| | | | (iii) | 77.3 | 19.439 | | |
| 784-04 | Wheat | 6.335 | (i) | 296.2 | 26.439 | 0.8573 | - |
| | | | (ii) | 195.0 | 22.666 | | |

Appendix F

Calibration of Burettes

Table F-1
Calibration of Large Burette (B)

| Bulb No. | Mass of mercury filled in, M (kg.) | Temperature (°K.) | Density of mercury, ρ_{Hg} (10) ($\text{kg}/\text{m}^3 \times 10^{-3}$) | Volume of the bulb $V = \frac{M}{\rho_{\text{Hg}}}$ ($\text{m}^3 \times 10^6$) | Average Volume of the bulb ($\text{m}^3 \times 10^6$) |
|----------|------------------------------------|-------------------|---|--|---|
| 1 | 0.0833 | 300.9 | 13.5268 | 6.1581 | 6.145 |
| | 0.0831 | 300.9 | 13.5268 | 6.1434 | |
| | 0.0830 | 299.3 | 13.5308 | 6.1342 | |
| 2 | 0.2426 | 300.9 | 13.5268 | 17.9348 | 17.919 |
| | 0.2424 | 300.9 | 13.5268 | 17.9200 | |
| | 0.2422 | 299.3 | 13.5308 | 17.8999 | |
| 3 | 0.3710 | 300.9 | 13.5268 | 27.4270 | 27.417 |
| | 0.3710 | 300.9 | 13.5268 | 27.4270 | |
| | 0.3707 | 299.3 | 13.5308 | 27.3968 | |
| 4 | 0.7507 | 300.9 | 13.5268 | 55.4972 | 55.489 |
| | 0.7506 | 300.9 | 13.5268 | 55.4898 | |
| | 0.7507 | 299.3 | 13.5308 | 55.4808 | |
| 5 | 1.8478 | 300.9 | 13.5268 | 136.6029 | 136.599 |
| | 1.8481 | 300.9 | 13.5268 | 136.6251 | |
| | 1.8479 | 299.3 | 13.5308 | 136.5699 | |

Table F-2
Calibration of Small Burette(S)

| Bulb No. | Mass of Mercury filled in, M (kg) | Temperature ($^{\circ}$ K) | Density of mercury ρ_{Hg} (10) ($\text{kg}/\text{m}^3 \times 10^{-3}$) | Volume of the bulb, $V = \frac{M}{\rho_{\text{Hg}}}$ ($\text{m}^3 \times 10^6$) | Average Volume of the bulb ($\text{m}^3 \times 10^6$) |
|----------|-----------------------------------|-----------------------------|--|---|---|
| 1 | 0.0812 | 298.2 | 13.5336 | 5.9999 | 5.990 |
| | 0.0810 | 298.2 | 13.5336 | 5.9851 | |
| | 0.0810 | 298.2 | 13.5336 | 5.9851 | |
| 2 | 0.1552 | 298.2 | 13.5336 | 11.4678 | 11.468 |
| | 0.1551 | 298.2 | 13.5336 | 11.4604 | |
| | 0.1553 | 298.2 | 13.5336 | 11.4751 | |
| 3 | 0.2445 | 298.2 | 13.5336 | 18.0662 | 18.059 |
| | 0.2446 | 298.2 | 13.5336 | 18.0735 | |
| | 0.2441 | 298.2 | 13.5336 | 18.0366 | |
| 4 | 0.3046 | 298.2 | 13.5336 | 22.5069 | 22.500 |
| | 0.3048 | 298.2 | 13.5336 | 22.5217 | |
| | 0.3041 | 298.2 | 13.5336 | 22.4700 | |
| 5 | 0.3688 | 298.2 | 13.5336 | 27.2507 | 27.359 |
| | 0.3727 | 298.2 | 13.5336 | 27.5389 | |
| | 0.3693 | 298.2 | 13.5336 | 26.2876 | |
| 6 | 0.4729 | 298.2 | 13.5336 | 34.9427 | 34.802 |
| | 0.4684 | 298.2 | 13.5336 | 34.6102 | |
| | 0.4717 | 298.2 | 12.5336 | 34.8540 | |

Appendix G

Calibration of the McLeod Gauge

The calibration of the McLeod gauge consists of three steps.

(a) Calibration of the capillary

It can be seen from Table G-1 that the capillary is uniform in diameter and this fact is used in part (c). The average diameter of the capillary is 1.043×10^{-3} m.

(b) Calibration of the gauge bulb

This is shown in Table G-2. The volume of the bulb used is found to be $217.078 \times 10^{-6} \text{ m}^3$.

(c) Calibration of the McLeod gauge scale

The McLeod gauge used is shown in Fig. G-1.

$$\text{Volume of the gauge bulb} = 217.078 \times 10^{-6} \text{ m}^3$$

$$\text{Total length of the capillary, } H = 0.323 \text{ m}$$

If the pressure in the system is P_s and the distance of the mercury level in the capillary from the top is h , then,

$$\text{pressure of the gas trapped} = (P_s + h) \text{ m. of mercury}$$

and

$$\text{volume of the gas trapped} = \frac{\pi}{4} \times (1.043)^2 \times h \times 10^{-6} \text{ m}^3.$$

$$\begin{aligned} \text{Initial volume of the gas trapped (at pressure } P_s) \\ = 217.078 \times 10^{-6} + \frac{\pi}{4} \times (1.043)^2 \times 0.323 \times 10^{-6} \text{ m}^3. \end{aligned}$$

According to Boyle's law,

$$PV = A \text{ constant}$$

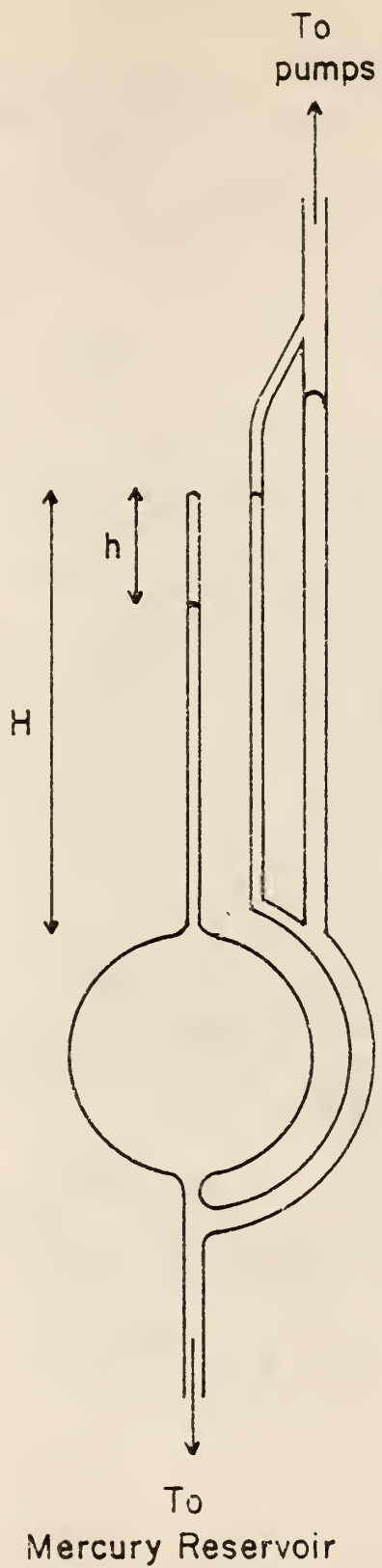


Fig. G-1 The McLeod Gauge

Table G-1
Calibration of the Capillary

| Position No. | Mass of mercury thread, M (kg x 10 ³) | Temperature (°K) | Density of mercury ρ_{Hg} (10) (kg/m ³ x 10 ⁻³) | Volume of the mercury thread, V $= \frac{M}{\rho_{\text{Hg}}}$ (m ³ x 10 ⁶) | Height of the mercury thread, h (m x 10 ³) | | | | Diameter of the capillary, $d = \sqrt{\frac{4V}{\pi h}}$ (m x 10 ³) |
|--------------|--|------------------|---|--|---|-------|-------|---------|---|
| | | | | | (i) | (ii) | (iii) | Average | |
| 1 | 0.42741 | 295.9 | 13.5404 | 0.031566 | 37.75 | 36.75 | 37.80 | 37.43 | 1.0362 |
| 2 | 0.42741 | 295.9 | 13.5404 | 0.031566 | 37.70 | 38.20 | 38.05 | 37.98 | 1.0287 |
| 3 | 0.42741 | 295.9 | 13.5404 | 0.031566 | 37.45 | 37.55 | 37.40 | 37.47 | 1.0357 |
| 4 | 0.42741 | 295.9 | 13.5404 | 0.031566 | 36.85 | 37.70 | 37.00 | 37.18 | 1.0397 |
| 5 | 0.42741 | 295.9 | 13.5404 | 0.031566 | 37.75 | 36.95 | 37.45 | 37.39 | 1.0368 |
| 6 | 0.42741 | 295.9 | 13.5404 | 0.031566 | 37.10 | 37.05 | 37.75 | 37.30 | 1.0380 |
| 7 | 0.35652 | 297.1 | 13.5362 | 0.026338 | 31.05 | 30.50 | 30.55 | 30.70 | 1.0451 |
| 8 | 0.35652 | 297.1 | 13.5362 | 0.026338 | 30.50 | 30.65 | 30.20 | 30.45 | 1.0494 |
| 9 | 0.35652 | 297.1 | 13.5362 | 0.026338 | 31.55 | 30.80 | 30.90 | 31.08 | 1.0387 |
| 10 | 0.35652 | 297.1 | 13.5362 | 0.026338 | 30.20 | 29.95 | 30.05 | 30.07 | 1.0567 |
| 11 | 0.35652 | 297.1 | 13.5362 | 0.026338 | 30.30 | 29.65 | 30.45 | 30.13 | 1.0549 |
| 12 | 0.35652 | 297.1 | 13.5362 | 0.026338 | 29.80 | 30.25 | 30.35 | 30.13 | 1.0549 |

∴ Average diameter of the capillary = 1.043 x 10⁻³ m.

Table G-2

Calibration of McLeod Gauge Bulb

| S. No. | Temperature (°K) | Density of mercury, ρ_{Hg} (10) (Kg/m ³ x 10 ⁻³) | Length of mercury in the capillary, h (m x 10 ³) | Mass of mercury taken, M (kg) | Volume of mercury taken, $v = \frac{M}{\rho_{\text{Hg}}}$ (m ³ x 10 ⁶) | Volume of mercury in the capillary $V_1 = \frac{\pi d^2}{4} h$ (m ³ x 10 ⁶) | Volume of the bulb, $V_2 = V - V_1$ (m ³ x 10 ⁶) |
|--------|---------------------|--|---|---|---|--|--|
| 1 | 295.4 | 13.5403 | 59 | 2.9390 | 217.0558 | 0.0504 | 217.0053 |
| 2 | 295.4 | 13.5403 | 57 | 2.9395 | 217.0927 | 0.0487 | 217.0540 |
| 3 | 295.9 | 13.5391 | 74 | 2.9412 | 217.2375 | 0.0632 | 217.1743 |
| | | | | | | | |

Average volume of the gauge bulb = $217.078 \times 10^{-6} \text{ m}^3$

$$\begin{aligned} \text{or, } P_s & \{217.078 \times 10^{-6} + \frac{\pi}{4} \times (1.043)^2 \times 0.323 \times 10^{-6}\} \\ & = (P_s + h) \times \frac{\pi}{4} \times (1.043)^2 \times h \times 10^{-6} \end{aligned}$$

or,

$$\begin{aligned} P_s & \{217.078 + \frac{\pi}{4} \times (1.043)^2 \times (0.323 - h)\} \\ & = \frac{\pi}{4} \times (1.043)^2 \times h^2 \end{aligned} \tag{G-1}$$

The values of h corresponding to various values of the pressure P_s as calculated using Eq. (G-1) are given in Table G-3.

Table G-3
 Calibration of the Gauge Scale

| Pressure in the system, p_s (m. of $H_g \times 10^3$) | Distance of the level of mercury from the closed end of the capillary, h (m. $\times 10^3$) |
|--|---|
| 1×10^{-4} | 5.0 |
| 5×10^{-4} | 11.3 |
| 1×10^{-3} | 16.0 |
| 5×10^{-3} | 35.7 |
| 1×10^{-2} | 50.4 |
| 5×10^{-2} | 112.8 |
| 0.1 | 159.5 |
| 0.2 | 225.5 |
| 0.3 | 276.1 |
| 0.4 | 318.8 |
| | |

Appendix H

A Sample Calculation for an Adsorption Run On the Static BET Apparatus

According to the Ideal gas law,

$$n_{\text{Tot}} = \frac{PV_1}{RT_1} + \frac{PV_d}{RT_2} + n_{\text{ads}}$$

where,

n_{Tot} = Total number of kmoles of the adsorption gas trapped in the system.

P = Equilibrium pressure in the system (N/m^2)

V_1 = Volume of the free space + Volume of the burette bulbs filled with the gas (m^3)

V_d = Volume of the dead space (m^3)

T_1 = Room Temperature ($^{\circ}\text{K}$)

T_2 = Temperature of the constant temperature bath surrounding the sample tube ($^{\circ}\text{K}$)

R = Universal gas constant ($= 8314.3 \text{ N}\cdot\text{m}/\text{kmole } ^{\circ}\text{K}$)

n_{ads} = Total number of kmoles of the adsorption gas that are adsorbed by the sample.

Table H-1 shows the measurements made for the adsorption run.

Average of PV_1 for 'closed' stopcock position = 3.20425 N.m

$$\begin{aligned} \therefore n_{\text{Tot}} &= \frac{PV_1}{RT_1} = \frac{3.20425}{8314.3 \times 294.8} \\ &= 1.3070 \times 10^{-6} \text{ kmole} \end{aligned}$$

S. No. 5

$$p = 2.687 \times 10^4 \text{ N/m}^2, T_1 = 294.8^\circ\text{K}, T_2 = 195.2^\circ\text{K}$$

$$\begin{aligned} \therefore 1.3070 \times 10^{-6} &= \frac{2.687 \times 10^4 \times 5.97 \times 10^{-6}}{8314.3 \times 294.8} + \frac{2.687 \times 10^4 \times 22.67 \times 10^{-6}}{8314.3 \times 195.2} + n_{\text{ads}} \\ &= 0.0648 \times 10^{-6} + 0.3741 \times 10^{-6} + n_{\text{ads}} \end{aligned}$$

$$\therefore n_{\text{ads}} = 0.8681 \times 10^{-6} \text{ kmole}$$

S. No. 6

$$p = 2.140 \times 10^4 \text{ N/m}^2, T_1 = 295.9^\circ\text{K}, T_2 = 195.1^\circ\text{K}$$

$$\begin{aligned} \therefore 1.3070 \times 10^{-6} &= \frac{2.140 \times 10^4 \times 18.10 \times 10^{-6}}{8314.3 \times 295.9} + \frac{2.140 \times 10^4 \times 22.67 \times 10^{-6}}{8314.3 \times 195.1} + n_{\text{ads}} \\ &= 0.1574 \times 10^{-6} + 0.2990 \times 10^{-6} + n_{\text{ads}} \end{aligned}$$

$$n_{\text{ads}} = 0.8506 \times 10^{-6} \text{ kmole}$$

S. No. 7

$$p = 1.580 \times 10^4 \text{ N/m}^2, T_1 = 297.1^\circ\text{K}, T_2 = 194.8^\circ\text{K}$$

$$\begin{aligned} \therefore 1.3070 \times 10^{-6} &= \frac{1.580 \times 10^4 \times 47.63 \times 10^{-6}}{8314.3 \times 297.1} \\ &\quad + \frac{1.580 \times 10^4 \times 22.67 \times 10^{-6}}{8314.3 \times 194.8} + n_{\text{ads}} \end{aligned}$$

$$\therefore n_{\text{ads}} = 0.7812 \times 10^{-6} \text{ kmole}$$

Table H-1

Adsorption Measurement of Carbon Dioxide On A Wheat Dust
Sample At Dry Ice-Acetone Temperature

System: B

Room Temperature, $T_1 = 294.8 \text{ }^\circ\text{K}$ (71°F)

Sample taken: 784-04 (Wheat)

Mass of the sample taken = $6.33545 \times 10^{-3} \text{ kg}$.

Mass of glass wool placed = $15.52 \times 10^{-6} \text{ kg}$.

Pretreatment: The sample is placed in a P_2O_5 desiccator for ~ 4 months and then evacuated upto $1.33 \times 10^{-3} \text{ N/m}^2$ ($1 \times 10^{-5} \text{ mm. Hg}$) within 2 hrs.

Volume of the dead space at 195°K , $V_d = 22.67 \times 10^{-6} \text{ m}^3$.

| S. No. | Position of the sample tube stopcock | Bulb(s) filled with gas (CO ₂) | Volume of the gas in the free space and in the burettes in the burettes $V_1 \times 10^6$ (m ³ x 10 ⁶) | Time given for Equilibration (hr.) | Equilibrium Pressure (N/m ² x 10 ⁻⁴) | PV ₁ (N·m) | Temperature of the bath, T ₂ (°K) | Room Temperature, T ₁ (°K) |
|--------|--------------------------------------|--|---|------------------------------------|---|-----------------------|--|---------------------------------------|
| 1 | Closed | 2B + 1S | 35.85 | --- | 8.897 | 3.1893 | --- | 294.8 |
| 2 | | 2B + 2S | 47.32 | --- | 6.760 | 3.1986 | --- | 294.8 |
| 3 | | 2B + 3S | 65.38 | --- | 4.910 | 3.2099 | --- | 294.8 |
| 4 | | 2B + 4S | 87.88 | --- | 3.663 | 3.2192 | --- | 294.8 |
| 5 | Open | None | 5.97 | 33 | 2.687 | --- | 195.2 | 294.8 |
| 6 | | 1B + 1S | 18.10 | 15.5 | 2.140 | --- | 195.1 | 295.9 |
| 7 | | 1B + 3S | 47.63 | 7.5 | 1.580 | --- | 194.8 | 297.1 |
| 8 | | 2B + 4S | 87.88 | 10 | 1.253 | --- | 194.9 | 295.9 |
| 9 | | 3B + 6S | 177.45 | 5.5 | 0.760 | --- | 194.9 | 297.1 |

S. No. 8

$$\begin{aligned}
 p &= 1.253 \times 10^4 \text{ N/m}^2, T_1 = 295.9 \text{ }^\circ\text{K}, T_2 = 194.9 \text{ }^\circ\text{K} \\
 \therefore 1.3070 \times 10^{-6} &= \frac{1.253 \times 10^4 \times 87.88 \times 10^{-6}}{8314.3 \times 295.9} \\
 &\quad + \frac{1.253 \times 10^4 \times 22.67 \times 10^{-6}}{8314.3 \times 194.9} + n_{\text{ads}} \\
 &= 0.4476 \times 10^{-6} + 0.1753 \times 10^{-6} + n_{\text{ads}} \\
 \therefore n_{\text{ads}} &= 0.6841 \times 10^{-6} \text{ kmole}
 \end{aligned}$$

S. No. 9

$$\begin{aligned}
 p &= 0.760 \times 10^4 \text{ N/m}^2, T_1 = 297.1 \text{ }^\circ\text{K}, T_2 = 194.9 \text{ }^\circ\text{K} \\
 \therefore 1.3070 \times 10^{-6} &= \frac{0.760 \times 10^4 \times 177.45 \times 10^{-6}}{8314.3 \times 297.1} \\
 &\quad + \frac{0.760 \times 10^4 \times 22.67 \times 10^{-6}}{8314.3 \times 194.9} + n_{\text{ads}} \\
 &= 0.5460 \times 10^{-6} + 0.1062 \times 10^{-6} + n_{\text{ads}} \\
 \therefore n_{\text{ads}} &= 0.6548 \times 10^{-6} \text{ kmole}
 \end{aligned}$$

Fig. H-1 gives the adsorption isotherm obtained from these calculations. The calculations required for the BET plot (Fig. H-2) are shown in Table H-2.

From the BET plot,

$$\text{Slope} = S = 0.06639 \times 10^6 \text{ m}^{-3}$$

$$\text{y- Intercept} = I = 0.00054 \times 10^6 \text{ m}^{-3}$$

$$\begin{aligned}
 \therefore \text{Monolayer capacity of the sample (STP), } V_m &= \frac{1}{S+I} \\
 &= 14.94 \times 10^{-6} \text{ m}^3
 \end{aligned}$$

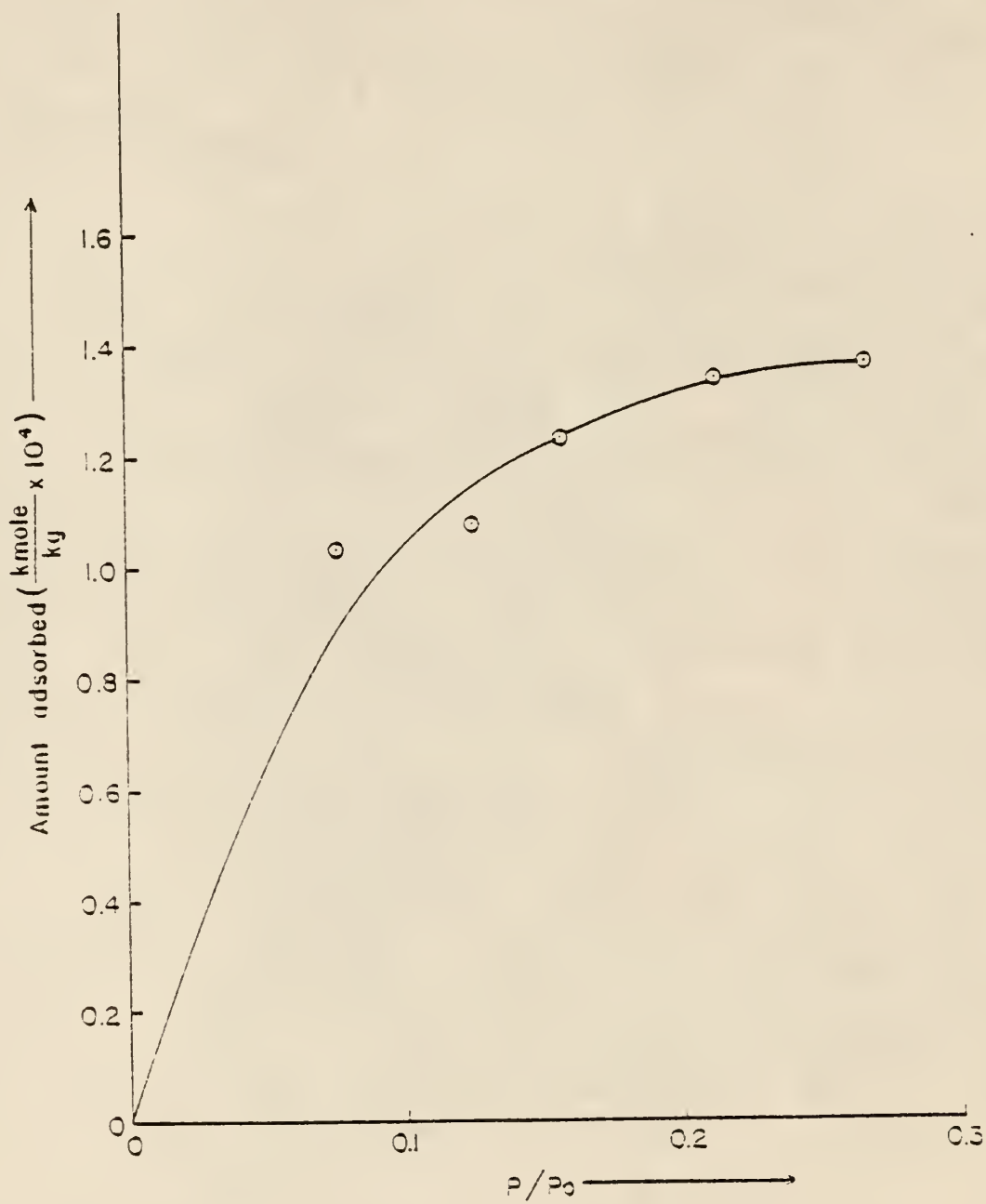


Fig. H-1 Adsorption Isotherm For Carbon Dioxide On a Wheat Sample At 195° K

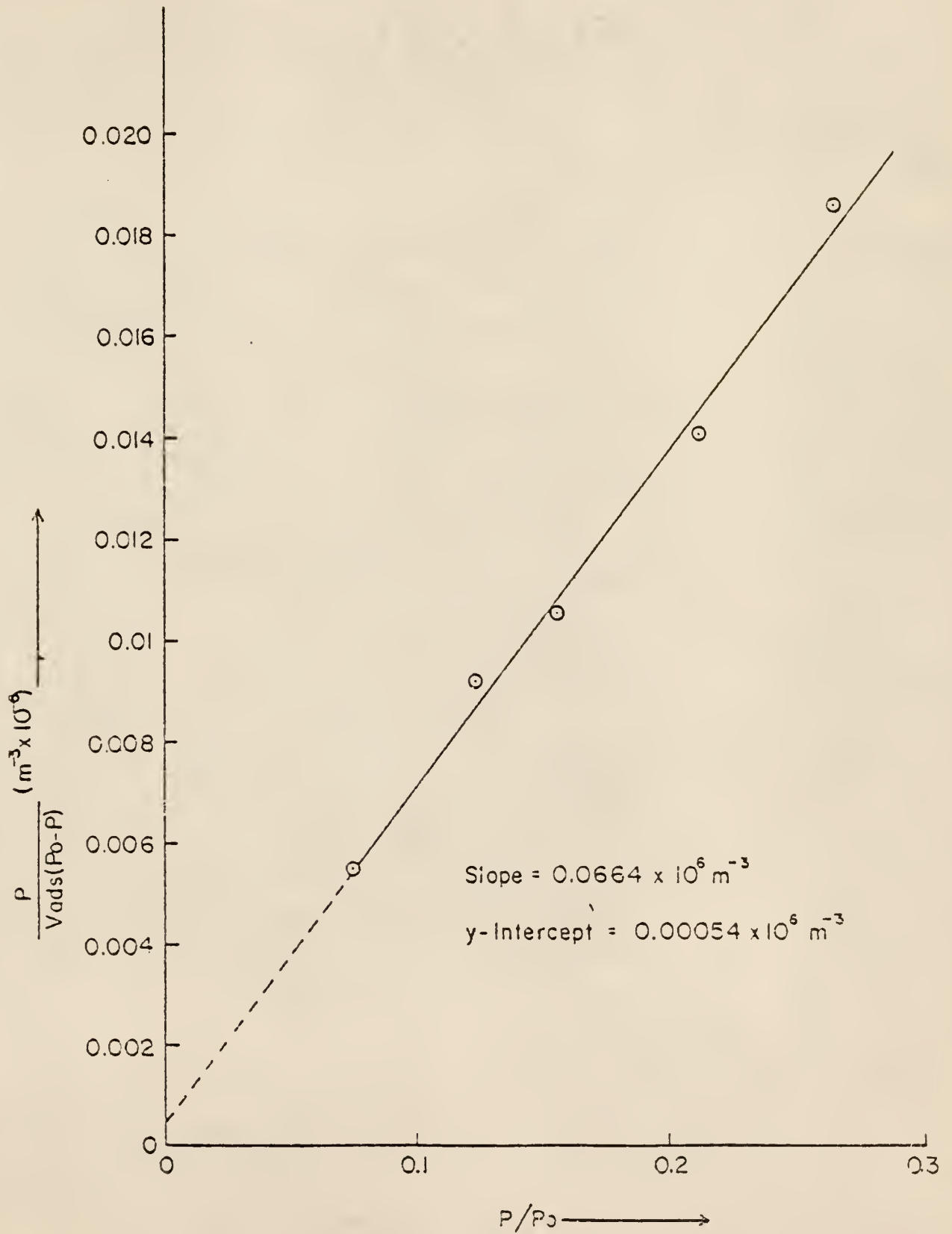


Fig. H-2 The BET Plot

Table H-2

Calculations For the BET Plot

Vapor pressure of carbon dioxide at 195°K. = $1.013 \times 10^5 \text{ N/m}^2$ (1 atm.)

| Equilibrium Pressure, p ($\text{N/m}^2 \times 10^{-4}$) | No. of kmoles of carbon dioxide adsorbed, n_{ads} ($\text{K mole} \times 10^7$) | Relative Pressure, p/p_0 | Volume (STP) of carbon dioxide adsorbed, $(V_{\text{ads}})_{\text{STP}} = n_{\text{ads}} \times 0.08206 \times 273.16$ ($\text{m}^3 \times 10^6$) | $\frac{p}{V_{\text{ads}}(P_0 - P)}$ ($\text{m}^{-3} \times 10^{-6}$) |
|---|--|-------------------------------|---|---|
| 2.687 | 8.681 | 0.265 | 19.459 | 0.0185 |
| 2.140 | 8,506 | 0.211 | 19.065 | 0.0140 |
| 1.580 | 7.812 | 0.156 | 17.511 | 0.0106 |
| 1.253 | 6.841 | 0.124 | 15.335 | 0.0092 |
| 0.760 | 6.548 | 0.075 | 14.678 | 0.0055 |

Area covered by a monolayer of 1 m³ (STP) of carbon dioxide,
 $s_o = 3.791 \times 10^6 \text{ m}^2/\text{m}^3$. (11)

$$\begin{aligned} \therefore \text{Specific surface area, } S_s &= \frac{V_{m_o} s_o}{w} \\ &= \frac{14.94 \times 10^{-6} \times 3.791 \times 10^6}{6.33545 \times 10^{-3}} \\ &= 8.94 \times 10^3 \text{ m}^2/\text{kg}. \end{aligned}$$

Appendix I

A Sample Calculation For Measurement of Surface Area
Using Carbon Dioxide At Room Temperature

Table I-1 shows the measurements made for the adsorption run. The amount of carbon dioxide adsorbed at a particular equilibrium pressure is calculated using the Ideal gas law as shown in Appendix H. These values with the other calculations necessary for the Dubinin-Polanyi plot (Fig. I-2) are shown in Table I-2. Fig. I-1 is the adsorption isotherm obtained from the measurements shown in Table I-1.

From the Dubinin-Polanyi plot (Fig. I-2),

$$y\text{-Intercept} = (\log n_{\text{ads}})_0 = -5.8762$$

$$\therefore (n_{\text{ads}})_0 = 1.330 \times 10^{-6} \text{ kmole}$$

$$\therefore \text{Monolayer capacity of the sample (STP), } V_m = n_{\text{ads}} RT$$

$$= 1.330 \times 10^{-6} \times 0.08206 \times 273.16$$

$$= 29.81 \times 10^{-6} \text{ m}^3$$

Area covered by a monolayer of 1 m^3 (STP) of carbon dioxide,

$$s_0 = 3.791 \times 10^6 \text{ m}^2/\text{m}^3 \quad (11)$$

$$\therefore \text{Specific surface area, } S_s = \frac{V_m s_0}{W}$$

$$= \frac{29.81 \times 10^{-6} \times 3.791 \times 10^6}{6.33545 \times 10^{-3}}$$

$$= 17.84 \times 10^3 \text{ m}^2/\text{kg}.$$

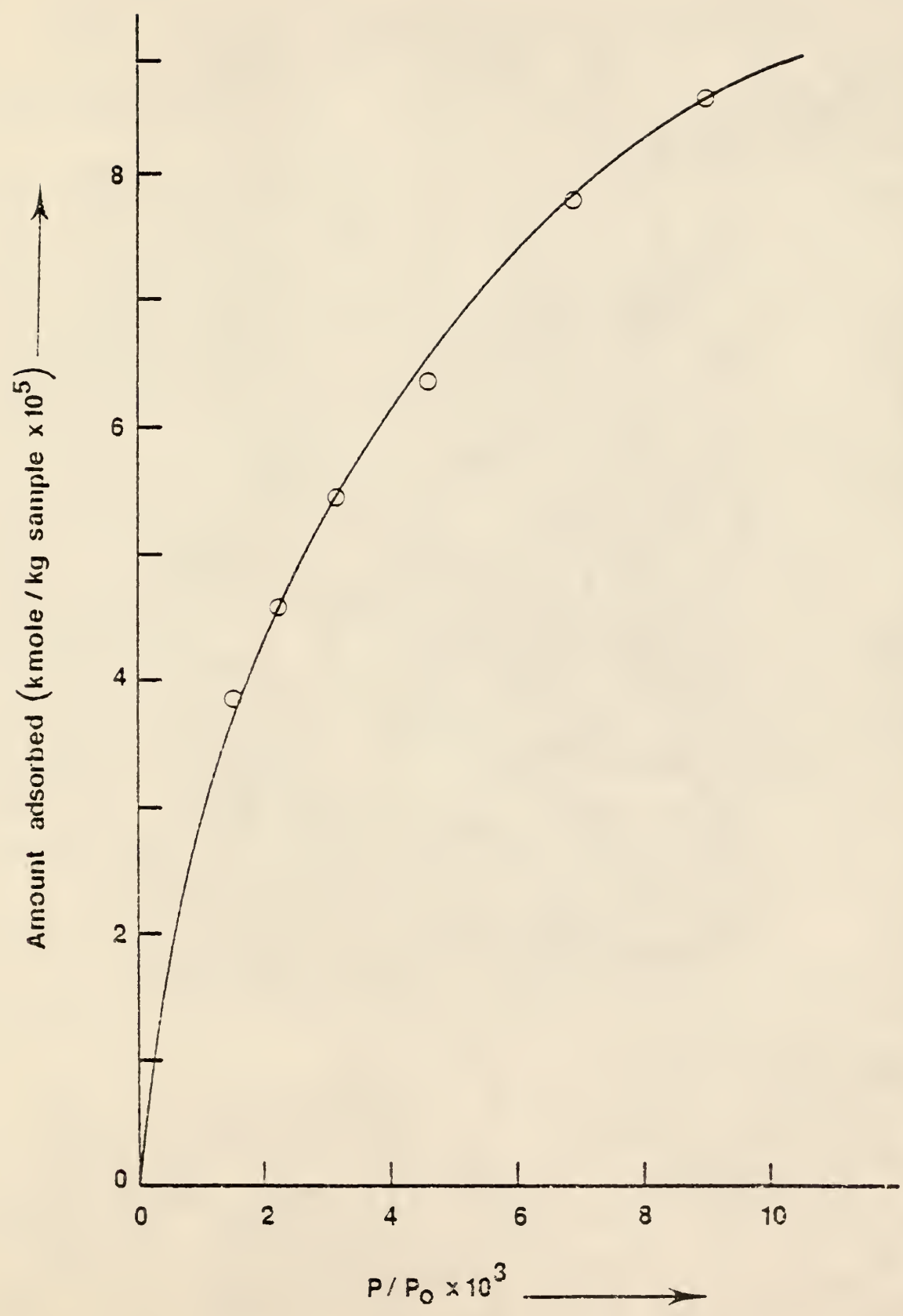


Fig. I-1 Adsorption Isotherm For Carbon Dioxide On A Wheat Sample At 301° K

Table I-1

Adsorption Measurement of Carbon Dioxide On A
Wheat Dust Sample At 301.2°K

System: B

Room Temperature, $T_1 = 297.1^\circ\text{K}$ (75°F.)

Temperature of the water bath, $T_2 = 301.2^\circ\text{K}$.

Sample taken: 784-04 (Wheat)

Mass of the sample taken = 6.33545×10^{-3} kg.

Mass of glass wool put = 15.52×10^{-6} kg.

Pretreatment: The sample is put in a P_2O_5 desiccator for ~ 4 months and then evacuated upto 1.33×10^{-3} N/m² (1×10^{-5} mm. Hg) within 2 hrs.

Volume of the dead space at 296.2°K, $V_d = 26.44 \times 10^{-6}$ m³

| S. No | Position of the sample tube stopcock | Bulb(s) filled with gas (CO ₂) | Volume of the gas in the free space and in the burettes V_1 (m ³ x 10 ⁶) | Time given for equilibration (hr.) | Equilibrium Pressure (N/m ² x 10 ⁻⁴) | P·V ₁ (N·m) | Room Temperature T ₁ (°K) |
|-------|--------------------------------------|--|---|------------------------------------|---|------------------------|--------------------------------------|
| 1 | Closed | 2B + 1S | 35.85 | -- | 9.283 | 3.328 | 297.1 |
| 2 | | 2B + 2S | 47.32 | -- | 7.037 | 3.329 | 297.1 |
| 3 | | 2B + 3S | 65.37 | -- | 5.100 | 3.334 | 297.1 |
| 4 | | 2B + 4S | 87.88 | -- | 3.800 | 3.339 | 297.1 |
| 5 | Open | None | 5.97 | 24 | 6.217 | -- | 297.9 |
| 6 | | 1B + 1S | 18.10 | 4 | 4.780 | -- | 295.4 |
| 7 | | 1B + 3S | 47.63 | 10.5 | 3.180 | -- | 297.6 |
| 8 | | 2B + 4S | 87.88 | 5 | 2.170 | -- | 295.4 |
| 9 | | 3B + 5S | 142.65 | 5 | 1.550 | -- | 297.3 |
| 10 | | 4B + 6S | 232.94 | 4 | 1.057 | -- | 297.9 |

Table I-2

Calculations For the Dubinin-Polanyi Plot

Vapor pressure of carbon dioxide at 301.2°K., $p_0 = 6.9077 \times 10^6 \text{ N/m}^2$ (68.17 atm.) (10)

| Equilibrium Pressure, p ($\text{N/m}^2 \times 10^{-4}$) | Amount adsorbed, n_{ads} ($\text{kmole} \times 10^7$) | Relative Pressure $p/p_0 (\times 10^3)$ | $\log (n_{\text{ads}})$ | $(\log (p_0/p))^2$ |
|---|---|---|-------------------------|--------------------|
| 6.217 | 5.432 | 8.999 | -6.265 | 4.185 |
| 4.780 | 4.923 | 6.920 | -6.308 | 4.665 |
| 3.180 | 4.015 | 4.603 | -6.396 | 5.461 |
| 2.170 | 3.441 | 3.141 | -6.463 | 6.264 |
| 1.550 | 2.913 | 2.244 | -6.536 | 7.017 |
| 1.057 | 2.440 | 1.530 | -6.613 | 7.927 |
| | | | | |

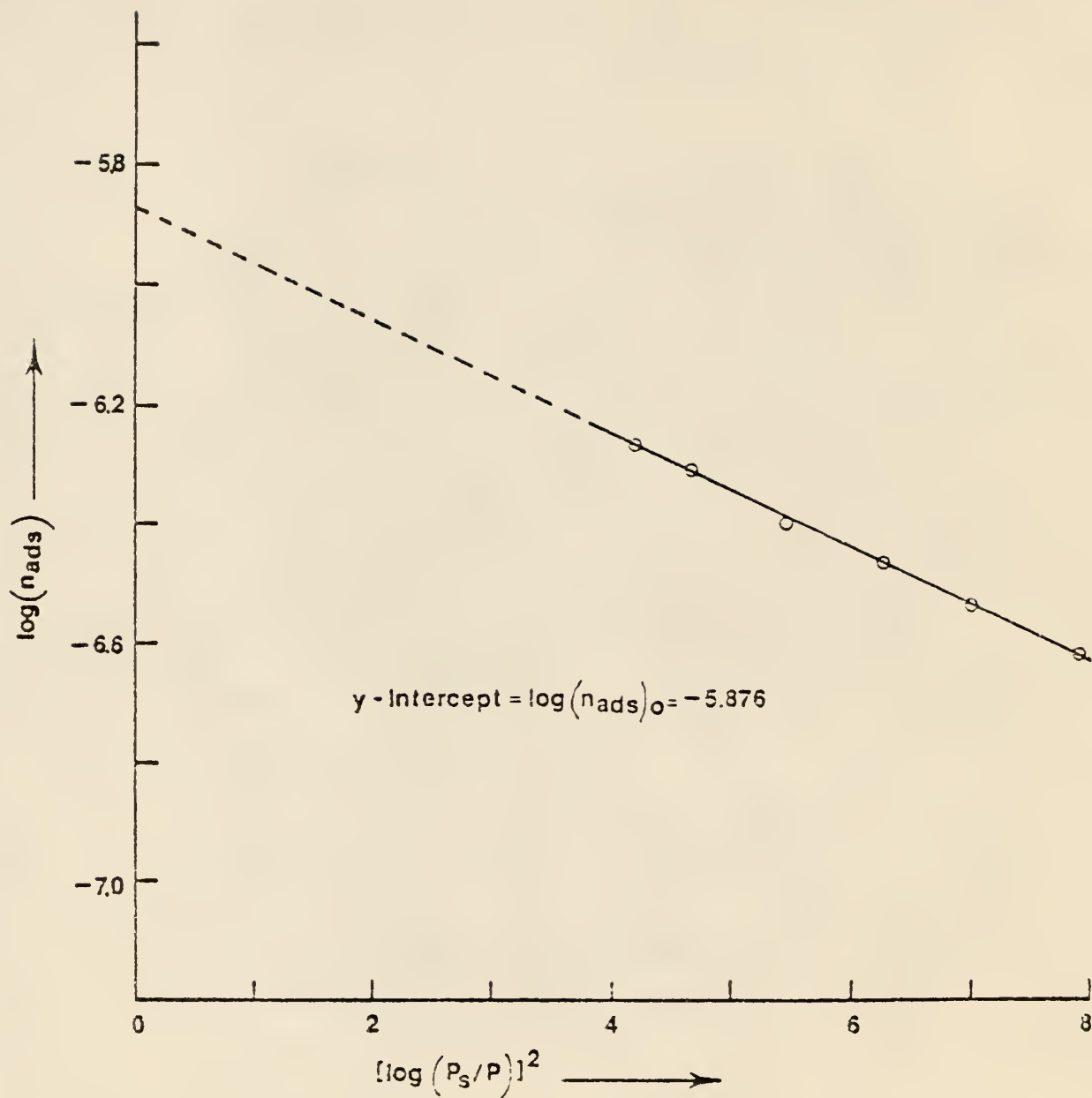


Fig. I-2 The Dubinin-Polanyi Plot

Appendix J

Pore Size Distribution Measurements Using the Static BET Apparatus

J-1 Introduction

A porous substance has pores of different sizes and shapes. The effectiveness of the internal surface can depend not only on the extent of void spaces, but also on the size of the openings. Too small pores would not be entered by most molecules and so would not offer the area required for any surface phenomenon. Therefore, it is desirable to know the distribution of void volume in a porous substance according to size of the openings. The void space in a porous substance is normally simulated as cylindrical pores. Hence the size of the void space is interpreted as a diameter of a cylindrical pore and the distribution of void volume is defined in terms of this variable. This distribution is known as the pore size distribution for the porous substance.

There are two established methods for measuring the pore size distribution. The mercury-penetration method depends on the fact that mercury has a significant surface tension and does not wet most solids. The pressure required to force mercury into the pores depends inversely on the diameter of the pores. So, the pore-volume distribution can be determined easily only down to 10 nm. and a special high-pressure apparatus is necessary to go below 10 nm., where much of the surface resides.

The second method involves adsorption of nitrogen. In surface area determination by the BET method, only the lower part of the adsorption

isotherm, from 0.05 to 0.30 relative pressure, is utilized. On the other hand, adsorption measurements are normally made over the relative pressure range of 0.05 to 0.98 when investigating the pore volume and the pore size distribution of the solids. As the nitrogen adsorption is continued to higher pressures, multilayer adsorption occurs and ultimately capillary condensation begins which fills up the pores with adsorbed nitrogen. This condensation is complete as the relative pressure approaches 1.0. If the pressure is now reduced in small intervals, some amount evaporates from the surface of the condensed nitrogen at the ends of the largest pores. The Kelvin equation gives the relationship between the vapor pressure and the curvature of the surface of the liquid that would evaporate. It may be written

$$\ln p/p_o = - \frac{\sigma V \cos\beta}{RT} \left(\frac{1}{r_1} + \frac{1}{r_2} \right) \quad (J-1)$$

where, p = Measured pressure, N/m^2

p_o = Saturation pressure of the adsorbate, N/m^2

σ = Surface tension of the adsorbate, N/m .

V = Molal volume of the liquid adsorbate, $m^3/kmole$

β = Angle of contact of the adsorbate meniscus with the pore surface, rad.

R = The universal gas constant

= $8314.3 \text{ N.m/kmole}^\circ\text{K}$.

T = Absolute temperature $^\circ\text{K}$.

and r_1, r_2 = Radii of curvature of the surface, m .

Application of the Kelvin equation involves several assumptions, the principal one among which is that liquid in the capillaries of the adsorbent has properties characteristic of the bulk liquid phase, such as the same surface tension and the same molal volume.

This adsorption method allows the measurement of the pore volume per unit mass of sample only when the pore diameters are smaller than approximately 85 nm. The pore volume existing in the pores larger than 85 nm. can be measured using the above stated mercury-penetration method. The pore volume obtained from either of these methods is, therefore, representative of only a part of the pores in the solid. These methods also provide means for determining the volume of pores having diameters all smaller than any selected size, in their respective ranges, thereby yielding a pore size distribution.

As mentioned earlier, the appropriate way of determining the pore size distribution for a sample, by the second method, is by making use of the desorption isotherm. However, it does not matter if one uses the adsorption isotherm when there is no hysteresis. Hysteresis is observed when a pore of particular size fills and empties at two different pressures. This gives different isotherms for adsorption and desorption on the same sample and the loop formed due to this is called a hysteresis loop. A small hysteresis loop is indicated in Fig. J-1. This is observed in case of samples having pores of certain shape and in fact, the shape of the pores can be determined theoretically by observing a hysteresis loop of certain shape (13). Whereas pores of most geometries exhibit hysteresis, "funnel" or V-shaped pores oriented with their large openings to the surface are noteworthy exceptions (11).

For cylindrical pores hysteresis is predicted by the Kelvin equation if the pore may be considered to fill from the sides (radially), but empty from the top. Thus for adsorption, $r_1 = r$ and $r_2 = \infty$ and the Kelvin equation becomes

$$\ln p/p_0 = - \frac{cV \cos\theta}{rRT} \quad (J-2)$$

But, for desorption, $r_1 = r_2 = r$ and the Kelvin equation becomes

$$\ln p/p_0 = -\frac{2 \sigma V \cos \theta}{rRT} \quad (\text{J-3})$$

Thus, the pore will empty at a lower pressure than it filled.

The Sorptometer from 'Perkin-Elmer', which was very successful in the specific surface area measurements, was not accurate at high relative pressures of nitrogen. Apparently, when large volumes are adsorbed the thermal conductivity cell detects both the change in the concentration and the change in the flow rate of the gas mixture because of the adsorption or desorption taking place. The adsorption measurements were therefore made on the static BET apparatus described in Chapter 3.

J-2 Sample Preparation and Experimental Procedure

Pore size distribution measurements were made on an alumina sample and a wheat sample. From the adsorption work using carbon dioxide, it is suspected that nitrogen does not enter the small pores. So, these experiments for determination of the pore size distribution of wheat dust are suspect. It was, however, decided to carry out these runs to see if some trend could be seen and pore size distribution is of interest to the U.S. Grain Marketing & Research Laboratory. Before starting the measurements on wheat, the alumina sample was run to ascertain whether meaningful results could be produced by the existing static apparatus.

The alumina sample (A201, 5 x 8 Mesh, produced by Kaiser Chemicals) was evacuated to $1.33 \times 10^{-3} \text{ N/m}^2$ ($1 \times 10^{-5} \text{ mm. Hg}$) at a temperature of about 710° K . for 6 hours, prior to start of the adsorption measurements, whereas the wheat sample (#784-04) was put in a P_2O_5 desiccator for 4 months and then evacuated to $1.33 \times 10^{-3} \text{ N/m}^2$ ($1 \times 10^{-5} \text{ mm. Hg}$) within 2 hours. Both of these pretreatments presumably free the internal surface of the solids from moisture or any other adsorbed gas.

The same procedure as described in Section 3.1 was carried out to obtain the adsorption isotherms. The dead space in the sample tube was measured prior to the adsorption measurements. Nitrogen was used as the adsorbate and the adsorption isotherms were obtained at liquid nitrogen temperature.

J-3 Necessary Data

For the calculation of the pore size distribution, a number of data are necessary.

(1) For the calculation of the amount of gas adsorbed at a particular pressure, one has to know the temperature of the liquid nitrogen bath surrounding the sample tube. The nitrogen vapor thermometer mentioned in Section 3.3.10 measures the vapor pressure of nitrogen and Table J-1 gives the temperature corresponding to the vapor pressure.

(2) In the pore size distribution measurement, the volume of adsorbed gas has to be converted to the corresponding liquid volume. The conversion factors for this, which are dependent on the liquid nitrogen temperatures, are tabulated against different temperature values in Table J-1.

(3) In the pore size distribution measurement, there is adsorption on the walls of unfilled pores which has to be accounted for. Also, the pore diameters corresponding to the relative pressure have to be established. This is done with the help of the Kelvin equation. Table J-2 lists values for statistical layers of nitrogen at various relative pressures as also the Kelvin diameter and the true pore diameter.

J-4 Results

The adsorption isotherms obtained are shown in Figures J-1 and J-4. A sample calculation for determining the pore size distributions from these adsorption isotherms is shown in Table J-3. The values obtained from such

Table J-1

Saturation Pressure and Liquid/Gas Ratio For Nitrogen(6)

| Temperature | | Saturation Pressure of Nitrogen | | Liquid/Gas Ratio $\frac{\text{m}^3 \text{ liquid}}{\text{m}^3 \text{ gas (STP)}}$ |
|-------------|-------|------------------------------------|------------------|--|
| T | | P _o | | f _{liq} |
| °C | °K | mm Hg | N/m ² | |
| -195.80 | 77.36 | 760 | 101332 | 0.0015482 |
| -195.69 | 77.47 | 770 | 102666 | 0.0015491 |
| -195.57 | 77.59 | 780 | 103999 | 0.0015501 |
| -195.47 | 77.69 | 790 | 105332 | 0.0015511 |
| -195.36 | 77.80 | 800 | 106666 | 0.0015520 |
| -195.25 | 77.91 | 810 | 107999 | 0.0015530 |
| -195.14 | 78.02 | 820 | 109332 | 0.0015540 |
| -195.04 | 78.12 | 830 | 110666 | 0.0015549 |
| -194.93 | 78.23 | 840 | 111999 | 0.0015558 |
| -194.83 | 78.33 | 850 | 113332 | 0.0015567 |
| -194.73 | 78.43 | 860 | 114666 | 0.0015576 |
| -194.63 | 78.53 | 870 | 115999 | 0.0015586 |
| -194.53 | 78.63 | 880 | 117332 | 0.0015596 |
| -194.43 | 78.73 | 890 | 118666 | 0.0015605 |
| -194.33 | 78.83 | 900 | 119999 | 0.0015614 |

Table J-2

Values For Statistical Layers of Nitrogen, the Kelvin Diameter
and the True Pore Diameter At Various Relative Pressures (6)

| Relative Pressure, P/P_0 | Statistical Layers of Nitrogen, n | Thickness of An Adsorbed Nitrogen Layer, $0.354 n$ (nm) | Diameter of Pore According To Kelvin Equation, d_k (nm) | True Pore Diameter, d_p ($= d_k + 2(0.354n)$) (nm) |
|----------------------------|-------------------------------------|---|---|--|
| 1.000 | 19.0 | 6.73 | . | |
| 0.980 | 14.0 | 4.95 | 94.6 | 104.5 |
| 0.975 | 13.0 | 4.60 | 75.4 | 84.6 |
| 0.970 | 11.9 | 4.20 | 62.6 | 71.0 |
| 0.960 | 10.1 | 3.58 | 46.3 | 54.0 |
| 0.950 | 9.8 | 3.12 | 37.2 | 43.4 |
| 0.925 | 6.7 | 2.37 | 24.4 | 29.2 |
| 0.900 | 5.6 | 1.98 | 18.2 | 22.2 |
| 0.850 | 4.4 | 1.56 | 11.3 | 14.9 |
| 0.800 | 3.5 | 1.24 | 8.6 | 11.1 |
| 0.700 | 2.5 | 0.88 | 5.36 | 7.12 |
| 0.600 | 2.08 | 0.74 | 3.74 | 5.22 |
| 0.500 | 1.78 | 0.63 | 2.76 | 4.02 |
| 0.400 | 1.56 | 0.55 | 2.08 | 3.18 |
| 0.300 | 1.38 | 0.49 | 1.58 | 2.56 |
| 0.200 | 1.22 | 0.43 | 1.18 | 2.04 |
| 0.100 | 1.09 | 0.385 | 0.83 | 1.60 |

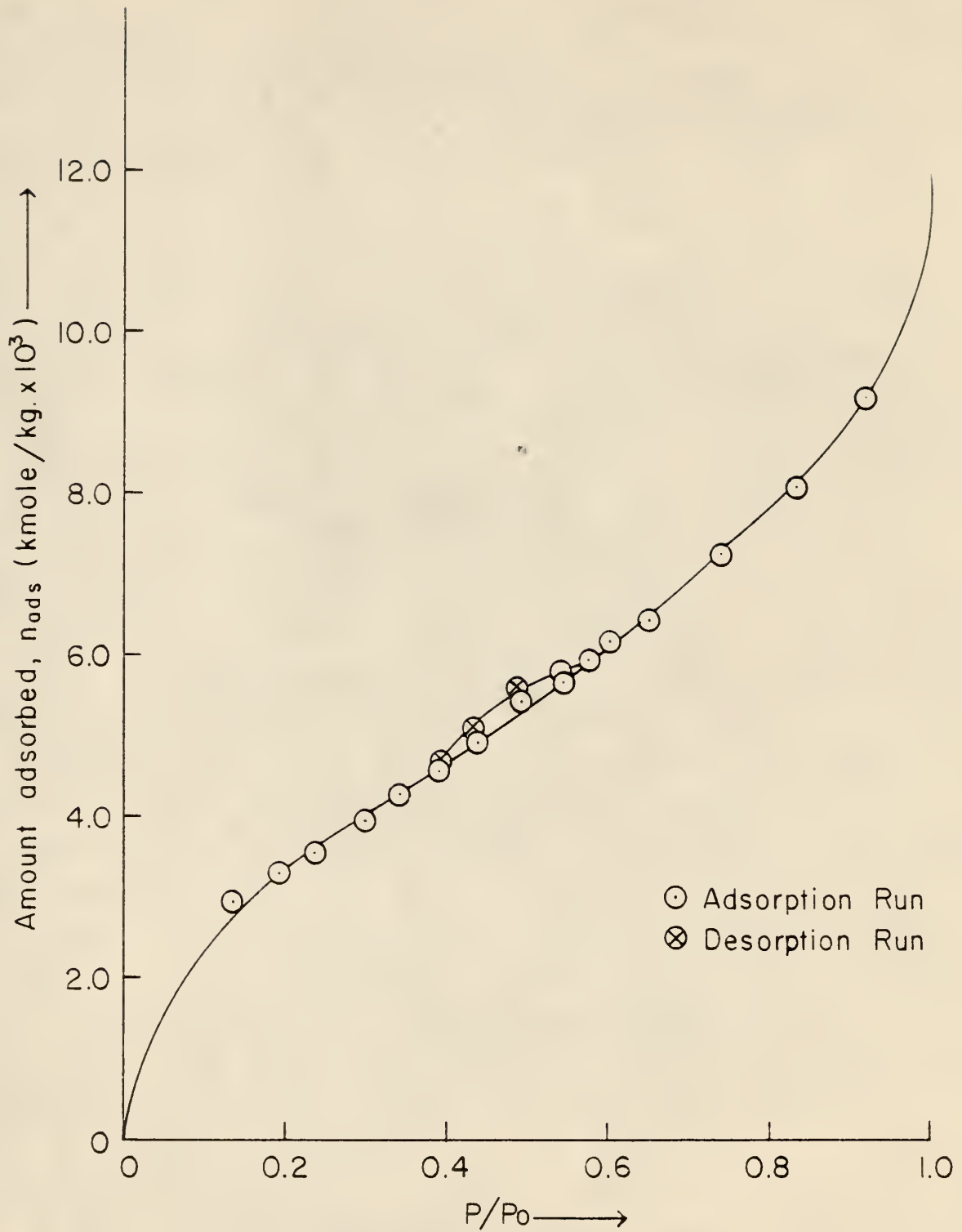


Fig. J-1 Adsorption Isotherm For Nitrogen On Kaiser Alumina At Liquid Nitrogen Temperature

Table J-3
Measurement of Pore Size Distribution

| (1) | (2) | (3) | (4) | (5) | (6) | (7) | (8) | (9) | (10) | (11) | (12) |
|-----|------------------|------------------------|---|---|---|---------------------|-----------------------------------|-----------------------------------|------------------|---|---|
| # | P/P ₀ | d _p (nm) | n _{ads} (kmole/ kg x 10 ³) | V_p (m ³ x 10 ⁶) = $\frac{82.06 \times 273.16 \times (4) \times f_{11q}}{f_{11q} \times 10^6}$ | ΔV_p (m ³ x 10 ⁶) | \bar{d}_p (nm) | ΔA_p (m ²) | ΣA_p (m ²) | 0.354 n (nm.) | (9) x (10) x 10 ⁻⁹ (m ³ x 10 ⁶) | V _p (corr.) (m ³ x 10 ⁶) = (5) - (11) |
| | | 100 | 12.25 | 0.42514 | 0.05388 | 93 | 2.31742 | 2.31742 | 6.8 | | |
| 0 | 0.975 | 86 | 10.7 | 0.37126 | 0.05233 | 58.5 | 3.57812 | 5.89554 | 4.6 | 0.01066 | 0.3606 |
| 1 | 0.9184 | 31 | 9.1896 | 0.31893 | 0.03824 | 22.1 | 6.92127 | 12.81681 | 2.2 | 0.012297 | 0.30663 |
| 2 | 0.8329 | 13.2 | 8.0858 | 0.28069 | 0.02911 | 10.9 | 10.68257 | 23.49938 | 1.38 | 0.017687 | 0.26300 |
| 3 | 0.7388 | 8.6 | 7.2514 | 0.25158 | 0.02910 | 7.4 | 15.72973 | 39.22911 | 0.98 | 0.02303 | 0.22855 |
| 4 | 0.6497 | 6.2 | 6.4090 | 0.22248 | 0.00774 | 5.1 | 6.07059 | 45.4256 | 0.80 | 0.03138 | 0.1911 |
| 5 | 0.6030 | 5.2 | 6.1584 | 0.21365 | 0.00929 | 4.75 | 7.82316 | 59.31935 | 0.74 | 0.03362 | 0.18003 |
| 6 | 0.5763 | 5.0 | 5.9355 | 0.20591 | 0.00882 | 4.2 | 8.4 | 67.71935 | 0.71 | 0.03656 | 0.16935 |
| 7 | 0.5454 | 4.5 | 5.6641 | 0.19662 | 0.01719 | 3.7 | 18.58378 | 86.30313 | 0.68 | 0.04034 | 0.15628 |
| 8 | 0.4934 | 3.9 | 5.4102 | 0.18780 | 0.01223 | 3.3 | 14.82424 | 101.12737 | 0.625 | 0.04232 | 0.14548 |
| 9 | 0.4378 | 3.5 | 4.9139 | 0.17061 | 0.00991 | 2.95 | 13.43729 | 114.56466 | 0.58 | 0.05006 | 0.12055 |
| 10 | 0.3905 | 3.1 | 4.5635 | 0.15838 | 0.01114 | 2.675 | 16.65794 | 131.2226 | 0.54 | 0.05461 | 0.10377 |
| 11 | 0.3424 | 2.8 | 4.2789 | 0.14847 | 0.01540 | 2.39 | 25.77406 | 156.99666 | 0.51 | 0.058428 | 0.09004 |
| 12 | 0.2987 | 2.55 | 3.9590 | 0.13733 | 0.00867 | 2.125 | 16.32 | 173.31666 | 0.485 | 0.06364 | 0.07369 |
| 13 | 0.2372 | 2.23 | 3.5423 | 0.12293 | 0.01223 | 1.885 | 25.95225 | 199.26891 | 0.455 | 0.07143 | 0.0515 |
| 14 | 0.1921 | 2.02 | 3.2925 | 0.11426 | 0.01223 | | | | 0.43 | 0.07453 | 0.03973 |
| 15 | 0.1355 | 1.75 | 2.9389 | 0.10203 | | | | | 0.405 | 0.08070 | 0.02133 |

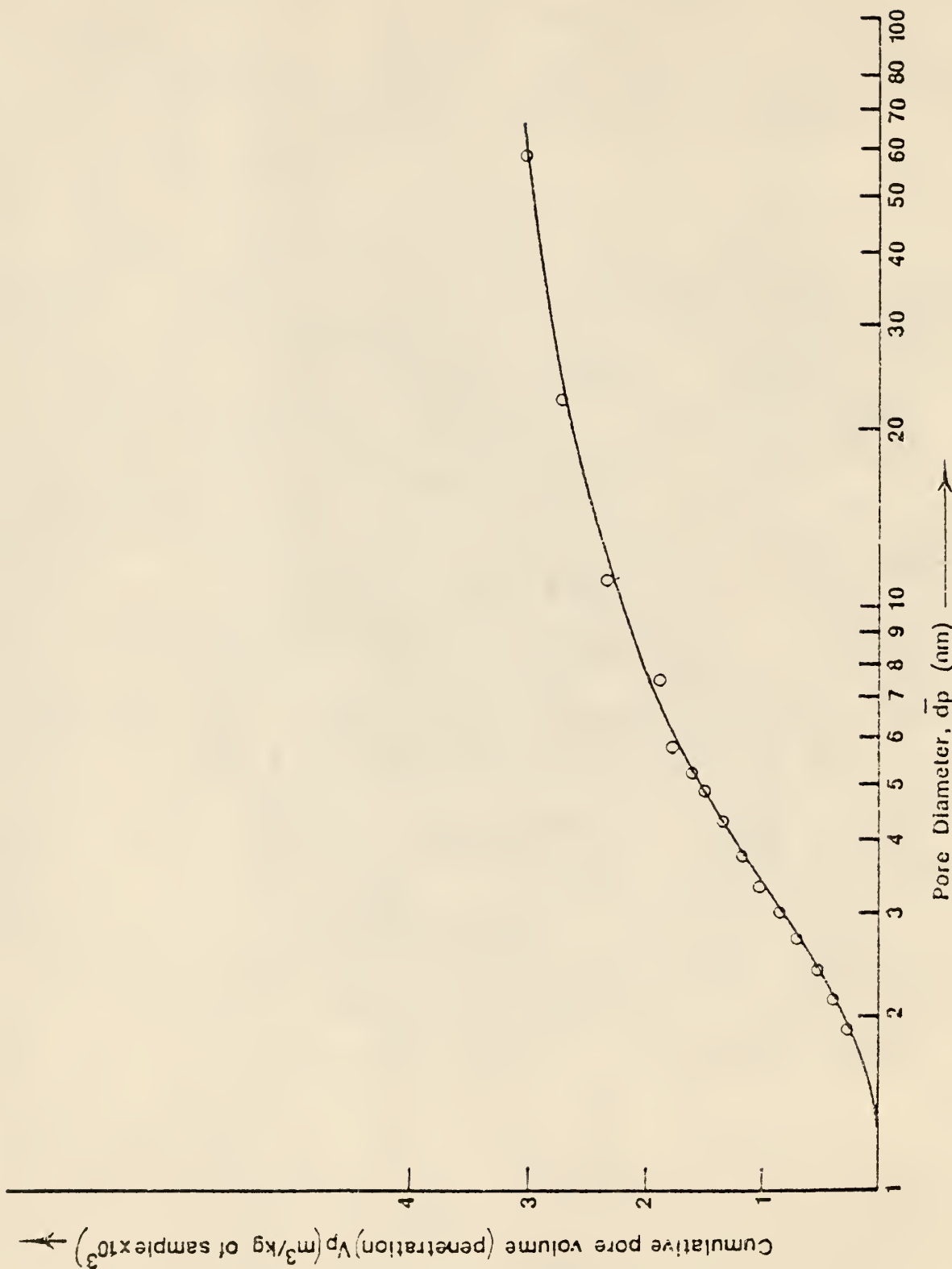


Fig. J-2 Cumulative Pore Volume Against Pore Diameter For Kaiser Alumina

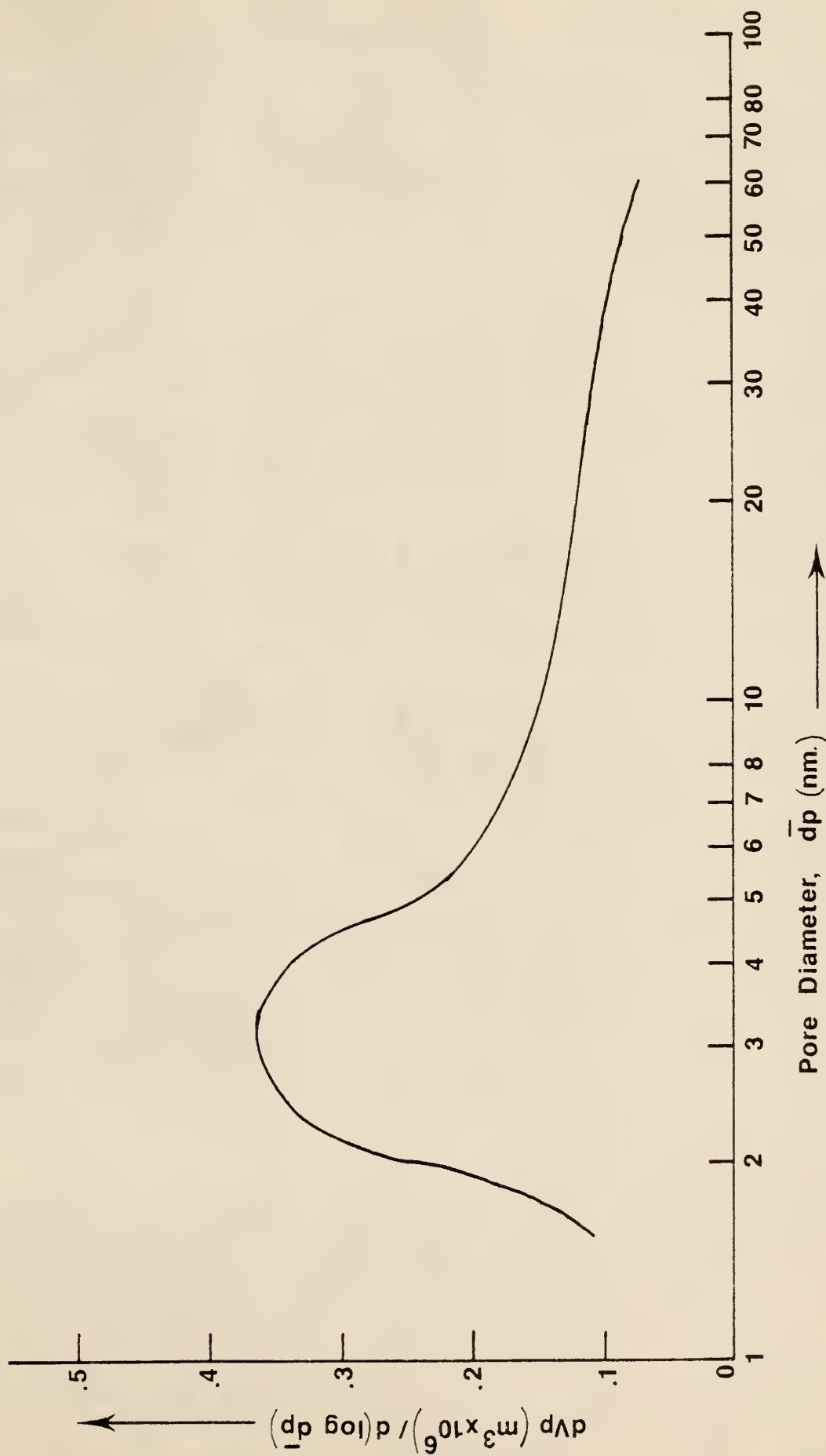


Fig. J-3 $\frac{dV_p}{d(\log d_p)}$ against \bar{d}_p For Kaiser Alumina

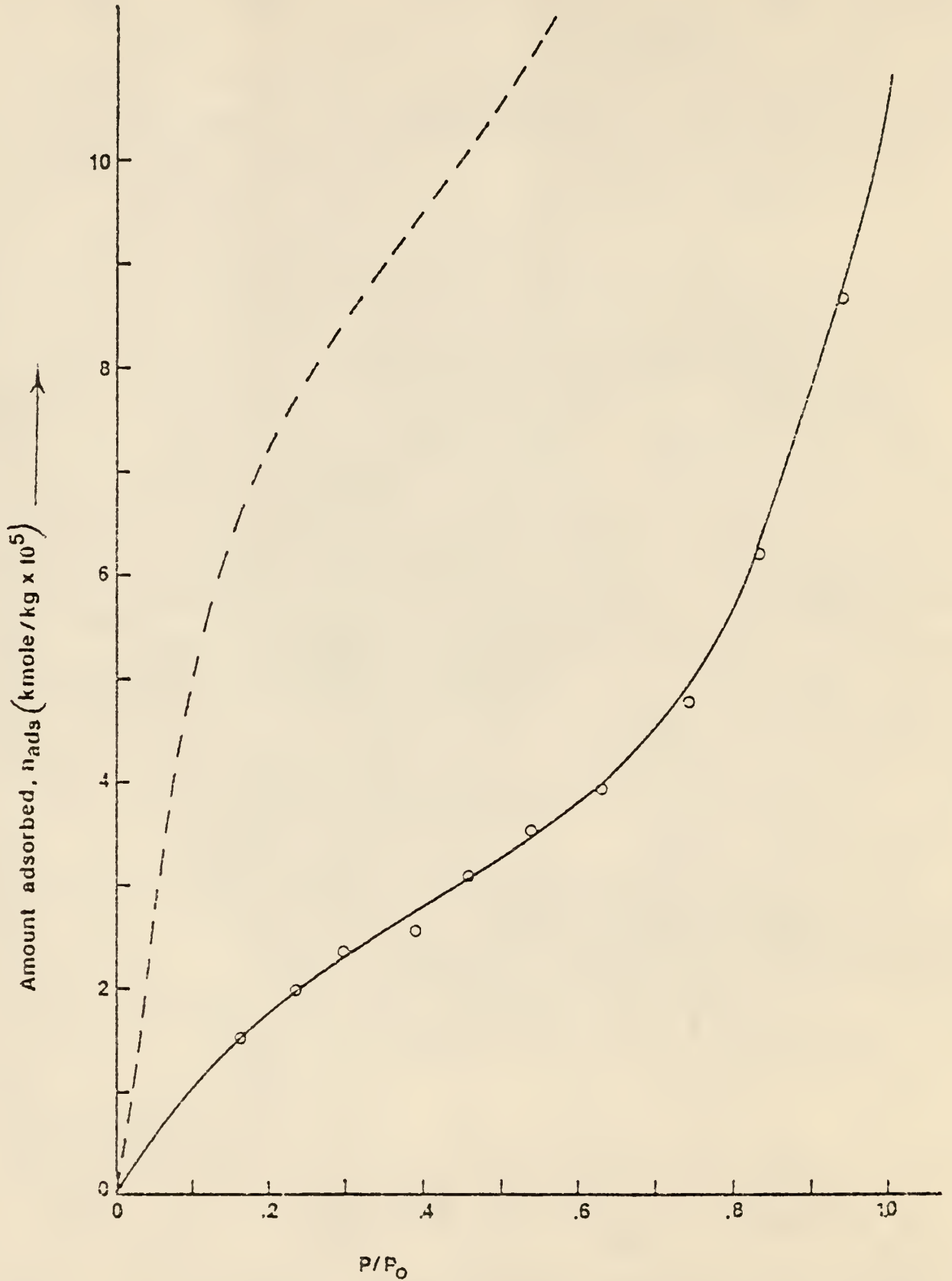


Fig. J-4 Adsorption Isotherm For Nitrogen On #784-04 (Wheat) At Liquid Nitrogen Temperature

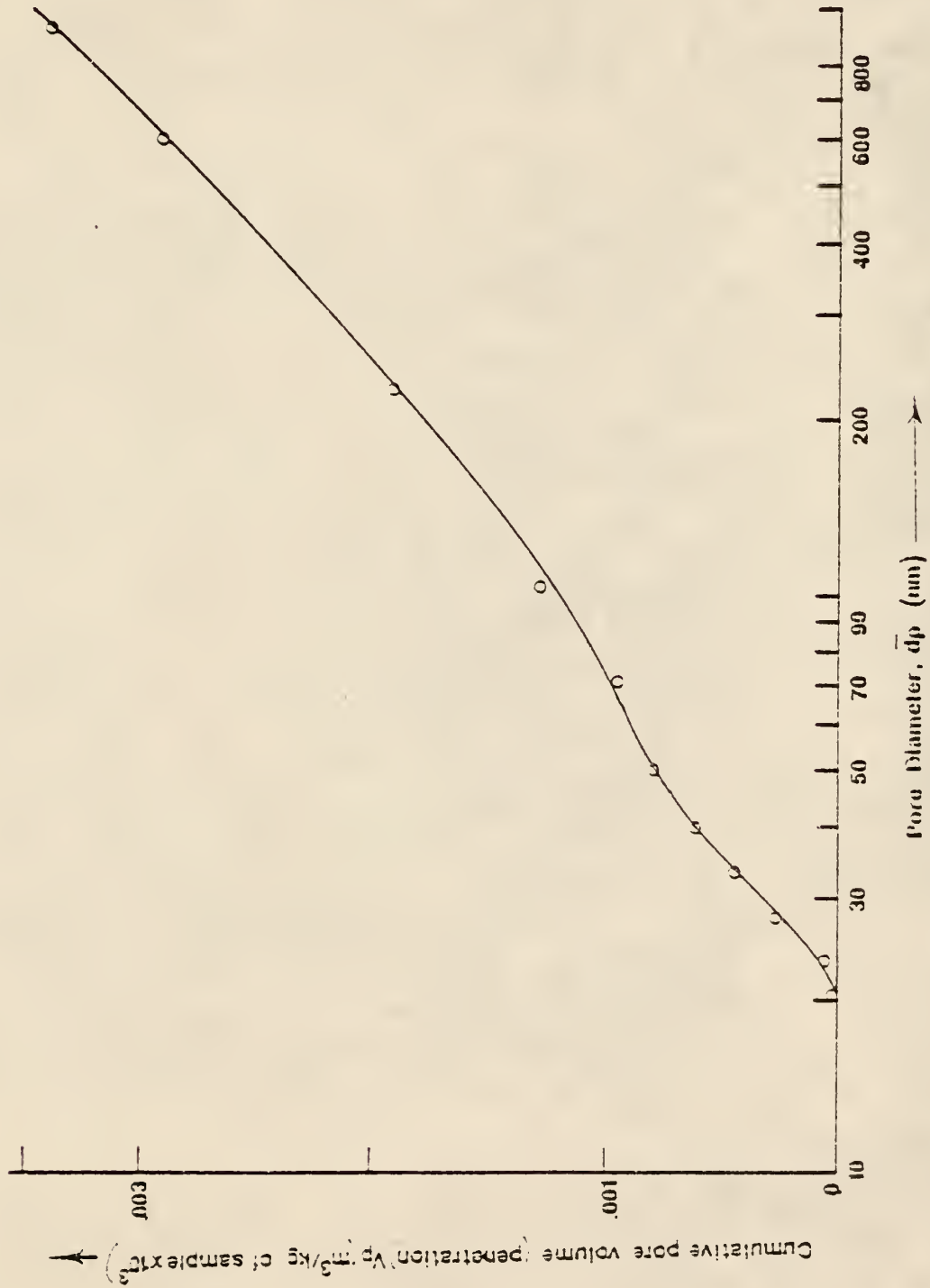


Fig. J-5 Cumulative Pore Volume Against Pore Diameter For #784-04 (Wheat)

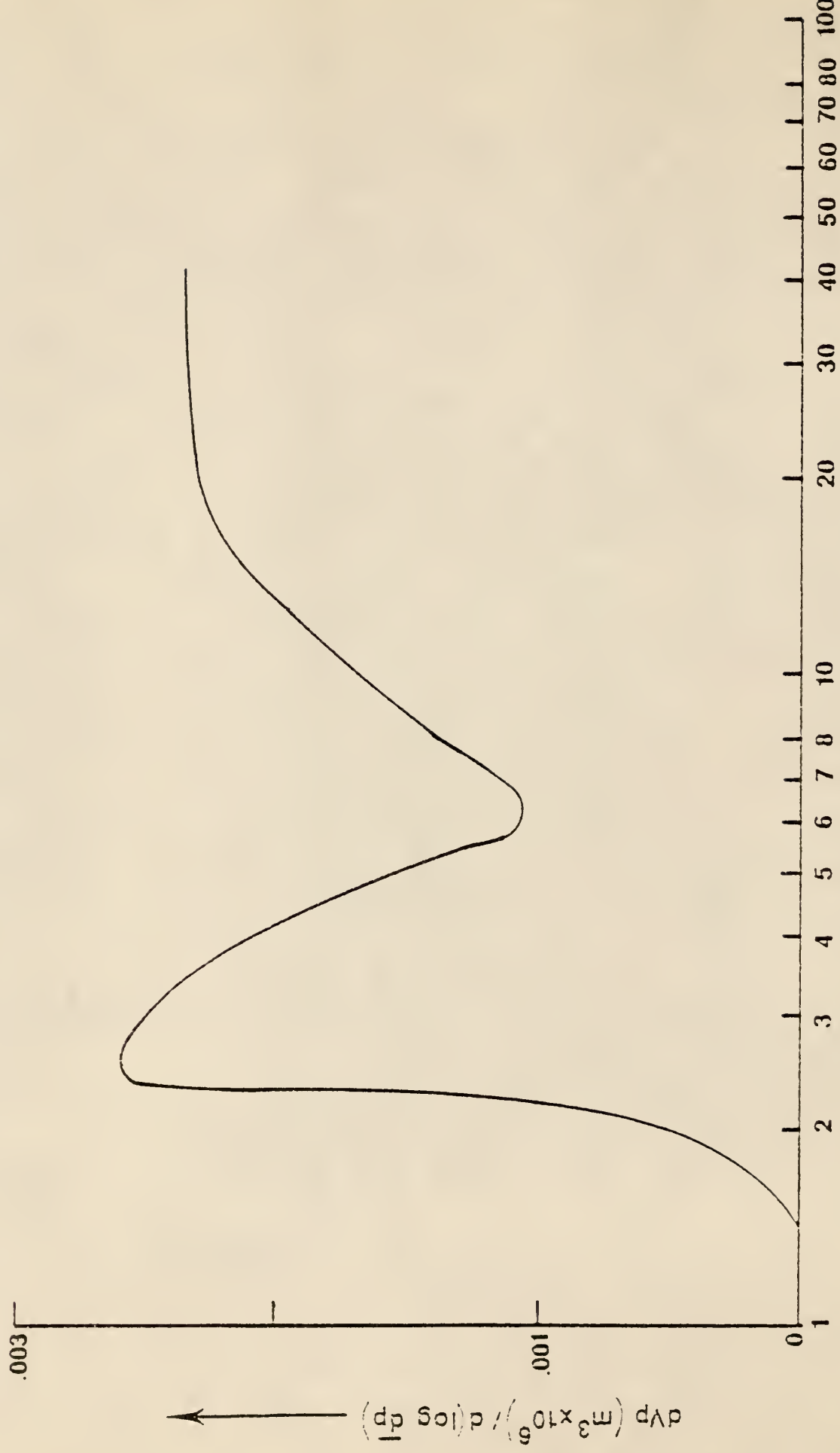


Fig. J-6 $\frac{dV_p}{d(\log \bar{d}_p)}$ against \bar{d}_p For #784-04 (Wheat)

calculation are shown as plots of cumulative pore volume against pore diameter in Figures J-2 and J-5. The pore size distributions are shown as plots of $\frac{d V_p}{d (\log d_p)}$ against pore diameter in Figures J-3 and J-6.

J-5 Discussion

The adsorption isotherms obtained for both samples (Figures J-1 and J-4) appear to be of type II. The amount of nitrogen filling the pores of a particular size in the alumina sample is approximately two orders of magnitude more than for the wheat dust sample. This was expected since the specific surface area of the alumina sample is much more than that of the wheat dust sample.

The shapes of the plots of cumulative pore volume V_p against pore diameter d_p and of $\frac{d V_p}{d (\log d_p)}$ against pore diameter for the alumina sample are typical of porous substances (12). However, the value of the pore volume obtained is much larger than the one reported by 'Kaiser Chemicals' (0.31 lit./kg. against the reported value of 0.104 lit./kg.). The alumina sample was found to have maximum of its pore volume offered by the pores of diameter around 3.0-3.5 nm.

Unlike the alumina, wheat was found to have an unusual pore size distribution (Figures J-5 and J-6). It was found to have a pore volume passing through a relative maximum at a pore diameter around 2.5-2.7 nm. and then monotonously increasing after a pore diameter of around 6.0-6.5 nm. As mentioned earlier, poor results with the wheat dust was considered a distinct possibility. It does appear that the results obtained can be explained with the assumption that nitrogen cannot enter small pores in the wheat dust. If nitrogen could enter the small pores, the adsorption isotherm would move upwards as shown by the dashed curve in Fig. J-4, with a sharper bend at the relative pressure corresponding to the monolayer

capacity. This dashed curve corresponds to one which would give the value of the surface area close to that obtained by carrying out the adsorption of carbon dioxide at room temperature. As can be seen easily, this would modify both the Figures J-5 and J-6 with the new shapes approaching those that have been observed in the literature for a porous substance (12).

It may be noted that both the adsorption isotherms that have been used to determine the pore size distributions are "adsorption isotherms" and not the "desorption isotherms". However, adsorption isotherms and desorption isotherms are identical when there is no hysteresis. Whether or not there would be a hysteresis depends on shapes of the pores. In both the samples tried, no sizeable hysteresis were found. However, if there were hysteresis, the desorption isotherms would have been used.

It may also be noted that while calculating the pore volume corresponding to a pore diameter, an assumption was made that the pores are cylindrical in shape. This may not always be the case and so the "pore diameters" found are actually the "equivalent pore diameters".

Also, the mode value of pore diameter calculated from these measurements may be slightly lower than the actual. This is because the cumulative surface area as calculated from the pore size distribution calculations is less than that calculated from the BET equation. This is indicative of the pores being not perfectly cylindrical (13). In this case, the correction in the pore volume for the amount adsorbed on the surfaces of the pores not filled should be higher than has been accounted for. This causes the inflexion point in the plot of cumulative pore volume V_p against the pore diameter d_p to move rightwards (corresponding to a higher value of pore diameter) and so also should the most occurring value of the diameter of the pores.

ADSORPTION STUDIES ON GRAIN DUSTS

by

UJWAL ANANT DESHPANDE

B.S., Indian Institute of Technology (Bombay), 1977

AN ABSTRACT OF A MASTER'S THESIS

submitted in partial fulfillment of the

requirements for the degree

MASTER OF SCIENCE

Department of Chemical Engineering

KANSAS STATE UNIVERSITY
Manhattan, Kansas

1979

ABSTRACT

The objective of this work was to measure the specific surface areas of grain dusts and to measure the extent of adsorption of carbon monoxide and methane on them. The specific surface areas were measured by carrying out adsorption of nitrogen on the dust samples at liquid nitrogen temperature and using the BET equation to calculate the monolayer capacities. These measurements were made on a standard volumetric BET apparatus as well as on a commercial flow-type adsorption apparatus. The samples were subjected to different treatments for moisture removal before the adsorption measurements and their results were compared.

The specific surface areas were also measured, on the static apparatus, at higher temperatures to reduce a suspected resistance to pore diffusion. Carbon dioxide was used for this and the measurements were made at 195°K. and at room temperature. The Dubinin-Polanyi equation was used for the surface area calculation from the latter measurement.

The specific surface area values obtained from the nitrogen measurements varied from 420 m²/kg. for a soybean dust sample to around 2240 m²/kg. for a wheat sample. The values of the surface area obtained using carbon dioxide were higher than those from nitrogen measurements. For example, a wheat dust sample which gave a surface area of 1770 m²/kg. from the Sorptometer measurements, gave a value of 3940 m²/kg. from adsorption at 195°K. and 17840 m²/kg. at room temperature.

The extent of adsorption of carbon monoxide and methane on the dust samples was measured at 195°K. and also at room temperature. The results at room temperature were compared with the Lower Explosive Limits of these gases and were found to give a composition in the void space of the solids less than the Lower Explosive Limits, except at very high partial pressures.



